FCTUC FACULDADE DE CIÊNCIAS E TECNOLOGIA
UNIVERSIDADE DE COIMBRA

PHILIPS
sense and simplicity

Integrated Master in Biomedical Engineering
Faculty of Sciences and Technology
University of Coimbra

Prediction of Critical Blood Pressure Changes Based on Surrogate Measures

Tobias Correia

Coimbra, 2012

FCTUC FACULDADE DE CIÊNCIAS E TECNOLOGIA
UNIVERSIDADE DE COIMBRA

PHILIPS
sense and simplicity

Integrated Master in Biomedical Engineering
Faculty of Sciences and Technology
University of Coimbra

Prediction of Critical Blood Pressure Changes Based on Surrogate Measures

Dissertation submitted to the University of Coimbra to fulfill the requirements for the degree of Master in Biomedical Engineering under the supervision of:

Jens Muehlsteff
Philips Research Europe

Paulo de Carvalho
Department of Informatics Engineering
Faculty of Sciences and Technology of University of Coimbra

Tobias Correia

Coimbra, 2012

Contents

Contents ... iii

List of Figures ... v

List of Tables ... viii

Acronyms ... ix

Acknowledgments ... x

Abstract ... xi

Sumário ... xii

1. Introduction ... 1

2. Clinical Background ... 2

2.1. Cardiovascular System ... 2
2.2. Heart ... 2
2.3. Types of circulation ... 3
2.3.1. Systemic circulation ... 4
2.3.2. Pulmonary circulation ... 4
2.4. Blood Pressure Regulation ... 4
2.5. Local Autoregulation ... 5
2.6. Hormonal Regulation ... 5
2.7. Neural regulation ... 6
2.7.1. Baroreflex Regulation ... 6
2.7.2. Chemoreflex Regulation ... 7
2.8. Cardiac Output ... 8
2.9. Cerebral Perfusion ... 9
2.10. Syncope ... 9
2.10.1. Reflex Syncope (Neurally Mediated Syncope or Vasovagal Syncope) ... 10
2.10.2. Syncope Secondary to Orthostatic Hypotension ... 10
2.10.3. Cardiac Syncope ... 11
2.11. Syncope Epidemiology ... 11
2.12. Tilt Table Testing ... 11
2.13. Windkessel Model ... 12

3. State of The Art ... 14

3.1. Photopletysmography and Its Features ... 14
3.1.1. Photoplethysmography ... 14
3.1.2. Heart Rate Variability (HRV) ... 16
3.1.3. Pulse Wave Velocity (PWV) ... 16
3.1.4. Left Ventricular Ejection Time (LVET) ... 17
3.1.5. Pulse Arrival Time (PAT) ... 18
3.1.6. Inflection Point Area Ratio (IPA) ... 19
3.1.7. Inflection and Harmonic Area Ratio (IHAR) ... 19

3.1.8. Dicrotic Index 19
3.1.9. Reflection Index (RI) 20
3.1.10. Augmentation Index (AI) 20
3.1.11. Shape Analysis 20
3.2. Blood Pressure from PPG 22
3.3. PPG Signal Processing 23
3.4. Syncope Prediction 24

4. Methods 25

5. Conclusion 26

6. References 30

A Appendices I

A.1 Tables I
A.2 PCA IX
A.3 ROC curves XVIII
A.4 Demonstration of relationship between thresholds of nPAT XXIII
A.5 Uncertainity of nPAT XXIV
A.6 Methods XXV
Clinical Databases XXV
PPG from MIMIC and its annotation XXV
Head-up tilt table test data XXVI
Feature Extraction from PPG and ECG XXVIII
Pulse Segmentation XXIX
Feature Extraction XXXIII
Artifact Removal XL
First Algorithm Approach XL
Second Algorithm Approach XLV
Feature Interpolation XLVIII
Syncope Detection L

List of Figures

Figure 1 Schematic illustration of human heart. [3] 2
Figure 2 Cardiac Cycle. [2] 3
Figure 3 The pulmonary and systemic circulations. [4] 4
Figure 4 The aortic blood pressure curve. [5] 5
Figure 5 Distribution of pressures and volumes in the vessels. [5] 5
Figure 6 Example of baroreflex mechanism. [1] 7
Figure 7 Example of chemoreflex mechanism referred from [Colorado University, 2004] 8
Figure 8 Distribution of age of first episode of syncope in general population. [11] 11
Figure 9 Example of tilt table test performing. [14] 12
Figure 10 3-element Windkessel model [6]. 13
Figure 11 Comparison between the PPG pulse wave and the pressure pulse wave. [18] 14
Figure 12 Normal PPG pulse wave. [20] 15
Figure 13 Schematic representation of the PPG features. 15
Figure 14 Spectrum of the frequency domain analysis of a normal PPG pulse. [28] 16
Figure 15 Pulse delay (Pdelay) between the two peaks of the PPG pulse wave. Adapted from [18]. 17
Figure 16 Comparison of stroke volume with LVET. [33] 18
Figure 17 Comparison of heart rate with LVET. [33] 18
Figure 18 Representation of an ECG and the first derivative of a PPG pulse. Adapted from [35]. 18
Figure 19 Domains of a pulse from a PPG. a) Time domain; b) Frequency domain. [40]. 19
Figure 20 A pulse wave from a PPG signal. Adapted from [44]. 20
Figure 21 Different types of PPG pulses. [18]. 21
Figure 22 Comparison between two different PPG pulses to their second derivative. [18] 22
Figure 23 Representation of a step function (a) and of the step response of the integrator from equation (12) (b). 27
Figure 24 Flowchart with an overview of the produced algorithm. 28
Figure 25 Explained Variance of the PATtop. X
Figure 26 Explained variance of PAT80. X
Figure 27 Explained variance of PAT50. XI
Figure 28 Explained variance of PAT20. XI
Figure 29 Explained variance of PATfoot. XII
Figure 30 Comparison between original PATtop segments and the reconstructed ones. XII
Figure 31 Comparison between original PAT80 segments and the reconstructed ones. XIII
Figure 32 Comparison between original PAT50 segments and the reconstructed ones. XIII
Figure 33 Comparison between original PAT20 segments and the reconstructed ones. XIV
Figure 34 Comparison between original PATfoot segments and the reconstructed ones. XIV
Figure 35 Power spectrum of PATtop segments after PCA reconstruction. XV
Figure 36 Power spectrum of PAT80 segments after PCA reconstruction. XV
Figure 37 Power spectrum of PAT50 segments after PCA reconstruction. XVI
Figure 38 Power spectrum of PAT20 segments after PCA reconstruction. XVI
Figure 39 Power spectrum of PATfoot segments after PCA reconstruction. XVII
Figure 40 ROC curve for Sensitivity and Specificity of the individual values of the normalized PATt during the late tilt. XVIII
Figure 41 ROC curve for Sensitivity and Specificity of the individual values of the normalized PAT80 during the late tilt. XVIII
Figure 42 ROC curve for Sensitivity and Specificity of the individual values of the normalized PAT50 during the late tilt. XIX
Figure 43 ROC curve for Sensitivity and Specificity of the individual values of the normalized PAT20 during the late tilt. XIX
Figure 44 ROC curve for Sensitivity and Specificity of the individual values of the normalized PATf during the late tilt. XX
Figure 45 ROC curve for performance of PATt with different prediction times. XX
Figure 46 ROC curve for performance of PAT80 with different prediction times. XXI
Figure 47 ROC curve for performance of PAT50 with different prediction times. XXI
Figure 48 ROC curve for performance of PAT20 with different prediction times. XXII
Figure 49 ROC curve for performance of PATf with different prediction times. XXII

Figure 50 Impact of the offset in the determination of a new threshold. XXIII
Figure 51 Screen shot from an example of the choice of 10 second segments. XXVI
Figure 52 Schematic representation of patient's posture during the test. Position 0 is the initial supine position, 1 corresponds to the upright position and -1 is the the final supine position after the back tilt (Patient number 5). XXVII
Figure 53 Representation of posture changes. In this case an additional phase is introduced, 1.5, which is the period after the administration of glycerol trinitrate and before the returning to supine position (Patient 12). XXVII
Figure 54 a) Task Force® Monitor [82]. b) Philips MP50® Monitor [83]. XXVIII
Figure 55 Flowchart of the algorithm for pulse segmentation. XXIX
Figure 56 Screenshot of the GUI to evaluate the segmentation algorithm. The bars represent the annotated points, blue for peaks and black for onsets and the dots are the points found by the algorithm, green for onsets and red for peaks. XXX
Figure 57 Example of a not consensual onset determination (record 410). XXXI
Figure 58 Example of wrong onset detection (record 224). XXXII
Figure 59 Pulse with a corrupted peak (record 208). XXXII
Figure 60 PPG pulses with 5 reference points (record 041). XXXIII
Figure 61 Example of heart rate calculation. The outliers caused by motion artifacts are more visible in the PPG foot HR (Patient 18). XXXIV
Figure 62 Comparison between the HR obtained from the ECG and from the PPG (Patient 9). XXXIV
Figure 63 Comparison between the ECG and PPG (subject 9)..... XXXV
Figure 64 Example of HR (from ECG) decrease before faint (patient 33). It is clear that the decrease of heart rate starts after the tilt up and it ends moments before the patient faints. That decrease reaches a minimum of less than 50 bpm, which is a critical value that might be the cause of this syncope episode along with the decrease of SBP. XXXVI
Figure 65 Example of decrease in HR (ECG) in a patient without syncope. In fact, the decrease takes place after an increase due to GTN administration. However, this example proves that a decrease of HR even in the ideal conditions for a syncope episode it is not always a good predictor measure (Patient 51). XXXVI
Figure 66 PAT extracted having as PPG reference points the foot, the heights at 20%, 50% and 80% of the amplitude and the top from top to bottom, respectively (Patient 39). XXXVII
Figure 67 Scheme of posture change (Patient 39). XXXVIII
Figure 68 Detail of the offset between different PATs. (Patient 10) XXXVIII
Figure 69 Pulse amplitude compared with SBP. The pulse amplitude keeps constant during all the record even after the administration of GTN when the SBP starts to decrease until the syncope. (Patient 39) XXXIX
Figure 70 Pulse amplitude changing with SBP. Although it is not a very well pronounced decrease it is still visible that the decrease in SBP is followed by the pulse amplitude. (Patient 26) XXXIX
Figure 71 Decrease in SBP followed by decrease in pulse amplitude. (Patient 46) XL
Figure 72 Screenshot of the procedure to annotate the records. XLI
Figure 73 Flowchart of the first algorithm developed to remove the noise and motion artifacts in the extracted features. XLII
Figure 74 Comparison of the HR before (first graph) and after the outliers' removal (second graph). (Patient 40) XLIII
Figure 75 Comparison of PAT before (first graph) and after outliers removal (second graph). (Patient 40) XLIII
Figure 76 Comparison of PAT before (first graph) and after outliers removal (second graph). (Patient 26) XLIV
Figure 77 Detail of the different PATs after outliers removal. A large number of segments without data (for example 47 and 17 seconds in PAT top and PAT80, respectively) can be seen in a critical period for syncope prediction, which is just before the fainting. (Patient 44) XLV
Figure 78 Comparison between the heart rates from the PPG and the one from the ECG. (Patient 21) XLVI
Figure 79 Flowchart of the second algorithm developed to remove the noise and motion artifacts in the extracted features. XLVI
Figure 80 Comparison between the PAT after the artifact removal algorithms. In the top graph the removal is processed with the first algorithm, while in the bottom the removal is done with

the HR comparison algorithm. It is clear that the signal from the new approach is much cleaner, since it removed the spikes that the first algorithm was not able to deal with. (Patient 26) ... XLVII
Figure 81 Example of linear interpolation between the blue points in order to find the red one. XLVIII
Figure 82 Schematic representation of HUT sequences and PATref. (Patient 8) LI
Figure 83 Anotation example for the syncope prediction tests. (Patient 12) LI
Figure 84 Example of PATref measured during a variation of the PAT (Patient 24). LIV

List of Tables

Table 1 Blood Pressure Regulation by Hormones. [1] 6
Table 2 Sensitivity and specificity for choice of best threshold in HR variations. (d is the distance to the upper left corner of the ROC curve). I
Table 3 Sensitivity and specificity for choice of best threshold in PAT variations. (d is the distance to the upper left corner of the ROC curve). II
Table 4 Sensitivity and specificity for choice of best threshold in HR comparison. (d is the distance to the upper left corner of the ROC curve). III
Table 5 Segmented PAT's for the PCA. IV
Table 6 HUT sequences for patients with syncope. V
Table 7 HUT sequences for patients without syncope. VI
Table 8 Student's t-test for HUT sequences of Table 6 and Table 7 ($p < 0.05$). VII
Table 9 Student's t-test HUT sequences comparison of syncope vs. non syncope patients ($p<0.05$). VII
Table 10 Statistics for optimal threshold determination with the original PAT signal. The optimal threshold is the one closest to the upper left corner of the ROC space (d). VIII
Table 11 Explained Variances of each component from the PCA. IX
Table 12 Details of the used records. XXV
Table 13 Details of patients tested for the used dataset. XXVIII
Table 14 Sensitivity and PPV of the onsets and peak detection. XXXI
Table 15 Sensitivity and specificity of chosen thresholds. XLI
Table 16 Sensitivity and Specificity of the best thresholds for each PPG heart rate. XLVII
Table 17 Power Spectrum properties for the sampling rate determination. XLIX
Table 18 Optimal thresholds and their statistics for each PAT. LIII
Table 19 Optimal thresholds and their statistics obtained with the filtered PAT. LIV

Acronyms

BP	Blood Pressure
CABG	Coronary Artery Bypass Graft
CHF	Congestive Heart Failure
CO	Cardiac Output
ECG	Electrocardiogram
FFT	Fast Fourier Transform
GTN	Glycerol Trinitrate
H^+	Hydron
HUT	Head-up Tilt
HR	Heart Rate
MAP	Mean Arterial Pressure
pCO_2	Carbon Dioxide Partial Pressure
pO_2	Oxygen Partial Pressure
PPG	Photoplethysmogram or Photoplethysmography
PAT	Pulse Arrival Time
PPV	Positive Predictive Value
ROC	Receiver Operating Characteristic
SE	Sensitivity
SBP	Systolic Blood Pressure
SP	Specificity
STD	Standard Deviation

Acknowledgments

I would like to thank to my both supervisors, Paulo Carvalho and Jens Muehlsteff, for their support and constant concern about the progress of this project.

A special consideration to Professor Miguel Morgado from the physics department of the University of Coimbra for his dedication and effort in promoting and maintaining the degree in biomedical engineering.

I am also thankful to all my friends, in particular to the 5 special ones, for all the help and good times that we spent together as biomedical engineering students and, of course, for being part of one of the best chapters of my life.

Finally, I am very grateful to my family for always being there and for supporting all my decisions.

Abstract

Blood pressure (BP) is one of the most important physiological parameters, in particular regarding the cardiovascular system. Through this vital sign is possible to infer about the health of a subject in various different ways. However, its continuous monitoring is conditioned by methods, which are either invasive or not comfortable enough yet having high costs, which in a society increasingly changing to a preventive medicine and patient monitoring in non-clinical environments becomes hardly feasible.

This document describes a system for syncope prediction based on signals acquired simultaneously and in real time, the photoplethysmogram (PPG) and the electrocardiogram (ECG), from, which one can extract measures correlated to BP and its regulation, the pulse arrival time (PAT) and the heart rate (HR). Since a syncope episode, generally, happens due to critical BP drops, tracking these features allows to predict a fainting phenomenon.

In order to achieve the ultimate goal, several processes had to be taken into account involving the conjugation of the acquired signals, the removal of motion artifacts and noise and the creation of thresholding algorithms to identify critical situations of BP changes and presyncope stages in real time. These thresholds were determined with the aid of receiver operating characteristic (ROC) curves. The data used to evaluate the performance of the developed algorithm was acquired in a tilt table test from 44 patients with a history of syncope. Thus, a sensitivity of 90.48%, a specificity of 83.33% and a positive predictive value of 82.61% were obtained and the average prediction time, *i. e.* the time between the prediction alarm and the faint was 77.71 ± 71.78 seconds.

Therefore, the development of simple systems to predict faints in real time is feasible and can help to increase the quality of life of patients suffering from recurrent syncope.

Keywords: syncope; electrocardiogram; photoplethysmography; pulse arrival time; heart rate; prediction algorithms; blood pressure, tilt table test.

Sumário

A pressão sanguínea é um dos parâmetros fisiológicos mais relevantes, nomeadamente no que diz respeito ao sistema cardiovascular. Através deste sinal vital é possível inferir de diversas formas acerca do estado de saúde do doente. No entanto, a sua monitorização contínua está condicionada por métodos que ou sendo invasivos ou não sendo suficientemente confortáveis têm ainda custos muito elevados, o que num sistema cada vez mais virado para a medicina de prevenção e monitorização do doente em ambiente não clínico se torna pouco viável.

Neste documento é descrito um sistema de predição de síncopes baseado no uso de sinais adquiridos simultaneamente e em tempo real como o fotopletismograma e o electrocardiograma dos quais são extraídas medidas correlacionadas com a pressão sanguínea e com a sua regulação, o tempo de chegada de pulso e o ritmo cardíaco. Uma vez que um episódio de síncope ocorre devido a descidas críticas da pressão sanguínea, a monitorização destes parâmetros permite a previsão de desmaios.

De forma a atingir o objectivo final, tiveram de ser tomadas em conta diversas etapas que envolvem processos como conjugação dos sinais, a remoção de artifactos de movimento e ruído e a criação de algoritmos de limiar para a identificação de situações críticas e de estágios pré-síncope em tempo real. Esses limiares foram determinados com o auxílio de curvas da característica do receptor (ROC). Para avaliar o desempenho do algoritmo desenvolvido foram usados dados adquiridos em testes de mesa inclinada de 44 pacientes com historial de síncope. Assim, obteve-se uma sensibilidade de 90,48%, uma especificidade de 83,33% e um valor de predição positiva de 82,61%, sendo que a média de tempo de previsão, isto é, o tempo entre o alarme e a ocorrência do desmaio foi de 77,71 ± 71.78 segundos.

Conclui-se portanto que a criação de sistemas simples de predição de desmaios em tempo real é viável e podem ajudar no aumento da qualidade de vida de pacientes que sofrem de síncope recorrente.

Palavras-chave: síncope; electrocardiograma; fotopletismograma; tempo de chegada de pulso; ritmo cardíaco; algoritmos de predição; pressão sanguínea; teste de mesa inclinada.

1. Introduction

The risk of fainting is permanent threatening to the quality of life of people diagnosed with recurrent syncope.

Preventive medicine and promotion of healthy customs are increasingly relevant issues in today's society in such a way that they were officially introduced by the world health organization only in 1984. Contrasting with the curative medicine, the costs involved in the preventive medicine are much lower, as an example most of money that is spent every year in the treatment of obesity and smoking diseases could be saved if the patients simply do physical exercise or quit smoking. Besides, it is known that nowadays the majority of health problems are preventable, which is also a motivation for the investment on preventive medicine.

Initially, preventive medicine was based on educational efforts to avoid risk behaviours, however with the increase in chronic diseases there was an evolution on this concept and now the preventive medicine tries also to act in people who already suffer from a disease in order to cure them or at least to avoid the progress of the disease, reducing its impact in the quality of life of the patient.

Thus, the use of portable medical devices for continuous and real time monitoring of the patients in their daily environment, pHealth systems, makes more sense than ever. These devices can contribute to the increase not only in the quality of life of the patients, but also in the increase of their average life expectancy, enabling a better control of the disease, the anticipation of undesirable effects and the reduction of serious consequences resulting from a defective monitoring of the patient. So, as a complement to the traditional medical procedures there is a need of using simple and portable devices, so that the normal life of the patient is the least affected as possible.

Recurrent fainting is one of these chronic diseases that have a huge impact in the daily life of a person since it happens occasionally, but sometimes without precedents, which can result in uncontrolled falls, resulting in severe damage to the patient, majorly to the elderly. So, if there was a way of predicting the occurrence of syncope episodes that could allow to the patient to react with countermeasures such as laying down or doing isometric exercises in order to promote the blood circulation, that could be a good way of improving the quality of life of this patients.

Our goal is to develop a way of predicting syncope episodes based on the fact that they happen, most of the times, due to a critical decrease in systolic blood pressure.

Since the existent techniques to monitor BP are very limited for a continuously and portable application together with the fact that the existent portable devices are not comfortable to wear, in this work a different approach for BP monitoring was explored. We developed an algorithm for syncope prediction, which uses the pulse arrival time acquired from ECG and PPG signals as a surrogate measure of the SBP. From these surrogates it is possible to track SBP changes and detect the critical decreases that might cause a faint. This algorithm has to be simple enough to be applied in a portable device, but at the same time robust enough to deal with the motions artifacts caused by the movements of a patient in a continuous, portable and real-time application

So, in this document we describe the steps for the development of the algorithm, starting with an overview of the cardiovascular system and an introduction to the clinical background of the syncope. Then, a study of the state of the art in feature extraction, signal processing and syncope prediction is made followed by the presentation of the datasets used. From here, the creation of the algorithm is described step by step starting with the pulse detection of the PPG, feature extraction, artifacts removal and, finally, the syncope prediction. In the end, it is made a discussion regarding the obtained results, an overview of the algorithm and a reflection about future work that can be done in order to increase the performance of the algorithm.

2. Clinical Background

2.1. Cardiovascular System

The cardiovascular System is one of the most important systems of the organism. It is responsible for the transport and supply of nutrients, oxygen and hormones for all cells of the body through the blood. At the same time it collects carbon dioxide and other products of their metabolism. In addition, this system transports proteins and cells of the immune system, and it is also important on the defense, thermic and pH regulation of the organism. [1]

This circulatory system consists of a heart that pumps the blood through the blood vessels. So, when the heart is working, it creates pressure gradients that force the blood to circulate through the vessels. This movement is unidirectional and the oxygenated blood (arterial) never blends with the deoxygenated blood (venous) because it is divided in two circulations: the pulmonary and the systemic circulation. [2]

2.2. Heart

The heart is a muscular organ primarily composed of four chambers: two atria (input chambers) and two ventricles (output chambers), more specifically an atrium and a ventricle on the left side (whose connection is made through the mitral (or bicuspid) valve) and an atrium and a ventricle on the right (whose connection is made by the tricuspid valve), as shown in Figure 1This separation is done at the level of the atria by the interatria septum and at the level of the ventricles by the interventricular septum, this allows to have two types of circulation so there is no mixing between oxygenated and venous blood. [1]

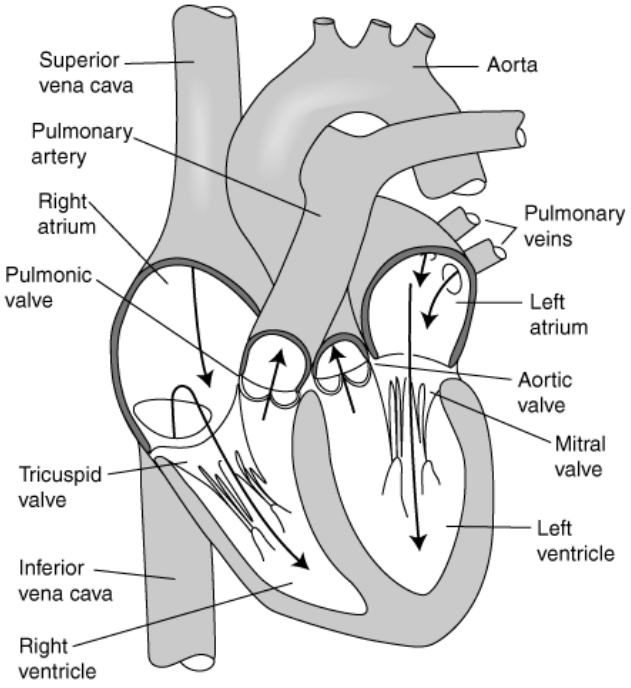

Figure 1 Schematic illustration of human heart. [3]

However, the left side is thicker than the right because this is the side where the oxygenated blood is pumped throughout the body (systemic circulation), while on the right side the

deoxygenated blood is ejected into the lungs (pulmonary circulation), which requires less effort since the distance and friction are reduced. [1]

Blood circulation is created by periodic contractions of the myocardium (heart muscle), which is stimulated electrically. The heart rate is then maintained by excitatory nodes: the sino-atrial node (which is located in the right atrium and sends impulses to the atria) and the atrio-ventricular node (which is located between the right atrium and right ventricle and stimulates the ventricles). The latter node creates a delay in the contraction of the ventricles in relation to the atria in order to the atria to contract and fill the ventricles before ventricular contraction occurs where the blood is released into the arteries. [3]

So, the cardiac cycle is a succession of contractions (systole) and relaxations (diastole) of the heart (Figure 2). While in the ventricular systole there are contractions of the ventricles at the same time that the mitral and tricuspid valves open to eject blood into the arteries, in the ventricular diastole this valves are closed and the ventricles are filled with blood from the atria. [2]

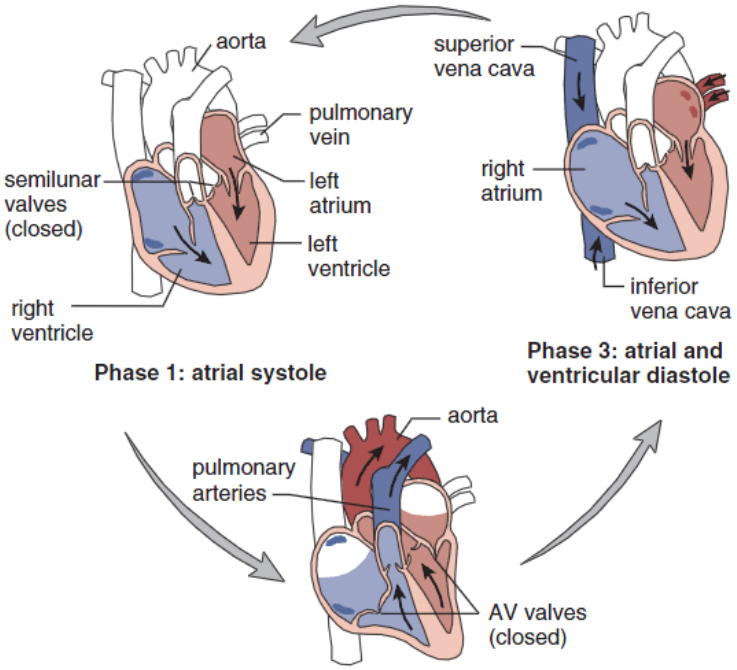

Figure 2 Cardiac Cycle. [2]

2.3. Types of circulation

As illustrated in Figure 3, there are two types of blood circulation, the systemic circulation in which the blood circulate to all body, and the pulmonary circulation that is when the blood flows to the lungs to be oxygenated. However, one can still consider a third circulation the coronary circulation that distributes the blood to the heart, although it is a part of the systemic circulation. [2]

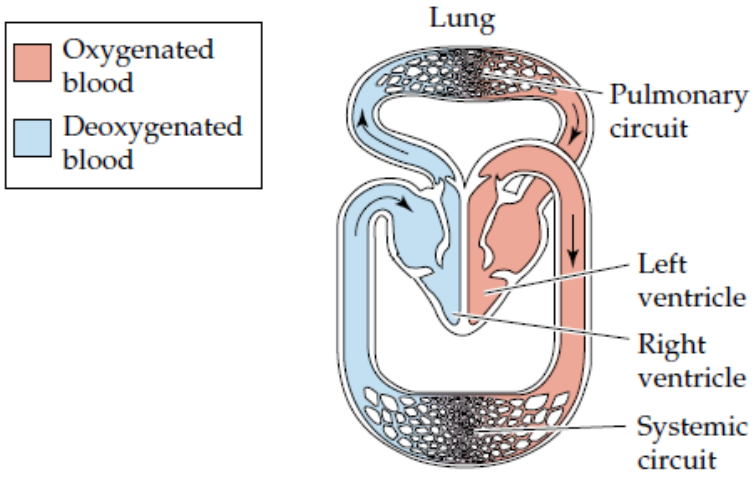

Figure 3 The pulmonary and systemic circulations. [4]

2.3.1. Systemic circulation

In the systemic circulation the oxygenated blood is provided to all tissues of the body. It leaves the left ventricle and flows to the aorta and its ramifications to the arterioles and then to the capillaries. The blood reaches the tissues where the exchange of oxygen and carbon dioxide takes place, so the blood passes from arterial to venous blood. After this, it returns to the right atrium by the veins, venules and (superior and inferior) vena cava. [1] [2]

2.3.2. Pulmonary circulation

The main targets of pulmonary circulation are to re-oxigenate the blood and remove carbon dioxide. Thus, the venous blood that reached the right atrium with the systemic circulation passes now to the right ventricle from where is ejected into the pulmonary arteries, which carry the blood to the lungs in progressive smaller vessels until the capillaries surrounding the alveoli. Here takes place the gas exchange that replaces the carbon dioxide for oxygen (the venous blood passes again to arterial blood). The blood then returns to the heart by increasing vessels up to the pulmonary veins that lead to the left atrium, and the cardiac cycle starts again. [1] [2]

2.4. Blood Pressure Regulation

Since the circulatory system operates with a pump (the heart), creating pressure gradients, it is possible to detect these variations in pressure in some areas of the body. From these variations one can have a curve that reflects different physiological parameters. In the case of arterial pressure curve shown in Figure 4, the systolic pressure corresponds to the peak (pressure in the artery when the blood is ejected from the left ventricle), while during ventricular diastole the pressure decreases until the exact moment before the new ejection of blood, which corresponds to the minimum point of the curve and, therefore, to the diastolic pressure. [5]

The values of mean pressure and the percent volume of blood in the vessels for a normal subject are represented in Figure 5, where we can notice a decrease in mean arterial pressure as we move to ever more distant vessels from the ventricles of the heart.

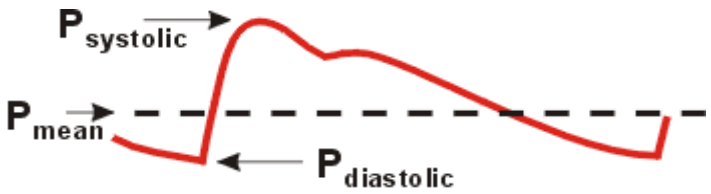

Figure 4 The aortic blood pressure curve. [5]

Arterial blood pressure is influenced by several physiological factors such as physical and mechanical characteristics of the fluid (e.g. volume and viscosity), heart rate, ventricular contractility, arterial stiffness, peripheral resistance of the cardiovascular system and venous return (which affects the level of left ventricular filling and, therefore, the force that is needed to carry out the blood from the heart, also known as cardiac preload). [1] [2] [5]

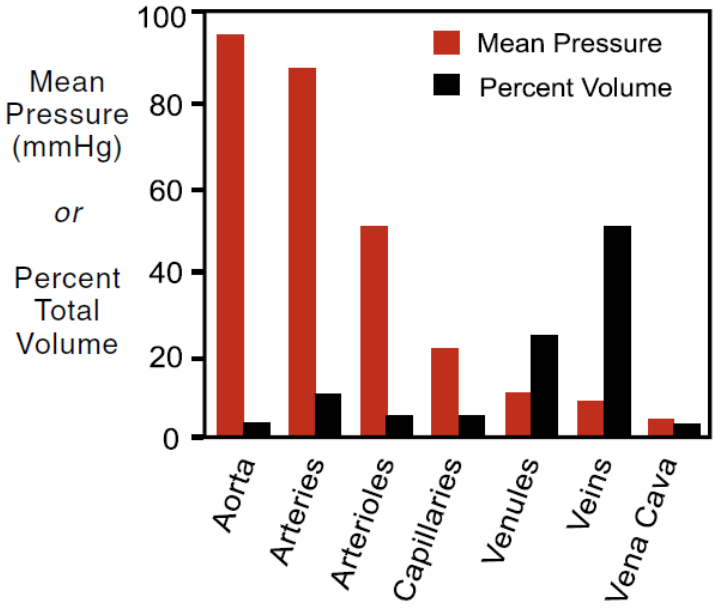

Figure 5 Distribution of pressures and volumes in the vessels. [5]

Depending on the needs of the body, either by metabolic factors (supplying of oxygen and nutrients and removal of carbon dioxide and other metabolic wastes), whether for circulatory reasons, the blood stream has to be regulated in order to optimize the blood flow that satisfies the needs of the body. This regulation can be made locally, by hormonal control or by neural control. [1] [2] [5]

2.5. Local Autoregulation

This is an emergency regulation that occurs depending on the tissue partial pressures of oxygen and carbon dioxide, nutrients or temperature. Thus, by releasing vasodilator substances or changing the muscle tone of blood vessels (since this depends on substances like oxygen or some nutrients), the vasodilatation or vasoconstriction of local microcirculation can be regulated. [1] [5]

2.6. Hormonal Regulation

Unlike the local autoregulation, hormonal regulation is made by binding substances, which can be stimulatory or inhibitory, to specific receptors that trigger a particular response,

regulating cell activity. Thus, this regulation is essentially made by the concentration of hormones to release in the target tissue to maintain the homeostatic balance. However, in spite of being precise, the hormonal regulation doesn't provide effective control in comparison with the neural regulation whose effects are longer lasting [1]. So the hormones help to adjust the blood pressure by regulating the cardiac output, the peripheral resistance and the blood volume and there are four main hormonal regulation systems: the renin-angiotensin-aldosterone system, the epinephrine and norepinephrine system, the antidiuretic hormone and the atrial natriuretic peptide [1]. The blood pressure regulation by hormones is resumed in Table 1.

Table 1 Blood Pressure Regulation by Hormones. [1]

Factor Influencing Blood Pressure	***Hormone***	***Effect on Blood Pressure***
Cardiac Output		
Increased Hear Rate and Contractility	Norepinephrine Epinephrine	Increase
Systemic Vascular Resistance		
Vasoconstriction	Angiotensin II Vasopressin Norepinephrine* Epinephrine**	Increase
Vasodilation	Atrial Natriuretic Peptide Epinephrine** Nitric Oxide	Decrease
Blood Volume		
Increase Decrease	Aldosterone Vasopressin Atrial Natriuretic Peptide	Increase Decrease

* Acts at α_1 receptors in arterioles of abdomen and skin.

** Acts at β_2 receptors in arterioles of cardiac and skeletal muscle; norepinephrine has a much smaller vasodilating effect.

2.7. Neural regulation

This type of regulation is done by the autonomic nervous system, specifically by control centers in the medulla, which are controlled by the brain and are stimulated by signals generated by receptors spread throughout the body like baroreceptors and chemoreceptors, for example in arteries. It is a very fast regulation and can be divided in two types depending on the type of receptors: baroreflex regulation and chemoreflex regulation. [1] [5]

2.7.1. Baroreflex Regulation

This type of regulation has the objective of maintaining the arterial blood pressure in normal values in cases of abrupt changes or its adaptation to acute conditions, meeting the needs of the body. This system of regulation is compound by receptors that are located in zones like the aortic arch, the carotid and in other areas of the venous and arterial peripheral circulation, by the efferent pathways and by the effector regulation. So, as resulting of this type of regulation one have the effect of the alteration of the cardiac rhythm, of the contractibility and elasticity of the vessels and of the volume of the venous return, to reach the ideal level of blood pressure. This regulation is illustrated in Figure 6. [1] [5]

These receptors can react to variations of blood pressure in a range of pressures from 60 to 180 mmHg. However, the optimal operating point, or at least the maximal sensitivity point is near the normal mean arterial pressure, which is about 95 mmHg in a healthy adult. This fact allows that a minimal deviation from the normal value can have a stronger, faster and more

effective response. So, if this variation is positive, in other words, if the blood pressure increases, the stretching of the baroreceptors fibers also increase and, consequently, their firing rate, which leads to a decrease in the sympathetic activity from the cardiovascular centers in the medulla and an increase in their parasympathetic outflow, causing a decrease in heart rate, vasoconstriction and ventricular contractility. It's important to note that sometimes (when happens an increase in venous return) the stretching of the baroreceptors fibers can cause the opposite effect, increasing heart rate, which is known as the Bainbridge effect. Otherwise, when the blood pressure decreases, the firing rate of the receptors also decrease leading to an increase in the sympathetic outflow accompanied by a decrease in parasympathetic activity causing vasoconstriction and heart rate and contractility augmentation. [5]

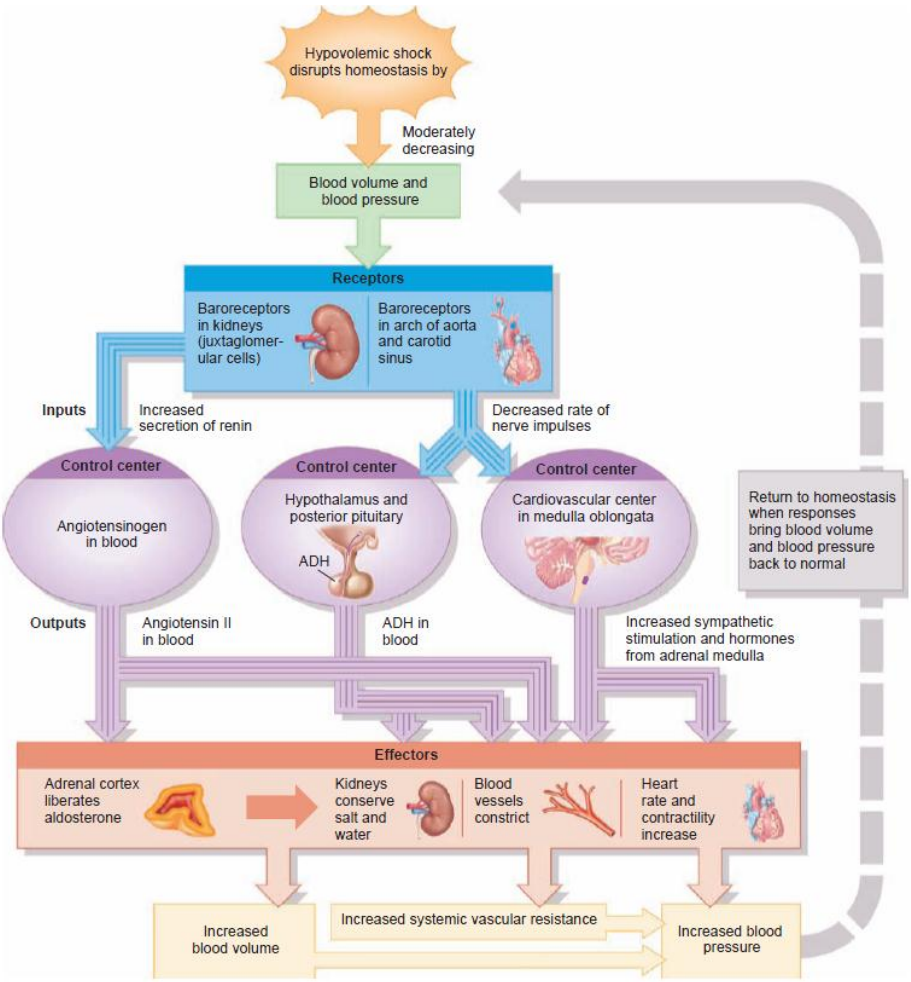

Figure 6 Example of baroreflex mechanism. [1]

2.7.2. Chemoreflex Regulation

Like the baroreflex regulation this regulation is also composed by receptors, in this case chemoreceptors, by the afferent and efferent pathways and by the regulatory effectors. This regulation has as control variables the partial pressures of oxygen and carbon dioxide and the H^+ concentration, which are used as the base of the function of the system. By this reason, there are two types of afferent pathways: one departs from peripheral chemoreceptors and is mainly controlled by the cardiovascular centers in the medulla and the other departs from the elasticity sensors of the lungs. So, to ensure the level of perfusion of oxygen necessary in the

tissues, we can also control the heart rate, the contractility and elasticity of the vessels and the volume of the venous return. This type of regulation is illustrated in Figure 7. [1] [5]

The chemoreceptors increase their firing response when the arterial pO_2 drops below 80 mmHg (the normal value is about 95 mmHg), when the arterial pCO_2 rises above the normal value of 40 mmHg or when de pH is below 7.4. In fact, it is known that the presence of carbon dioxide in the tissues increase the acidity, so the arterial pCO_2 and pH are highly related.

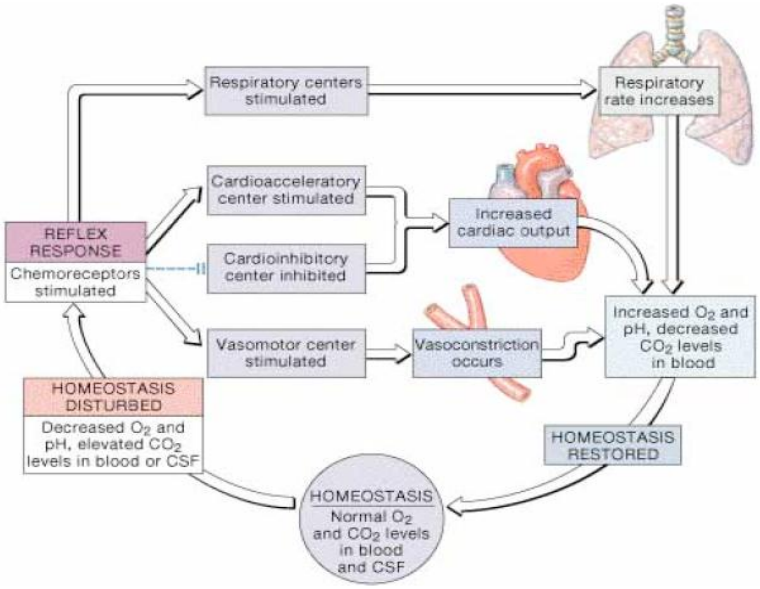

Figure 7 Example of chemoreflex mechanism referred from [Colorado University, 2004]

All of these regulations affect directly the cardiac output, which is the total volume of blood ejected by each ventricle per minute and it is a very important physiological parameter because one can take a lot of information about the cardiovascular function from it. [1] [2]

2.8. Cardiac Output

As said above, cardiac output is the amount of blood ejected from a ventricle in one minute. Cardiac output can vary because it is dependent of heart rate and stroke volume. In fact cardiac output equals the heart rate (beats/min) multiplied by stroke volume (mL/beat) and, because of that, an increase (or decrease) in any of these parameters cause a proportional increase (or decrease) in cardiac output. [1] [2]

In terms of quantization of cardiac output in a normal subject, the cardiac index is the best parameter to describe it, because it relates cardiac output with the surface area of the body. Thus, depending on the size of the person, the range of normal values for cardiac index varies from 2.6 to 4.2 L/min/m^2. [5]

Another important fact about cardiac output is that blood pressure is related to it. Indeed, blood pressure only depends on two factors: cardiac output and peripheral resistance, in other words the greater the volume of blood in the vessels, the greater the pressure exerted on its walls and, besides that, the smaller the vessel or the greater its length, the greater the resistance and, therefore, the pressure. To be more precise if the cardiac output can be calculated by dividing mean arterial pressure by peripheral resistance, it's easy to see that mean arterial pressure is only the cardiac output multiplied by resistance (Equation (1)). [1]

$$MAP = CO \times R \tag{1}$$

This equation will be further discussed in chapter 2.13. So, if the resistance is kept constant, a decrease in cardiac output leads to a decrease in arterial blood pressure. [1] [2]

Thus, if stroke volume depends on afterload, preload and contractility [1] [6], then the cardiac output and, therefore, the blood pressure are also dependent on these factors. In addition to that, we have seen that peripheral resistance and heart rate are also factors that constrain blood pressure. So, one can have at least five features that directly affect blood pressure and from which we can estimate its value.

2.9. Cerebral Perfusion

The brain and the nervous system are probably the most important systems of the human body, since they control all other systems or organs. Because of that, it is important to ensure that, in case of disturbance, this system keeps stable. However, because the brain is inside of an isovolumetric box (the skull), if the volume of any intracranial component is increased like blood volume or cerebrospinal fluid this must be balanced with a volume decrease of the other components in order to keep the right intracranial pressure and volume that ensures the right perfusion [7] [8].

Due to cerebral autoregulation, the cerebral blood flow is not entirely dependent of the cardiac output or arterial pressure [7] [9]. In other words, the cerebral blood flow, which is about 50-60 ml/min per 100g of brain tissue, is kept stable for an arterial pressure range between 60 to 160 mmHg. This is known as the autoregulation range. Between these values, the cerebral blood flow is controlled by mechanisms of cerebral autoregulation, which are not fully understood, but it seems to consist on vascular muscle fibers that respond to the transmural pressure: they relax if this pressure is decreasing (to allow more blood flow) or constrict if the pressure is increasing [7] [8]. Besides that, cerebral blood flow is also dependent on CO_2. In fact, carbon dioxide is a vasodilator, which can increase cerebral blood flood independently of cerebral autoregulation. However, if the arterial pressure drops below 60mmHg, autoregulation mechanisms are lost and cerebral blood flow becomes dependent of arterial pressure [9]. So, if the arterial pressure becomes too low (less than 50 mmHg) the cerebral perfusion cannot be ensured, which leads to syncope [9]. So, it is the cerebral autoregulation that allows the brain to have a reserve time for hypoxia (about 7 seconds), which means that, if the blood circulation is interrupted for less than that reserve time, the cerebral blood supply keeps stable, passing unnoticed by the patient [10].

2.10. Syncope

Syncope, also known as fainting, is a transient loss of consciousness due to a transient cerebral hypoperfusion. It is characterized by rapid onset, short duration and complete spontaneous recovery. [11]

In some types of syncope may be precursor symptoms such as dizziness, nausea, sweating, weakness or visual disturbances, which allows to know that a syncope is about to occur. However, it is very common to happen without any apparent precursor, so it is very difficult to estimate in advance the loss of consciousness and even its duration. Besides that, it is important to notice that the occurrence of this precursor symptoms, their duration and the duration of the unconsciousness can be different from patient to patient, being the age and sex the two most important determinative factors (in general women have more symptoms than men, and the elderly have less symptoms than younger patients) . [10] [11]

Regardless of the type of syncope, a fall in systemic blood pressure accompanied by a decrease in cerebral blood flow is usually the cause of syncope. With just a cessation of 6 to 8 seconds of the blood flow to the brain or a value below 60 mmHg in systolic blood pressure is possible to verify a complete loss of consciousness. [5] [11]

Thus, as cause of low transient cardiac output is, in the first place, a physiological reflex causing bradycardia (slow heart rate, less than 60 bpm), known as neurally mediated syncope, in the second there are the cardiovascular diseases such as arrhythmia and structural diseases

like pulmonary embolism or hypertension, and finally the inadequate venous return. These compose the three types of syncope: reflex syncope, cardiac syncope and syncope secondary to orthostatic hypotension, respectively. [11]

2.10.1.Reflex Syncope (Neurally Mediated Syncope or Vasovagal Syncope)

A reflex syncope is the result of a set of conditions in which cardiovascular reflexes that normally regulate the blood flow becomes irregular and inadequate in response to an unexpected stimulus such as emotional stress or the post exercise condition. This leads to the vasodilatation and/or bradycardia and, therefore, to a reduction in arterial blood pressure and consequent decrease of blood flow in the brain. This abnormality in the cardiovascular reflexes is occasional and not a permanent disability of these reflexes. [11]

The prodromal symptoms of vasovagal syncope begin to be noticed from 30 to 60 seconds before the loss of consciousness, which is enough time to sit or lie down preventing the syncope. However, this duration depends largely on the patient, and there are patients that don't notice the prodromal symptoms, particularly the elderly. Thus, the symptoms of the prodromal phase are common to the other types of syncope and to the ones that were described above and their occurrence and intensity increase with the reduction of blood pressure until the fainting occurs. [10]

The duration of the unconsciousness phase is normally less than 10 to 20 seconds, but in some cases it can extend for a few minutes (up to 5 minutes). An important condition that is related to the duration of this phase is the position of the patient: in a standing position the cerebral blood flow is insufficient for a greater amount of time than lying or sitting down, which leads to a slower recovery. [10]

2.10.2.Syncope Secondary to Orthostatic Hypotension

The orthostatic hypotension is defined as an atypical decrease of systolic blood pressure upon standing. Thus, unlike the reflex syncope, in autonomic failure the efferent pathways are permanently impaired, which means that there are defects in the vasoconstriction regulation despite the symptoms are identical, which can make the diagnosis of these two distinct types of syncope quite hard. Thus, when standing, there is a sudden drop in blood pressure at which the body is unable to respond and syncope occurs. [11]

This type of syncope is characterized for having three stages of succession of events: the presyncope phase (before syncope), the loss of consciousness and the postsyncope phase (after syncope). So, the presyncope is the earlier phase when people start to feel the prodromal symptoms such as weakness, dizziness, blurred vision, nausea, abdominal discomfort and sweating (there also another symptoms such as headache, tunnel vision or vertigo, but these described above are the most common ones), it may last 30 seconds, which can be enough time for the subject to sit or lie down in order to prevent injuries due to a fall when the loss of consciousness happens. The second phase is the loss of consciousness, which last for just a few seconds (it can be just 5 seconds, but in the worst cases it may last up to 20 seconds) and the person who faints is normally pale or ashen, with cold skin, but sweating, and sometimes is having convulsions. The last phase, postsyncope, corresponds to the moment after the fainting, when the patient regains consciousness, which is associated to nervousness, headache and nausea. [12] [10]

In patients with syncope due to orthostatic hypotension the prodromal effects start to occur when the systolic blood pressure drops to 60 mmHg, which means that this pressure in the brain is between 30 to 40 mmHg. The loss of consciousness phase happens at 20 mmHg of blood pressure in the brain (at eye level). [10]

2.10.3.Cardiac Syncope

Arrhythmias are the main cause of cardiac syncope by causing hemodynamic dysfunction, which leads to decreased cardiac output and, therefore, to decreased cerebral blood perfusion level [11]. The duration of loss of consciousness is clearly related with the duration of the arrhythmia and it happens from 20 to 120 seconds after the onset of the arrhythmia, which means that this type of syncope is much slower than the other types because the blood pressure drops slower, offering enough time for the patient to notice the prodromal symptoms and take the right steps to minimize injuries [10].

Structural cardiovascular diseases are another cause of syncope since by decreasing the ability to increase cardiac output does not allow that the body's circulatory requirements are met. This is aggravated when there are obstructions in the left ventricular outflow tract. Thus, loss of consciousness is due to inadequate blood flow to the brain. [11]

2.11. Syncope Epidemiology

As seen from Figure 8, the first occurrence of syncope arises at characteristic ages, mainly between 10 and 30 years old and at older ages (over 60 years old). [11]

Besides that, it appears that reflex syncope is the most common type of syncope at any age and situation, followed by cardiovascular syncope, which are most frequent in the elderly, and, finally, the orthostatic hypotension syncope, which also occur mostly in elderly. [11]

Being a common disorder in the general population, syncope recurrence has a serious impact on quality of life for many people. The difficulties inherent in a patient of recurrent syncope are comparable with those of other chronic diseases such as arteritis. Furthermore, psychosocial disturbances have an impact estimated at 33% of the activities of daily life, since syncope reduces mobility and usual abilities and increases discomfort, depression and even pain that can result from inanimate falls resulting from fainting. Thereby, although syncope takes place intermittently, the continuous threat of recurrence implies the loss of quality of life, especially with advancing age. [11]

Figure 8 Distribution of age of first episode of syncope in general population. [11]

2.12. Tilt Table Testing

As shown in Figure 9 a tilt table test consists of a table that spins from supine to erect posture causing a gravitational shift. This gravitational shift makes an estimated blood volume of 0.5 to 1 liter to flow to the vascular system below the diaphragm and reduces the plasma volume by about 700ml. This effects cause a reduction in venous return and, therefore, a decrease of stroke volume and, consequently, in cardiac output. However, the short-term mechanisms

that ensure the correct arterial blood pressure when standing up, like the neural mediated vasoconstriction of vessels, which work as blood reservoirs, have the capability to compensate the fall of arterial blood pressure caused by this decrease in cardiac output. [13]

In situations of prolonged orthostatic stress the normal venous return and, therefore, the cardiac output and arterial blood pressure is ensured by the skeletal muscle pump together with the neural orthostatic reflexes that depends of baroreceptors and chemoreceptors. As we have seen, the failure of these mechanisms can lead to episodes of syncope and this is the basic principle of tilt table tests. In other words, tilt table test pretend to simulate the failure of this compensatory systems causing a reduction in arterial blood pressure (normally a decrease to 90 mmHg of systolic blood pressure is associated with impending syncope and if this value is reduced to 60 mmHg syncope happens) and, consequently, a decrease in cerebral blood flow. [13]

Although tilt table tests are used to make scientific investigation, they can also be used in diagnosis of syncope in healthy patients or, at least, in patients without structural heart diseases or arrhythmias. [13]

Figure 9 Example of tilt table test performing. [14]

2.13. Windkessel Model

In order to make easier the understanding of all these concepts like blood pressure, blood flow and resistance, we can compare the cardiovascular system to a 3-element Windkessel model, which is an electric circuit composed by one battery, two resistors and a capacitor as shown in Figure 10. Besides, it is important to keep in mind that this is not the only type of Windkessel model. In fact, there are several other variations, some of them more realistic, but also more complex which might include diodes, representing the valves that prevent the return of blood flow, and inductances that represent the inertia of the fluid (blood) [6].

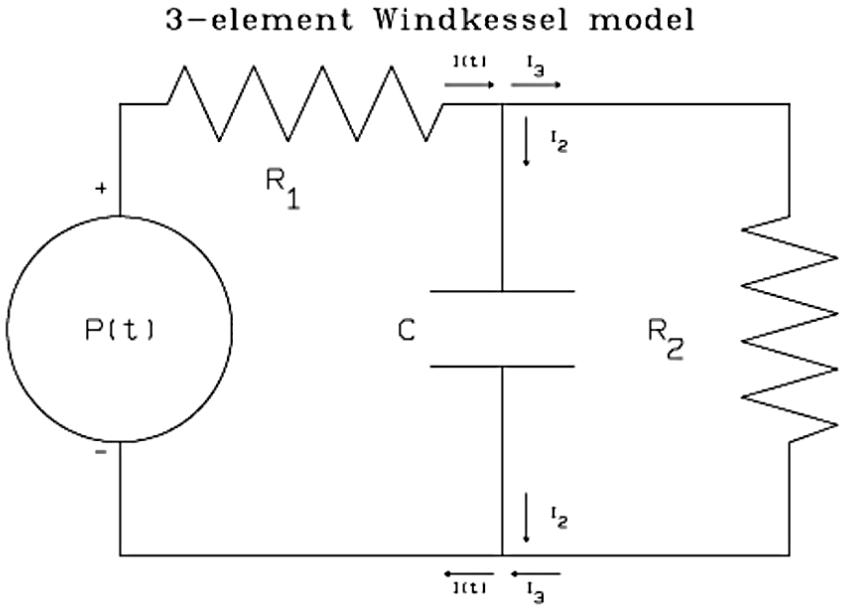

Figure 10 3-element Windkessel model [6].

In this system we can consider the input as being the current I(t), which is the equivalent of blood flow from the heart to the main arteries, P(t) or the potential corresponds to the blood pressure also in the main arteries and it is created by the battery, which is symbolically represented by the heart because it creates the pressure gradient, C represents the arterial compliance and, finally, R_2 is the peripheral resistance, while R_1 pretends to represent the resistance created due to cardiac valves (aortic or pulmonary). [6]

Thus, from this Windkessel model it's easier to understand the equation presented in chapter 2.8, which relates mean arterial pressure with cardiac output and peripheral resistance. From Ohm's law, the potential equals the product between resistance and current (Equation (2)).

$$V = R \times I \tag{2}$$

So, as said above, the potential of the circuit is the pressure, here represented by mean arterial pressure (MAP), and the current corresponds to the blood flow, which can be approximated to cardiac output since it is also the quantity of blood per time unit. Finally, joining the resistance of the circuit, which represents the peripheral resistance of the cardiac circulation, and replacing this three factors in the Ohm's law equation, one can obtain the analogue Ohm's law for the cardiac system presented in equation (2). Note that the presence of the capacitor was neglected since its resistance was not considered because it was assumed that it is an ideal capacitor and that this is a simplified model.

So, using the electrical circuit laws and using some known values for these parameters one can obtain a fully description of the cardiovascular system and even get values of parameters that are not possible to obtain easily such as the peripheral resistance. However, although this model is able to make a good representation of the cardiovascular system there are many other possible variations of Windkessel models with also good results [15].

3. State of The Art

3.1. Photopletysmography and Its Features

Being the blood pressure regulation failure the effective cause of syncope one can use the physiological parameters related to blood pressure, such as heart rate, vasodilation, stroke volume and others to detect the moment when de prodromal phase or even the syncope starts, and, eventually, to predict it. In order to do that, one can use the photoplethysmography (PPG) from where one can obtain various features that are correlated with these variables.

3.1.1. Photoplethysmography

Photoplethysmography or just PPG is a simple, non-invasive, low-cost and well-known method used to detect blood volume changes. It is an optical measurement technique whose principle is based on the interaction of light with biological tissues and, because of that, one light emitter and one photodetector (at least) are needed. However, this interaction is not simple and there are a few factors that affect the reception of light by the photodetector: the blood volume, the wall movement of blood vessels, the orientation of the red blood cells and even the amount of fat in the tissues. [16]

The most important issue that influences the quality of measurements from a PPG is the wavelength of the emitted light. So, this wavelength must be chosen considering three factors: avoid wavelengths that are absorbed by water, which is the main constituent of tissues, and melanin; use an isobestic wavelength, which is the wavelength that allows the signal not to be affected by the oxygen saturation, or in other words, the wavelength in, which oxyhemoglobin and reduced hemoglobin have the same absorbance (590 and near 800 nm); use a wavelength that provides a deep penetration in tissue. Thus, the red or near infrared wavelengths are the most used in photoplethysmography because they assemble these three conditions. [16]

From the PPG one can obtain a pulsatile signal like the one showed in Figure 11 identified as “digital volume” pulse or in Figure 12. Although the pulse waveform of the PPG is very similar to the arterial blood pressure waveform (compare the digital volume pulse with the radial pressure pulse in Figure 11), they are not the same wave and they have different features [17].

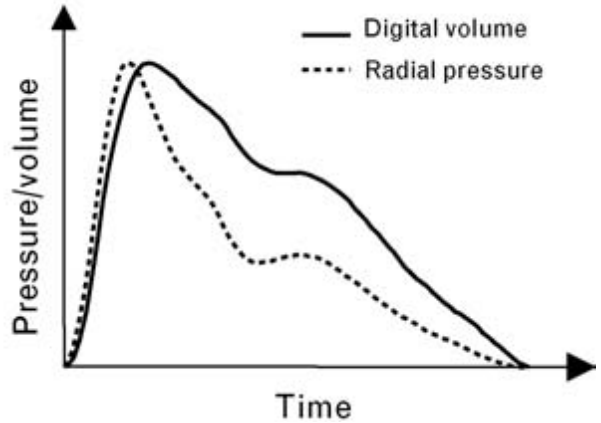

Figure 11 Comparison between the PPG pulse wave and the pressure pulse wave. [18]

In fact, the pulsatile component of PPG pulse wave, also known as “AC” component reflects the peripheral pulse and it is obviously synchronized with the heartbeat [16], while the “DC” component, which is indeed a slow varying component and composes the baseline of the signal is related to the respiratory and sympathetic nervous system activity and thermoregula-

tion [16] [19]. So, the pulse wave can be divided in two main parts: the rising edge or anacrotic phase, which is related to systole, and the falling edge, which is associated with diastole. In the latter phase there is usually a dicrotic notch (Figure 12), which results from the closure of heart valves after ventricular ejection.

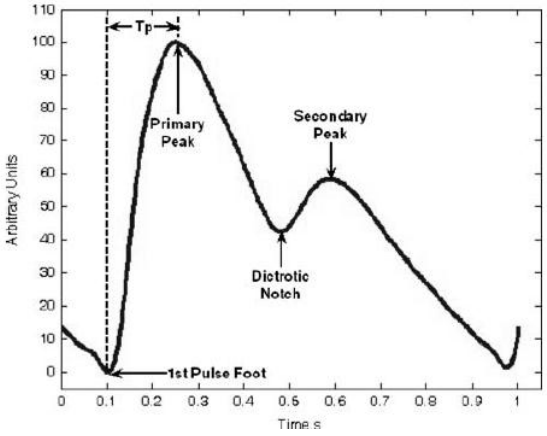

Figure 12 Normal PPG pulse wave. [20]

However, despite the similarity with arterial pulse wave and simplicity of the technique, the features from PPG pulse wave are not fully understood. However, there are already various features that have been documented and highly related with the operation of cardiovascular system and the autonomic control, which can be used as surrogates for the blood pressure changes. It is important to note that the PPG pulse waveform varies from subject to subject, mainly due to age, and it is very susceptible to movement artifacts like the ones caused by deep breathing and by probe movement [16].

For all these reasons, the photoplethysmography is a good method to acquire information to achieve our goal, i. e., to predict syncopes. As we have seen, every cause of syncope has a common factor, which is the failure in blood pressure regulation. Nevertheless we have also seen that blood pressure depends on resistance of the vessels, which is essentially affected by vasodilation, and on cardiac output, which is a function of heart rate and stroke volume. To determine this parameters one can use surrogates extracted from some of the features of the PPG, which are summarized in Figure 13 and will be further discussed in the next section.

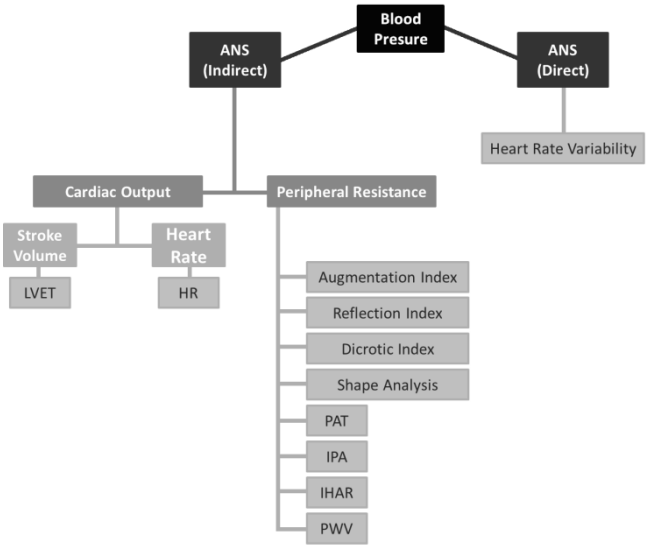

Figure 13 Schematic representation of the PPG features.

3.1.2. Heart Rate Variability (HRV)

The evaluation of heart rate is a reliable indicator of cardiovascular disorders [16]. Since the analysis of heart rate variability is based on the fact that the normal heart beat is not regular, the loss of heart rate variability can be an indicator sign of heart or vessel diseases [21] [22]. Besides that, knowing that heart rate is controlled by autonomic nervous system, a change in heart rate variability reflects a change in the modulation of the heart rate. For example, if the heart rate variability increases, this reveals an increase in the autonomic modulation, while low heart variability reflects a deficiency in the autonomic modulation [23].

In photoplethysmography one can have the pulse rate variability, which is an approximation to heart rate variability, and can be used as so [24]. Thus, the heart rate variability is the variance of the intervals between pulses and these fluctuations in heart rate reflect the influence of the autonomic nervous system in the cardiovascular system along time [21] [25]. However, when analyzing the heart rate variability, it is important to have in account that there are subject-dependent factors that influence HRV such as age and gender [26] [27].

The most used methods of analyzing the heart rate variability data are the time and the frequency domain analysis. In the frequency domain one can obtain a heart rate variability spectrum (Figure 14) by measuring the time intervals between instantaneous pulses and applying a frequency transformation to the obtained time series [16]. The normal spectrum has two peaks, one (centered near 0.1 Hz) corresponds to the sympathetic component of the heart rate, or the accelerating component, and the other (centered near 0.3 Hz) refers to the parasympathetic component, or the heart rate diminishing component [16]. The time domain analysis is simpler to make. Here there are two kinds of variables: the statistics derived from the interbeat intervals and statistics obtained from the differences between sucessive intervals [23].

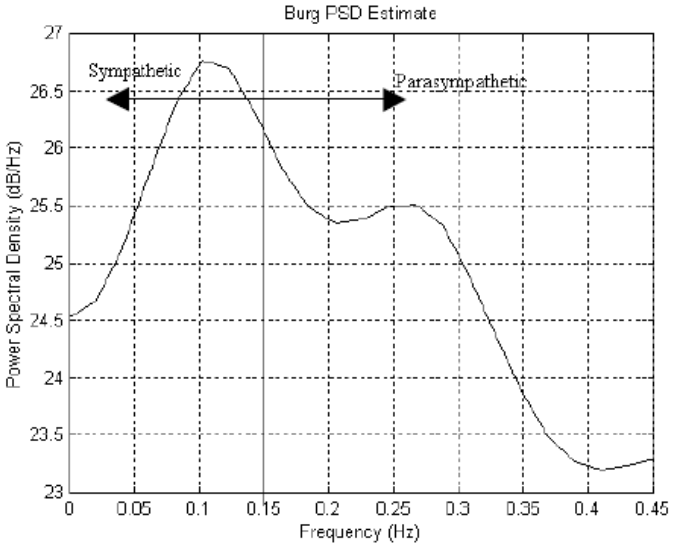

Figure 14 Spectrum of the frequency domain analysis of a normal PPG pulse. [28]

3.1.3. Pulse Wave Velocity (PWV)

During systole, the pressure in the aorta increases. Although this increase in pressure is not transmitted instantaneously, this creates a pressure pulse that travels along the arterial tree at a given speed. This speed is known as the pulse wave velocity [18] and there are different ways of measuring it. For example, one can place two probes in different body sites and recording both the photoplethysmographys at the same time, another example consists in recording the pulses at different sites, but comparing the time delay with the QRS complex of the ECG, which is also recording simultaneously [29].

An important concept that is associated with pulse wave velocity is the pulse transit time (PTT), which is the time that the pulse wave takes to travel from the heart to the local of the photoplethysmography measurement in the periphery. This can be achieved dividing the pulse wave velocity by the distance traveled by the pulse waveform, but it can also be approximated by the time delay between the two peaks of the PPG waveform (Pdelay in Figure 15) [18].

Pulse wave velocity provides information about the dilation of the vessels and BP and can be calculated in two different ways. The Moens-Koerteweg equation (equation (3)), uses the Young's modulus of elasticity of wall material (E), the wall thickness (h), the inside radius of vessel (r) and the density of blood (ρ), the Bramwell-Hill equation (equation (4)) relates pulse wave velocity to distensibility (D) using the relative volume elasticity of the vessel segment ($\frac{\Delta PV}{\Delta V}$) and the blood density (ρ) [30].

$$PWV = \sqrt{\frac{Eh}{2r\rho}} \tag{3}$$

$$PWV = \sqrt{\frac{\Delta PV}{\Delta V \rho}} = \sqrt{\frac{1}{\rho D}} \tag{4}$$

From equation (4) it is easy to see that if the distensibility decreases, for example with vasoconstriction, the pulse wave velocity increases.

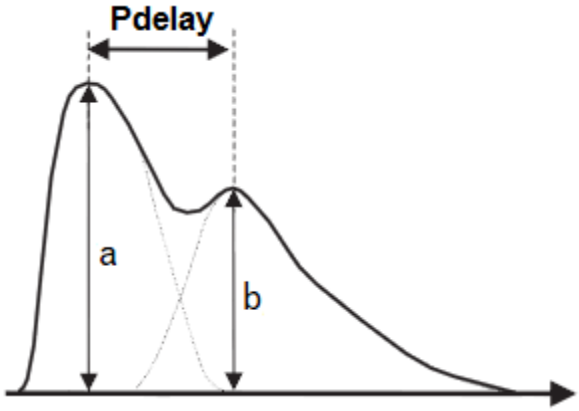

Figure 15 Pulse delay (Pdelay) between the two peaks of the PPG pulse wave. Adapted from [18].

However, the parameters needed to calculate the pulse wave velocity with the above equations are not easy to determine. So, if we have the pulse transit time, or at least the time delay between the two peaks of the PPG pulse, one can use a surrogate for measuring the pulse wave velocity, the stiffness index (SI), which can be calculated with equation (5), where H is the subject's height [31].

$$SI = \frac{H}{Pdelay} \tag{5}$$

As reference, for a normal subject the pulse wave velocity is 690±297 cm/s if it is male and 577±171 cm/s if it is female [32].

3.1.4. Left Ventricular Ejection Time (LVET)

The left ventricular ejection time is the duration of time that blood takes to flow out of the heart [33]. It is dependent of ventricular contractility and because of that is correlated with stroke volume (Figure 16) [33]. Nevertheless, it is also associated with heart rate since both affect the

duration of cardiac cycle. Thus, if the heart rate increases, LVET tend to decrease as shown in Figure 17, however, this dependency can be eliminated by using normalized LVET.

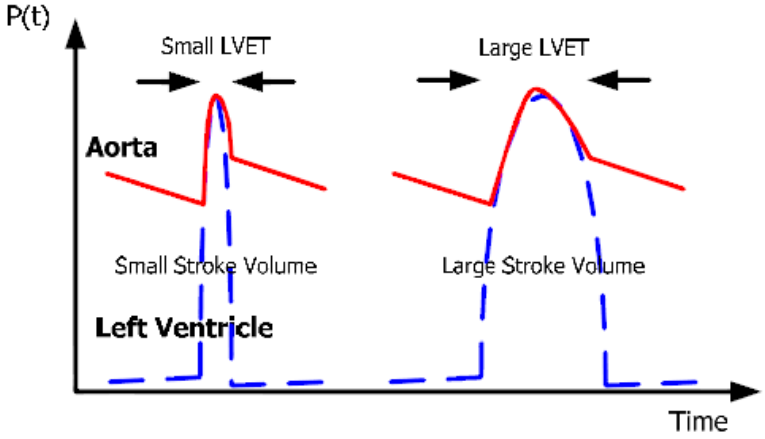

Figure 16 Comparison of stroke volume with LVET. [33]

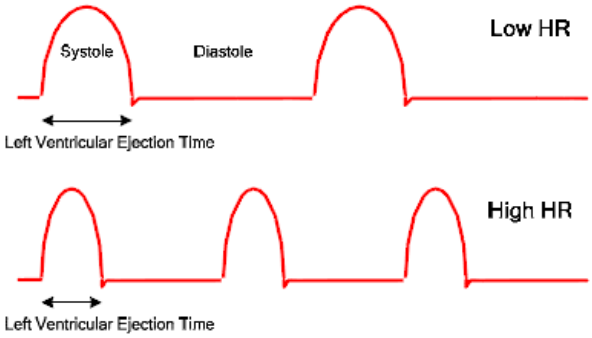

Figure 17 Comparison of heart rate with LVET. [33]

Since LVET is not affected by changes caused by the arterial tree, one can obtain it directly from a PPG [34]. LVET corresponds to the time interval from the onset to the end of ventricular ejection estimated from PPG first derivative (Figure 18). [35]

3.1.5. Pulse Arrival Time (PAT)

Pulse arrival time is defined as the time interval between the R-peak of the ECG and the arrival of the arterial pulse wave at periphery, as seen in Figure 18, more precisely to the local where measurements are made. This includes the sum of the pre-ejection period, which is the isovolumetric ventricular contraction phase, and the pulse transit time [36]. PAT can be a good estimator of blood pressure, since they are correlated, especially with the systolic blood pressure. In fact, an increase in blood pressure leads to a decrease in arterial compliance and, consequently, to a decrease in PAT and vice-versa, which reveals that PAT is inversely related with blood pressure [37] [38] [39].

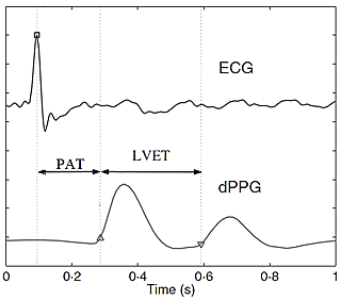

Figure 18 Representation of an ECG and the first derivative of a PPG pulse. Adapted from [35].

3.1.6. Inflection Point Area Ratio (IPA)

The inflection point area ratio, IPA, is a recent revealed feature of photoplethysmography and it is associated with pulse wave reflection, which results from the impedance difference between the arterial system constituents and, therefore, with vasoconstriction. Thus, knowing that the area ratio of the second and first peak in the PPG wave is mainly influenced by the strength of pulse wave reflection, this feature is a clear indicator of the vessel dilation. So, IPA is given by the ratio of the areas of each peak:

$$IPA = \frac{S_2}{S_1} \tag{6}$$

Where S_1 and S_2 are the areas of each peak, as shown in

*Figure 19*a. Hence, if arteries contract, the total peripheral resistance will change (in this case will increase), which will change the impedance mismatch and further change IPA. [40]

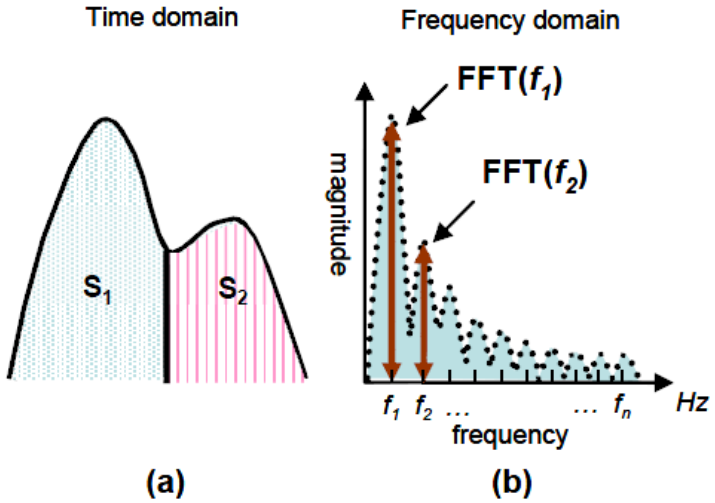

Figure 19 Domains of a pulse from a PPG. a) Time domain; b) Frequency domain. [40].

3.1.7. Inflection and Harmonic Area Ratio (IHAR)

The inflection and harmonic area ratio is also a recent feature, which also reproduces the pulse wave reflection as a result of the impedance mismatch in the arterial system. Because of that, it is highly related with cardiac output and, therefore, with blood pressure. IHAR is a parameter derived from the frequency domain analysis of the PPG pulse wave (

*Figure 19*b). It can be calculated dividing the normalized harmonic area by IPA.

$$IHAR = \frac{\sum_{n=2}^{N} FFT^2(f_n) / \sum_{n=1}^{N} FFT^2(f_n)}{IPA} \tag{7}$$

Where $FFT^2(f_n)$ is the square of the magnitude at the n^{th} harmonic. [40]

3.1.8. Dicrotic Index

In the PPG, the dicrotic notch is the minimum of the depression between the two main peaks (the systolic wave peak and the reflected wave peak) as represented in Figure 12. This point is the result of the pressure produced when the aortic valves close at the end of left-ventricular ejection, which is transmitted along the circulatory path [41], but it is also related to the reflected wave from the periphery, which makes that this point becomes clearly influenced by vasodilation [42]. Thus, the incisura rise with vasoconstriction and with the age as the result of the loss of elasticity in the vessels to a point that can be visually indistinguishable because both of two peaks appear to join in a single one. On the other hand, with vasodilation the dicrotic notch tends to decrease, separating the two main peaks of PPG [18].

3.1.9. Reflection Index (RI)

When the pressure pulse travels along the arterial tree, a part of it is reflected backwards in different points of the systemic vasculature. Nevertheless, the arterial system acts as if a single wave is reflected back from the lower body [18].

As seen in the dicrotic index section, the dicrotic notch and, consequently, the existence of the second peak in the PPG pulse wave is directly related to the reflection of the pulse wave in the arterial system, and also to vasodilation. So, a reflection index can be defined as the ratio of the amplitude of the reflected wave (b in figure Figure 15) to the amplitude of the first peak (a in Figure 15), as seen in equation (8). An important fact is that the effects of vasodilation in reflection index can be firstly detected than alterations in heart rate or blood pressure. [18]

$$RI = \frac{b}{a} \tag{8}$$

However, RI is highly dependent of the detection of the second peak, which is not always possible since the second peak is less pronounced with age. Besides that the RI determination is dependent of temperature since it changes the vasodilation of vessels, which can also change the amplitude of the PPG second peak [43] [31].

3.1.10. Augmentation Index (AI)

The augmentation index of photoplethysmography is another feature that is related to vasodilation and peripheral resistance of the circulatory system. It is defined as the ratio of the late systolic peak to the early systolic peak in the pulse [44]. So, the augmentation index can be calculated with the following equation:

$$AI = \frac{PT_2 - PT_1}{MA} \tag{9}$$

Where PT_2 is the height of the second systolic peak, PT_1 is the height of the first systolic peak and MA is the maximum amplitude of the pulse, as represented in Figure 20. As reference, augmentation index calculated for a normal subject is 0.252 ± 0.09 for subjects with ages in the interval of 57 ± 6 years [44]. So, augmentation index increase is associated to vasoconstriction increase, on the other hand with the increase in vasodilation, the augmentation index decreases [45] [46].

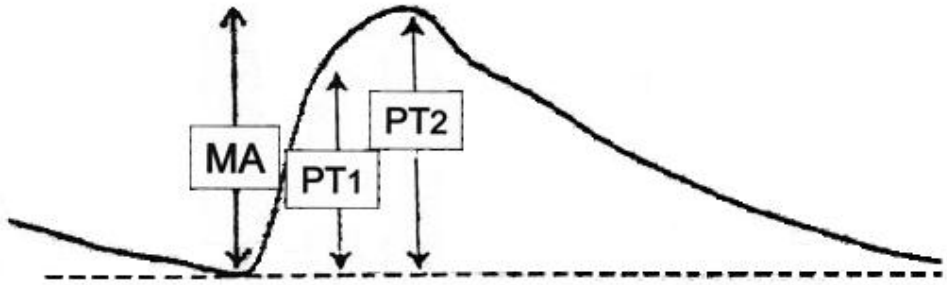

Figure 20 A pulse wave from a PPG signal. Adapted from [44].

3.1.11. Shape Analysis

All the PPG pulses had common features such as the systolic rising edge or the dicrotic notch. Knowing that the PPG pulse is correlated to the real pressure pulse, it reflects the alterations of the cardiac system. Some of these alterations have already been seen such as the dicrotic notch position, which varies with the vessel dilation. However there are other conclusions that can be taken from the pulse shape of PPG. It is known that the amplitude of the

pulsatile component of the PPG is influenced by respiration, sympathetic nervous system activity and temperature (cold acts as vasoconstrictor, which leads to reduced amplitude, while heat has the opposite effect, dilating the vessels). Furthermore, it is also known that age has great influence in the PPG pulse shape.

In fact, the pulse wave of a PPG can be classified in terms of its shape, which is presented in Figure 21. As can be observed, in class 1 the dicrotic notch is clearly visible; in class 2 the dicrotic notch is lost and the incisura becomes horizontal; the class 3 has no notch, but there is a visible angle change in the descent part, however in class 3-bis the first systolic pulse is separated from the second one; the fourth class has no notch and there is no visible angle change in the descent part of the pulse. While the class 1 is usually associated to young individuals, the class 4 is prevalent in older ages or in individuals with coronary artery diseases, since it is a typical pulse of high artery stiffness or reduced compliance.

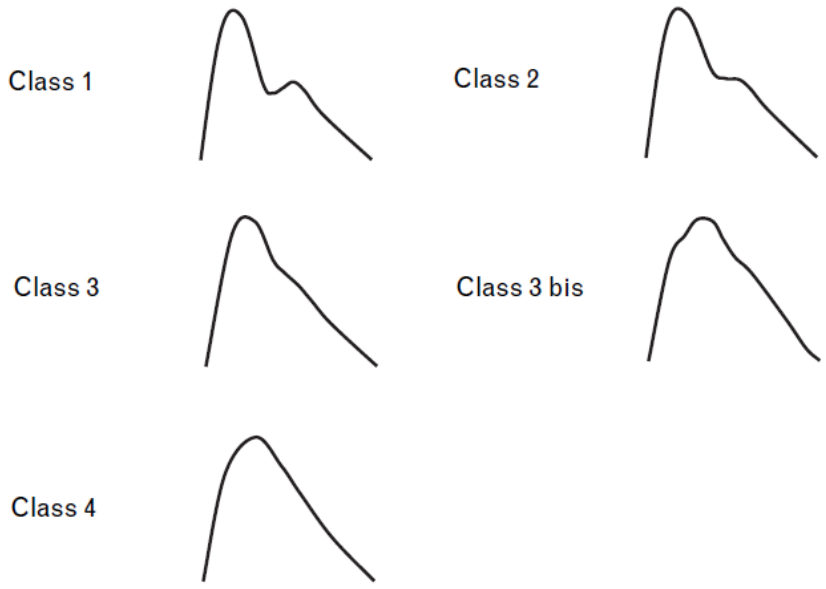

Figure 21 Different types of PPG pulses. [18].

The relevance of age in the pulse wave shape can be achieved with the second derivative of pulse wave (Figure 22), from where one can obtain the age index, which is given by:

$$age\ index = \frac{b - c - d - e}{a} \tag{10}$$

Where a, b, c, d and e are the heights of each wave in the second derivative of the photoplethysmography pulse. Apart from that the relative heights, b/a, c/a, d/a and e/a are also related to arterial blood pressure and artery stiffness. [18]

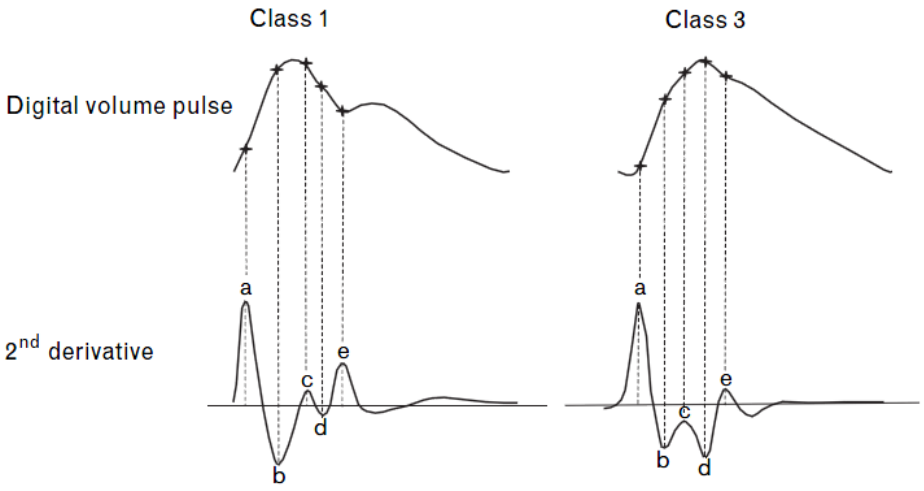

Figure 22 Comparison between two different PPG pulses to their second derivative. [18]

3.2. Blood Pressure from PPG

As seen before, a faint can be caused by a decrease in systolic blood pressure, which is a process that can be tracked in order to predict a syncope episode. However, current methods to monitor blood pressure are invasive or are not easy to wear, which means that another solution has to be found. Using already existing signals, like PPG and ECG, is a well known way of achieving BP surrogates. Moreover, these signals offer continuous measurement, low complexity and the devices to acquire them are easy to wear. This chapter is an overall review of the existent techniques of tracking blood pressure from PPG signals.

Although the pulse wave shape of the PPG is very similar to the blood pressure wave, it is not the same wave. In fact, they are correlated, but there is no consensus if this correlation is static or dynamic. Nevertheless, it is easy to understand that while in the PPG one obtain a wave where the amplitude is an electric potential from the PPG sensor, in the blood pressure curve the amplitude is a completely different physical quantity, the pressure, which can be argued with the fact that the PPG is the BP transformed by optical and vascular factors.

However, some authors have been trying to obtain the exact blood pressure from the PPG and other hardware such as accelerometers. Although the results are consistent with the blood pressure measurements through the conventional ways, the fact that the system is composed of additional hardware is a relevant drawback [47]. So, the more consensual way of accessing to BP using PPG is through computational methods using some of its features. In this case there is a wide range of possibilities starting with the determination of a transfer function obtained by Fourier transforms of the PPG pulse to obtain the BP one [48]. The possibility of using neural networks was also studied, but an individual calibration for each subject was needed as well as controlled laboratory conditions, which are not convenient for a practical usage [49].

More recently, several other methods have been used. One of them is the relation between the pulse amplitude of the PPG that has been studied in different ways, such as the width of the pulse at different portions of its amplitude. These gave promising preliminary results, but a validation of the method in patients with cardiovascular pathologies has to be carried out [50]. Another strategy is related to the amplitude of the pulse by itself, which has also a correlation with the blood pressure. There are authors who even argue that it is a better way of tracking the blood pressure than the PAT, although this is not consensually proved [51] [52].

One of the most used methods of accessing the blood pressure, mainly the SBP, is the PAT. As described above, this method needs an ECG measured at the same time as the PPG and it has been studied by several authors who concluded that there is a linear relationship

between PAT and BP in under specific conditions, e.g. during and after physical exercise. The potential of this technique is attested by the amount of literature available and the number of studies that has been done. Those are the reasons why the PAT was the feature chosen for the purpose of this thesis, to predict critical blood pressure changes that can cause a syncope [37] [38] [51] [53].

However, it is important to mention that PAT is actually the sum of the PTT and the pre-ejection period PEP. PTT is more directly related to blood pressure as discussed by equation (3) and (4), whereas it has been shown that PEP can vary even independently of Blood Pressure [53].

$$PAT = PTT - PEP \tag{11}$$

To compensate PEP contributions an alternative measurement has to be used, like the impedance cardiogram, heart sounds or echocardiography, and, therefore, is not as simple as using only the PAT. It has been also shown that PTT, e.g. during physical exercise, does necessarily correlate with BP [54] [53].

3.3. PPG Signal Processing

In order to extract the features needed to achieve our goal, several processing techniques must be designed. The first important fact to bear in mind is that the PPG signal is very subjected to noise and motion artifacts, which should be removed in an efficient way, but at the same time trying to keep the important information that can be present in the corrupted segments. Besides, features like PAT or HR are in a beat-to-beat domain, which means that a segmentation of the pulses should be implemented.

The filtering and motion artifacts removal of PPG signals is clearly a growing field, not only because of the need for faster and more effective filtering techniques in physiological measurements, but also due to the increasing usage of this signal particularly in personal health systems. These facts led the scientific community to test several techniques, such as singular value decomposition methods to extract the principal components of a signal, although it is not a very fast algorithm [55]. Principal component analysis using the covariance matrix and reconstructing the signal with the components of interest [56] [57] is another used technique, as well as the usage of wavelets transforms to decompose the signal and reconstruct it without the noise or motion artifacts components [58] [59]. Time-frequency methods, like pseudo Wigner-Ville distributions or Fourier series analysis based on the principle of periodicity of the PPG pulses [60] [61] [62], were also used offering good results, but being too complex for our purpose. Other possibilities regarding techniques based on least mean square errors, have been also studied, such as creating an artificial noise reference signal based in features from the original signal in order to detect the corrupted segments, or using accelerometers to generate that reference [63] [64] [65]. Finally, there is also reference to independent component analysis methods, if an independent relation between noise and signal is considered [66]. Besides that, it is important not to forget the filtering techniques, which can be a small part of the algorithms mentioned above, where they were only used to remove high or low frequency noise, but they can also compose entire methods to remove noise and even motion artifacts [67] [68].

Apart from the filtering and motion artifacts removal there is also the need for pulse segmentation in order to extract the features in a continuous way. There are some possible approaches in the literature that can be used. One of the most simple is finding the peaks and the valleys of the pulses using a thresholding method of the entire or, at least, long segments of the PPG record, which can be a fast algorithm, but it is highly affected by baseline fluctuations or even amplitude changes of the pulses [69]. Zhang et al. used wavelet transform to identify the characteristic points of the pulse waveform [70] and Aboy et al. tried a more simple methodology based on nearest neighbour criteria [71]. However, both of the algorithms are not very flexible, since they don't take into account the different types of pulses that can be caused by pathological or age reasons or even slightly corrupted ones. After a filtering procedure to

remove high and low frequency components, Couceiro et al. also used a different segmentation approach with the first and the third derivatives of the PPG in which the most significant local maxima and minima were chosen, respectively [72]. Another possible solution involves the creation of an analysis window, which has approximately the same duration of the pulse period, then, the segmentation is evaluated with comprehensible criteria like the number of peaks, for example. In case of an incorrect segmentation, another window is calculated and the process is repeated until a correct segmentation is achieved [73]. The last algorithm, although it was developed for BP pulses, offers very good results also in PPG with sensitivity and positive predictive accuracy of more than 99% with a simple implementation. This algorithm can be divided in 3 steps: low pass filtering in order to remove the high frequency noise, a slope sum function that enhances the upslope of the pulses and a decision rule, which is used to find the pulse onset of that slope sum function, which has to be compensated to match the original signal, due to the phase shift caused by the low pass filter [74].

3.4. Syncope Prediction

There are not too many studies about fainting prediction independently of the type of syncope that is involved. Besides, the majority of work that has been done in this field does not use the same signals that are going to be described in the following chapters. Some authors use the arterial blood pressure or systolic blood pressure that are very reliable measurements, but there is no comfortable way for continuously measuring them, not allowing them to be used in a personal health scenario. So, not surprisingly, the specificity and sensitivity were about 80% on a dataset with 80 patients [75] and 95% in another study with 1155 patients [76]. Another method using heart rate variability achieved very good results, although the tests were performed only with healthy subjects with no cardiovascular disease or even unstable heart rate [77]. The possibility of using neural networks it has been studied as well, however, it requires more computational effort than using simple techniques like thresholding [78].

Finally, there is another way of achieving the goal of syncope prediction. This method requires the extraction of PAT and HR from PPG and ECG, since the heart rate tends to decrease before syncope. In a primary stage, only the PAT was taken into account and then the algorithm was improved adding the HR variability information, which improved the sensitivity and specificity, although it reduced the prediction times. In the first case, the prediction time for the patients who effectively fainted varied between 41 and 724 seconds, while in the second the range is between 16 and 337 seconds. Attending to the results and to the fact that only 14 patients were tested (7 with syncope and 7 without syncope), there is a need to test the algorithm with more subjects, but, still, this study shows that there is a high potential in this technique and for that reason it will work as a base for the syncope prediction part of this thesis [79].

4. Methods

This chapter describes the developed algorithms that were used in this project. Besides, to test these algorithms two databases were used and are also described in this section. One contains PPG signals from patients of an intensive care unit and the other contains data from a HUT test in which PPG, ECG, BP and the position of the patient were acquired.

The first algorithm was used to detect the relevant points of the PPG, such as the peak and the onset. The sensitivity of the algorithm was 94.81% and 91.91% for onsets and peaks, respectively. The specificity was 95.77% and 99.38% for onsets and peaks respectively. Then, two other algorithms were used to extract the pulse amplitude, the PAT and the HR from the PPG and ECG signals. After the feature extraction, there was a need for artifact removal from the extracted features and this was done in two different ways, despite only the one with the best performance (optimal values of 80.17% and 76.71% for sensitivity and specificity, respectively) were chosen to integrate the final algorithm.

Finally, since our goal is to predict faints, a syncope predictor was also developed based on an already existent methodology. The optimal value that was obtained for sensitivity was 95.24%, for the specificity 83.33%, for positive predictive value 82.61 and the best average prediction time was 109.97 seconds.

For further details see appendix A.6.

5. Conclusion

From the results obtained in the last chapter, the best value for the specificity is 83.33%, for the sensitivity 95.24%, which corresponds to a syncope prediction of 20 cases from a total of 21 existent in the dataset, and for positive predictive value 82.61%. These are good indicators of the feasibility of this algorithm. Moreover, the general prediction times are long enough for the purpose of this algorithm, which is to avoid the consequences of a sudden syncope episode. The success of these results is influenced by every step of this work, which was chosen and developed with the intent of having the best performance as possible and trying to avoid the maximum number of limitations, but at the same time keeping in mind that the simpler the algorithm, the easier to use it in a daily life application.

Regarding the beat detection and pulse segmentation we have seen that while the top of the pulse is easily distinguishable by eye and through computational methods (the worst sensitivity and PPV achieved were 88.78% and 96.14%, respectively), the same does not happen with the foot of the pulse (83.22% and 91.58%, respectively). This issue affects the ability of the PAT foot in tracking BP drops and, consequently, reduces the performance of the prediction. So, in order to improve the performance of this PAT, the onset detection might be made in a different way such as the ones previously described in the state of the art. Still, with the other pulse points, the problem of the inaccuracy is attenuated, which results in more reliable PATs and, consequently, better specificity and sensitivity for the prediction alarms. Although the general prediction times from this features are shorter than with the PATfoot partially due to the delay between the foot of the pulse and the other points.

Although the PAT is well known as a surrogate of the BP and it worked properly in this case, the HR variability might also be used to help identifying a critical blood pressure change since the HR often decreases before a faint and it has been proved that it can improve the effectiveness of the prediction algorithm. However, introducing more features to analyse in the algorithm will increase the computational effort, despite it might help to increase the robustness when the signals are corrupted by motion artifacts. Furthermore, the pulse amplitude was also taken into account to use, however we have seen that in most of the cases any change of pulse amplitude is visible together with the decrease in SBP. In the two records where a variation is seen it is a negative variability while, theoretically, was expected an increase, since when the BP drops the vasoconstriction tries to compensate, which is reflected in the amplitude increase of the pulse, therefore, this feature was discarded.

The next step was to remove the influence of motion artifacts from the features since they affect their reliability. An algorithm based on the HR comparison of the ECG and PPG was developed showing better results than the simple threshold method developed before. Despite the improvement on the performance, this algorithm has also its limitations since the ECG is used as reference and, although this signal is less prone to artifacts than the PPG, it can also be affected by them, and when that happens the removal is not well performed, which creates corrupted values in the extracted features. Along with this limitation we have seen that after the removal of corrupted values, long segments without data remain, which might compromise the tracking of the increase of the PAT. Other possibilities could be taken into account, in the literature we have seen more complex approaches, which can work properly but need a lot more computational effort. However, there are also simpler ways of dealing with noise and motion artifacts, such has filtering and/or thresholding the input signals, instead of doing it after the feature extraction, as we did. This might offer a major advantage since after the signal processing, there might be no need for a cleaning procedure in the extracted features. However, processing the input signals is much more complicated since the signals have a complex periodic shape comparing with the linear behaviour of the PAT or HR. Besides, the changing of the signal shape can influence the values of the features extracted from them generating values that do not correspond to the real parameters.

The problem regarding all the filtering techniques is that nothing ensures that a long segment without data cannot be generated not only by normal moves in a daily life activity, but also during the increase in PAT, when there are a lot of motion artifacts caused by the natural reaction of trying to move when the presyncope symptoms appear. So, in order to avoid that the prediction times are affected by these segments we have seen that an interpolation of 2 Hz can solve this issue, since it easily allows tracking the increase of PAT.

Still in the chapter of the artifacts removal, some interesting conclusions can be taken. The computed spectrum for each PAT (Figure 35, Figure 36, Figure 37, Figure 38 and Figure 39) has the same behaviour of the frequency response of an integrator, whose transfer function, H(s), is given by:

$$H(s) = \frac{k}{s} \tag{12}$$

From this transfer function one can create a system that models the relation between the failure of BP regulation mechanisms and the increase in PAT (or decrease in BP). In fact, the PAT increase (Figure 30, Figure 31, Figure 32, Figure 33 and Figure 34) is also similar to the step response of an integrator (Figure 23). Thus, if we consider a Heaviside function where the step represents the failure of the BP regulation mechanisms, it might be possible to find the exact moment of this failure with this model and the PAT behaviour.

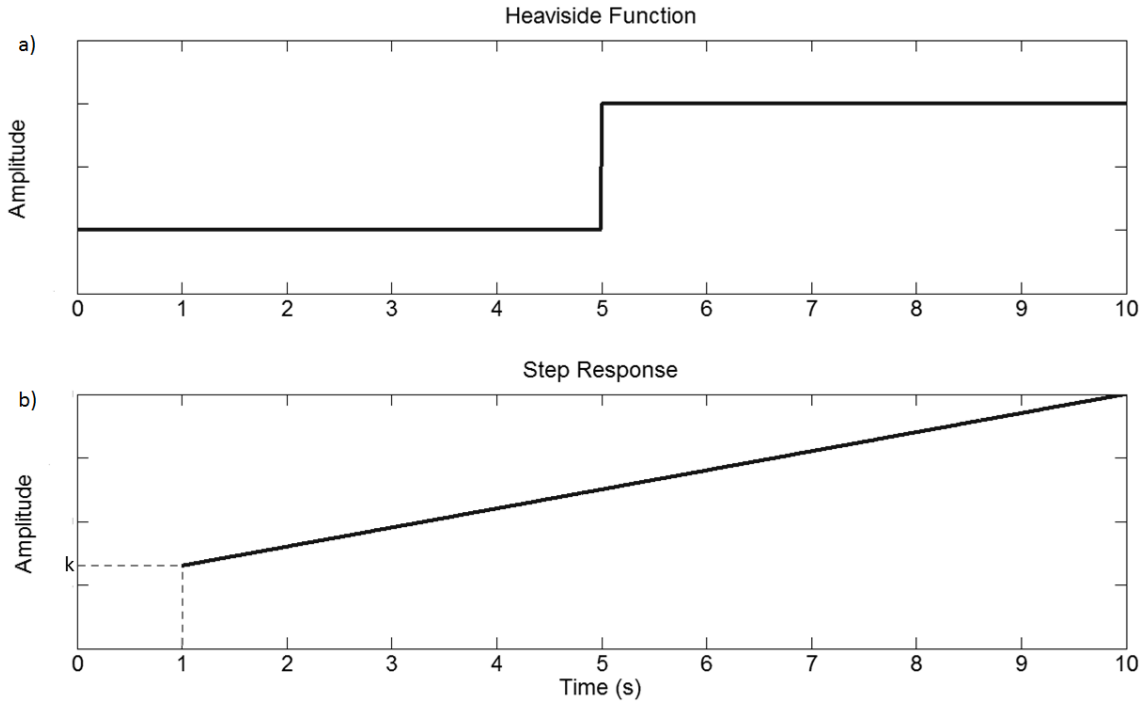

Figure 23 Representation of a step function (a) and of the step response of the integrator from equation (12) (b).

This might be a topic for further investigation in order to improve the detection of this failure, or to model it, which might be useful in understanding this phenomenon and improving the treatments for syncope.

Finally, we reached the syncope prediction algorithm based on the normalized PAT. The introduction of the normalized PAT brings some issues that can influence the final results. The PATref adds an additional error to the normalized PAT (Section A.5). So, redefine the place to acquire the PATref in a more stable situation, or at least in a later position after up tilt or even before, it is a good way of reducing the variance and improve the performance since in the actual situation the PATref is occasionally acquired during an adaptation phase of the BP to the standing position.

It is important to refer that in a real time situation there are no annotations of the posture changes, which means that there is no baseline to use as reference to measure the PATref. In a future real-time application this issue might be overcome by monitoring the patient at a resting position during a short period of time where the PATref can be acquired in a baseline situation with the minimum variance of the PAT.

Resuming, in Figure 24 there is a flowchart representing an overview of all the steps of the algorithm. Starting with the input data and resulting in an alarm generation in case of an impending syncope.

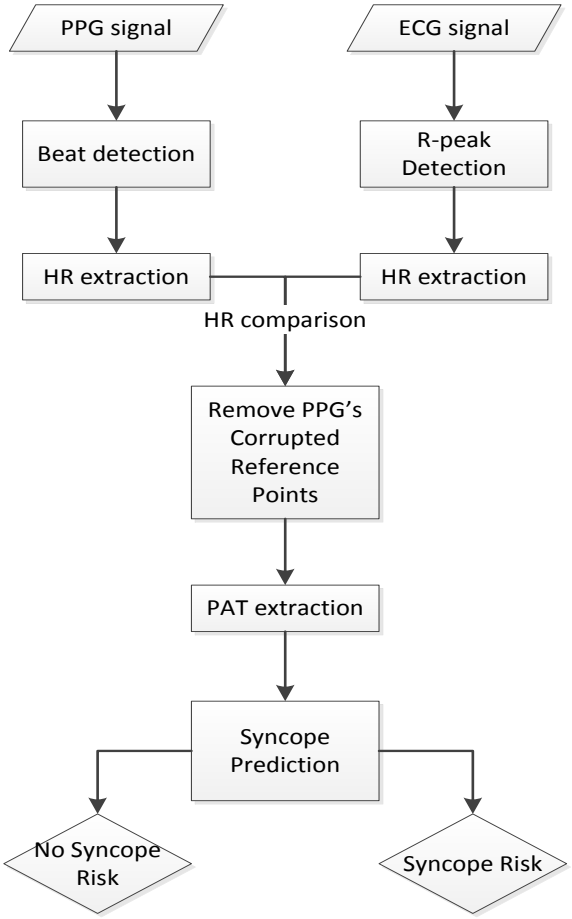

Figure 24 Flowchart with an overview of the produced algorithm.

In order to optimize the thresholds, or even find a better algorithm for prediction using additional features such as the heart rate or maybe the pulse amplitude, there are some researches that can still be done. In fact, it might be possible to improve every step of the algorithm, since all of them have their own limitations. Besides, the implementation in a real time device and the testing with the signal processing and prediction made at the same time as the signal is acquired are tasks to be realized.

Finally, the definition of optimal threshold is relative; in this work the optimal values were considered the ones that have the best relation between maximizing true positive rate and minimizing the false positive rate. However, if it is preferred to have a conservative algorithm, in order to increase the number of true positives, despite the reduction in true negatives, the optimal thresholds will be certainly different. Along with this, and despite the average of prediction time is enough for taking syncope preventive actions, if the priority is to have the longest prediction times as possible, it is also possible to increase them by reducing the threshold, which might compromise a good specificity.

This work proved that a real time and continuous monitoring of patients who suffer from recurrent syncope can be achieved using simple methodologies and already existent technologies. This might help to improve the quality of life of these patients, since the injuries and the discomfort of being constantly concerned about the possibility of a syncope episode to occur can be avoided. All of this using devices with low producing costs and comfortable enough to wear in daily life. However, some work has still to be done, starting with a refining of the segmentation, artifacts removal and syncope prediction algorithms, adapt and test the algorithm to work with real-time acquisition data, and, finally, evaluate the possibility of using some of the features that were described in the beginning of this work for syncope prediction.

6. References

[1] G. J. Tortora and B. Derrickson, Principles of Anatomy and Physiology, 12 ed., John Wiley & Sons, 2009.

[2] S. S. Mader, Understanding Human Anatomy and Physiology, 5 ed., McGraw-Hill, 2004.

[3] D. E. Mohrman and L. J. Heller, Cardiovascular Physiology, 7 ed., McGraw-Hill, 2010.

[4] W. Purves, D. Sadava, G. Orians e C. Heller, Life: The Science of Biology, 7 ed., Sinauer Associates and W. H. Freeman, 2003.

[5] R. E. Klabunde, Cardiovascular Physiology Concepts, 2 ed., Lippincott Williams & Wilkins, 2011.

[6] D. R. Kerner, "Solving Windkessel Models with MLAB," 2008.

[7] J. J. Van Lieshout, W. Wieling, J. M. Karemaker and N. H. Secher, "Syncope, Cerebral Perfusion and Oxygenation," *Journal of Applied Physiology,* vol. 94, no. 3, pp. 833-848, 2003.

[8] D. G. Benditt, M. Brignole, A. Raviele and W. Wieling, Syncope and Transient Loss of Consciousness, Blackwell Futura, 2007.

[9] R. Hainsworth, "Pathophysiology of Syncope," *Clinical Autonomic Research,* vol. 14, no. 0, pp. i18-i24, 2004.

[10] W. Wieling, R. D. Thijs, N. van Dijk, A. A. M. Wilde, D. G. Benditt e J. G. van Dijk, “Symptoms and signs of syncope: a review of the link between physiology and clinical clues,” *Brain - A Journal of Neurology,* n.º 132, pp. 2630-2642, 2009.

[11] A. Moya, R. Sutton, F. Ammirati, J.-J. Blanc, M. Brignole, J. B. Dahm, J.-C. Deharo, J. Gajek, K. Gjesdal, M. Massin, M. Pepi, T. Pezawas, R. R. Granell, F. Sarasin, A. Ungar, J. G. Van Dijk, E. P. Walma and W. Wieling, "Guidelines for the Diagnosis and Management of Syncope," *European Heart Journal,* vol. 30, no. 21, pp. 2631-2671, 2009.

[12] B. P. Grubb, The Fainting Phenomenon, 2 ed., Blackwell Futura, 2007.

[13] B. P. Grubb and B. Olshansky, Syncope: Mechanisms and Management, 2 ed., Blackwell Futura, 2005.

[14] G. Chang, "Early Detection of Blood Loss Using a Noninvasive Finger Photoplethysmographic pulse oximetry waveform," 2008.

[15] X.-Y. Zhang e Y.-T. Zhang, “A Model-based Study of Relationship Between Timing of Second Heart Sound and Systolic Blood Pressure,” em *Conf Proc IEEE Eng Med Biol Soc.*, 2006.

[16] J. Allen, “Photoplethysmography and its application in clinical physiological measurement,” *Physiological Measurement,* vol. 28, n.º 23, 2007.

[17] A. M. D. Reisner, P. A. Shaltis, D. McCombie e H. H. Asada, “Utility of the photoplethysmogram in circulatory monitoring,” *Anesthesiology,* vol. 108, n.º 5, pp. 950-958, 2008.

[18] S. C. Millasseau, J. M. Ritter, K. Takazawa e P. J. Chowienczyk, “Countour analysis of the photoplethysmographic pulse measured ate the finger,” *J Hypertens,* vol. 24, n.º 8, pp. 1449-1456, 2006.

[19] Z. Marcinkevics, S. Kusnere, J. I. Aivars, U. Rubins e A. H. Zehtabi, “The shape and dimensions of photplethysmographic pulse waves: a measurement repeatability study,” *Acta Universitatis Latviensis,* vol. 753, pp. 99-106, 2009.

[20] E. Zahedi, K. Chellappan, M. A. M. Ali e H. Singh, “Analysis of the effect of ageing on rising edge characteristics of the photoplethysmogram using a modified Windkessel model,” *Cardiovasc Eng,* vol. 7, n.º 4, pp. 172-181, 2007.

[21] H. M. Stauss, “Heart rate variability,” *AJP- Regu Physiol,* vol. 285, pp. 927-931, 2003.

[22] K. Srinivas, L. R. G. Reddy e R. Srinivas, “Estimation of hear rate variability from peripheral pulse wave using PPG sensor,” em *3rd Kuala Lumpur International Conference*, Kuala Lumpur, 2007.

[23] P. K. Stein e R. E. Kleiger, “Insights from the study of hear rate variability,” *Annual Review of Medicine,* vol. 50, pp. 249-261, 1999.

[24] E. Gil, M. Orini, R. Bailón, J. M. Vergara, L. Mainardi e P. Laguna, “Photoplethysmography pulse rate variability as a surrogate measurement of heart rate variability during non-stationary conditions,”

Phyisiological Measurement, vol. 31, pp. 1271-1290, 2010.

[25] P. Shi, Y. Zhu, J. Allen e S. Hu, "Analysis of pulse rate variability derived from photoplethysmography with the combination of lagged Poincaré plots and spectral characteristics," *Medical Engineering & Physics,* vol. 31, n.º 7, pp. 866-871, 2009.

[26] I. A. D. O'Brien, P. O'Hare e R. J. M. Corrall, "Heart rate variability in healthy subjects: effect of age and the derivation of normal ranges for tests of autonomic function," *Br Heart J.,* vol. 55, n.º 4, pp. 348-354, 1986.

[27] K. Umetani, D. H. Singer, R. McCraty e M. Atkinson, "Twenty-four hour time domain heart rate variability and heart rate: relations to age and gender over nine decades," *J Am Coll Cardiol,* vol. 31, pp. 593-601, 1998.

[28] V. S. Murthy, S. Ramamoorthy, N. Srinivasan, S. Rajagopal e M. M. Rao, "Analysis of photoplethysmographic signals of cardiovascular patients," em *23rd Annual International Conference of the IEEE*, 2001.

[29] J. I. Davies e A. D. Struthers, "Pulse wave analysis and pulse wave velocity: a critical review of their strengths and weaknesses," *J Hypertens,* vol. 21, n.º 3, pp. 463-472, 2003.

[30] I. S. Mackenzie, I. B. Wilkinson e J. R. Cockcroft, "Assessment of arterial stifness in clinical practice," *QJM: An international journal of medicine,* vol. 95, n.º 2, pp. 67-74, 2002.

[31] Y. K. Qawqzeh, M. B. I. Reaz, O. Maskon, K. Chellappan, M. T. Islam e M. A. M. Ali, "The investigation of the effect of aging through photoplethysmogram signal analysis of erectile dysfunction subjects," em *10th WSEAS international conference on Telecommunications and informatics and microelectronics, nanoelectronics, optoelectronics, and WSEAS international conference on Signal processing* , Wisconsin, 2011.

[32] Y. Lin, Z. Song and Y. Yimin, "Study of pulse wave velocity noninvasive detecting instrument based on radial artery and finger photoplethysmography pulse wave," in *International Symposium on Intelligent Information Technology Workshops, 2008*, Shanghai, 2008.

[33] J. O. Hahn, D. McCombie, A. H. Harry, A. Reisner, H. Hojman and R. Mukkamala, "Adaptive left ventricular ejection time estimation using multiple peripheral pressure waveforms," in *Conf Proc IEEE Eng Med Biol Soc*, Shanghai, 2005.

[34] T. Geeraerts, P. Albaladejo, A. D. Declère, J. Duranteau, J. P. Sales and D. Benhamou, "Decrease in left ventricular ejection time on digital arterial waveform during simulated hypovolemia in normal humans.," *J Trauma,* vol. 56, no. 4, pp. 845-849, 2004.

[35] P. M. Middleton, G. S. Chan, E. O'Lone, E. Steel, R. Carroll, B. G. Celler and N. H. Lovell, "Changes in left ventricular ejection time and pulse transit time derived from finger photoplethysmogram and electrocardiogram during moderate haemorrhage," *Clin Physiol Funct Imaging,* vol. 29, no. 3, pp. 163-169, 2009.

[36] J. Muehlsteff, X. A. Aubert and G. Morren, "Continuous cuff-less blood pressure monitoring based on the pulse arrival time approach: The impact of posture," in *30th Annual International Conference of the IEEE* , Vancouver, 2008.

[37] C. P. Chua and C. Heneghan, "Continuous Blood Pressure Monitoring using ECG and Finger Photoplethysmogram," in *28th Annual International Conference of the IEEE* , New York, 2006.

[38] W. Chen, T. Kobayashi, S. Ichikawa, Y. Takeuchi and T. Togawa, "Continuous estimation of systolic blood pressure using the pulse arrival time and intermittent calibration," *Medical and biological engineering and computing,* vol. 38, pp. 569-574, 2000.

[39] J. S. Kim, K. K. Kim, H. J. Baek and K. S. Park, "Effect of confounding factors on blood pressure estimation using pulse arrival time," *Physiological Measurement,* vol. 29, pp. 615-624, 2008.

[40] L. Wang, E. Pickwell-Macpherson, Y. P. Liang and Y. T. Zhang, "Noninvasive cardiac output estimation using a novel photoplethysmogram index.," in *31st Annual International Conference of the IEEE*, Minneapolis, 2009.

[41] W. B. Gu, C. C. Y. Poon and Y. T. Zhang, "A novel parameter from PPG dicrotic notch for estimation of systolic blood pressure using pulse transit time," in *The 5th International Summer School and Symposium on*

Medical Devices and Biosensors, Hong Kong, 2008.

[42] J. Allen and A. Murray, "Age-related changes in the characteristics of the photoplethysmographic pulse shape at various body sites," *Physiological Measurements,* vol. 24, no. 2, pp. 297-307, 2003.

[43] Y. K. Qawqzeh, M. B. I. Reaz e M. A. M. Ali, "The Analysis of PPG Contour in the Assessment of Atherosclerosis for Erectile Dysfunction Subjects," *WSEAS transactions on biology and biomedicine,* vol. 7, n.º 1, pp. 306-315, 2010.

[44] L. A. Bortolotto, J. Blacher, T. Kondo, K. Takazawa and M. E. Safar, "Assessment of vascular aging and atherosclerosis in hypertensive subjects: second derivative oh photoplethysmogram versus pulse wave velocity," *American journal of hypertension,* vol. 13, no. 2, pp. 165-171, 2000.

[45] K. Takazawa, N. Tanaka, M. Fujita, O. Matsuoka, T. Saiki, M. Aikawa, S. Tamura and C. Ibukiyama, "Assessment of vasoactive agents and vascular aging by the second derivative of photoplethysmogram waveform," *Hpertension,* vol. 32, pp. 365-370, 1998.

[46] K. Takazawa, "Augmentation index in heart disease," *Am J Hypertens,* vol. 1S, pp. 15S-18S, 2005.

[47] P. Shaltis, A. Reisner and H. Asada, "Calibration of the Photoplethysmogram to Arterial Blood Pressure: Capabilities and Limitations for Continuous Pressure Monitoring," in *Engineering in Medicine and Biology Society, 2005. IEEE-EMBS 2005. 27th Annual International Conference of the*, Shanghai, 2006.

[48] S. Millasseau, F. Guigui, R. Kelly, K. Prasad, J. Cockcroft, J. Ritter and P. Chowienczyk, "Noninvasive Assessment of the Digital Volume Pulse: Comparison with the Peripheral Pressure Pulse," *Hypertension,* no. 36, pp. 952-956, 2000.

[49] J. Allen e A. Murray, "Modelling the relationship between peripheral blood pressure and blood volume pulses using linear and neural network system identification techniques," *Physiological Measurement,* vol. 20, n.º 3, pp. 287-301, 1999.

[50] X. Teng and Y. Zhang, "Continuous and Noninvasive Estimation of Arterial Blood Pressure Using a Photoplethysmographic Approach," in *Engineering in Medicine and Biology Society, 2003. Proceedings of the 25th Annual International Conference of the IEEE*, Cancun, 2003.

[51] C. Chua and C. Heneghan, "Continuous Blood Pressure Estimation using Pulse Arrival Time and Photoplethysmogram," in *IET 3rd International Conference On Advances in Medical, Signal and Information Processing, 2006. MEDSIP 2006.*, Glasgow, 2006.

[52] E. Chua, S. Redmond, G. McDarby e C. Heneghan, "Towards Using Photo-Plethysmogram Amplitude to Measure Blood Pressure During Sleep," *Annals of Biomedical Engineering,* vol. 38, n.º 3, pp. 945-954, 2010.

[53] A. Payne, C. Symeonides, D. Webb e S. Maxwell, "Pulse transit time measured from the ECG: an unreliable marker of beat-to-beat blood pressure," *Journal of Applied Physiology,* vol. 100, n.º 1, pp. 136-141, 2005.

[54] J. Proença, J. Muehlsteff, X. Aubert e P. Carvalho, "Is pulse transit time a good indicator of blood pressure changes during short physical exercise in a young population?," em *Engineering in Medicine and Biology Society (EMBC), 2010 Annual International Conference of the IEEE*, Buenos Aires, 2010.

[55] K. Reddy and V. Kumar, "Motion Artifact Reduction in Photoplethysmographic Signals using Singular Value Decomposition," in *Instrumentation and Measurement Technology Conference Proceedings, 2007. IMTC 2007. IEEE*, Warsaw, 2007.

[56] R. Enríquez, M. Castellanos, J. Rodríguez and J. Cáceres, "Analysis of the photoplethysmographic signal by means of the decomposition in principal components," *Physiological Measurment,* vol. 23, no. 3, pp. 17-29, 2002.

[57] M. Ram, K. Madhav, E. Krishna, K. Reddy and K. Reddy, "Use of Multi-scale Principal Component Analysis for Motion Artifact Reduction of PPG Signals," in *Recent Advances in Intelligent Computational Systems (RAICS), 2011 IEEE*, Trivandrum, 2011.

[58] M. Raghuram, K. Madhav, E. Krishna and K. Reddy, "On the performance of wavelets in reducing motion artifacts from photoplethysmographic signals," in *2010 4th International Conference on Bioinformatics and Biomedical Engineering (iCBBE)*, Chengdu, 2010.

[59] R. Sukanesh and R. Harikumar, "Analysis of Photo-Plethysmography (PPG) Signals with Motion Artifacts (Gaussian Noise) Using Wavelet Transforms," *Biomedical Soft Computing and Human Sciences,* vol. 16, no. 1, pp. 135-139, 2009.

[60] K. Reddy, B. George and V. Kumar, "Use of Fourier Series Analysis for Motion Artifact Reduction and Data Compression of Photoplethysmographic Signals," *IEEE Transactions on Instrumentation and Measurement,* vol. 58, no. 5, pp. 1706-1711, 2009.

[61] S. Kim, E. Hwang and D. Kim, "Reduction of Movement Artifacts in Photoplethysmograph Using SFLC (scaled Fourier linear combiner)," in *3rd Kuala Lumpur International Conference on Biomedical Engineering 2006*, Springer Berlin Heidelberg, 2007, pp. 427-430.

[62] Y. Yan, C. Poon and Y. Zhang, "Reduction of motion artifact in pulse oximetry by smoothed pseudo Wigner-Ville distribution," *Journal of Neuroengineering and rehabilitation,* vol. 2, pp. 3-11, 2005.

[63] M. Ram, K. Madhav, E. Krishna, K. Reddy and K. Reddy, "Adaptive reduction of motion artifacts from PPG signals using a synthetic noise reference signal," in *2010 IEEE EMBS Conference on Biomedical Engineering and Sciences (IECBES)*, Kuala Lumpur, 2010.

[64] H. Han, M. Kim e J. Kim, "Development of real-time motion artifact reduction algorithm," em *29th Annual International Conference of the IEEE EMBS*, Lyon, 2007.

[65] F. Coetzee and Z. Elghazzawi, "Noise-resistant pulse oximetry using a synthetic reference signal," *IEEE Transactions on Biomedical Engineering,* vol. 47, no. 8, pp. 1018-1026, 2000.

[66] B. Kim and S. Yoo, "Motion artifact reduction in photoplethysmography using independent component analysis," *IEEE Transactions on Biomedical Engineering,* vol. 53, no. 3, pp. 566-568, 2006.

[67] H. Lee, J. Lee, W. Jung and G. Lee, "The Periodic Moving Average Filter for Removing Motion Artifacts from PPG Signals," *International Journal of Control, Automation, and Systems,* vol. 5, no. 6, pp. 701-706, 2007.

[68] K. Chan and Y. Zhang, "Adaptive reduction of motion artifact from photoplethysmographic recordings using a variable step-size LMS filter," in *IEEE Sensors, 2002.*, Orlando, 2002.

[69] K. Li and S. Warren, "Principle component analysis on photoplethysmograms: Blood oxygen saturation estimation and signal segmentation," in *Annual International Conference of the IEEE Engineering in Medicine and Biology Society,EMBC, 2011*, Boston, 2008.

[70] P. Zhang e H. Wang, "A framework for automatic timedomain characteristic parameters extraction of human pulse signals," *EURASIP Journal on Advanced in Signal Processing,* vol. 2008, n.º 55, pp. 1-9, 2008.

[71] M. Aboy, J. Mc Names, T. Thong, D. Tsunami, E. M. and B. Goldstein, "An automatic beat detection algorithm for pressure signals," *IEEE Transactions on Biomedical Engineering,* vol. 52, no. 10, pp. 1662-1670, 2005.

[72] R. Couceiro, P. Carvalho, R. Paiva, J. Henriques, M. Antunes, I. Quintal and J. Muehlsteff, "Multi-Gaussian fitting for the assessment of left ventricular ejection time from the Photoplethysmogram," in *34th International Conference of the IEEE Engineering in Medicine and Biology Society – EMBC 2012*, San Diego, 2012.

[73] D. Jang, M. Hahn, U. Farroq, J. Jang and S. Park, "A morphological approach to pulse feature extraction from the digital volume pulse," in *8th International Conference on Information, Communications and Signal Processing (ICICS) 2011*, Singapore, 2011.

[74] W. Zong, T. Heldt, G. Moody and R. Mark, "An open-source algorithm to detect onset of arterial blood pressure pulses," in *Computers in Cardiology*, Thessaloniki, 2003.

[75] M. Pitzalis, F. Massari, P. Guida, M. Iacoviello, F. Mastropasqua, B. Rizzon, C. Forleo and P. Rizzon, "Shortened Head-Up Tilting Test Guided by Systolic Pressure Reductions in Neurocardiogenic Syncope," *Circulation,* vol. 105, pp. 146-148, 2002.

[76] N. Virag, R. Sutton, R. Vetter, T. Markowitz and M. Erikson, "Prediction of vasovagal syncope from heart rate and blood pressure trend and variability: Experience in 1,155 patients," *Hearth Rhythm,* vol. 4, no. 11, pp. 1375-1382, 2007.

[77] Z. Mallat, E. Vicaut, A. Sangaré, J. Verschueren, G. Fontaine and R. Frank, "Prediction of Head-Up Tilt Test Result by Analysis of Early Heart Rate Variations," *Circulation,* vol. 96, pp. 581-584, 1997.

[78] M. Feuilloy, D. Schang and P. Nicolas, "A Quick Low Cost Method For Syncope Prediction," in *14th European Signal Processing Conference (EUSIPCO 2006)*, Florence, 2006.

[79] C. Meyer, G. Morren, J. Muehlsteff, C. Heiss, T. Lauer, P. Schauerte, T. Rassaf, H. Purefellner and M. Kelm, "Predicting Neurally Mediated Syncope Based on Pulse Arrival Time: Algorithm Development and Preliminary Results," *Journal of Cardiovascular Electrophysiology,* vol. 22, no. 9, pp. 1042-1048, 2011.

[80] A. Goldberger, L. Amaral, L. Glass, M. Hausdorff, P. Ivanov, R. Mark, J. Mietus, G. Moody, C. Peng and H. Stanley, "PhysioBank, PhysioToolkit, and PhysioNet: Components of a New Research Resource for Complex Physiologic Signals," *Circulation,* vol. 101, no. 23, pp. e215-e220, 2000.

[81] J. Muehlsteff, A. Ritz, T. Drexel, E. C., P. Carvalho, R. Couceiro, M. Kelm and C. Meyer, "Pulse Arrival Time as Surrogate for Systolic Blood Pressure Changes during Impending Neurally Mediated Syncope".

[82] "Task Force® Monitor," [Online]. Available: http://accuramed.be/?page_id=373. [Accessed 22 August 2012].

[83] "IntelliVue MP40 and MP50 patient monitors," [Online]. Available: http://www.healthcare.philips.com/in_en/products/patient_monitoring/products/intellivue_mp50_mp40/. [Accessed 22 August 2012].

[84] J. Pan and W. Tompkins, "A real-time qrs detection algorithm.," *IEEE Transactions on Biomedical Engineering,* vol. 32, no. 3, pp. 230-236, 1985.

[85] M. Akay, Wiley Encyclopedia of Biomedical Engineering, John Wiley & Sons, Inc., 2006.

A Appendices

A.1 Tables

Table 2 Sensitivity and specificity for choice of best threshold in HR variations. (d is the distance to the upper left corner of the ROC curve).

Threshold (bpm)	Foot			Top			20%			50%			80%		
	SE (%)	SP (%)	d	SE (%)	SP (%)	d	SE (%)	SP (%)	d	SE (%)	SP (%)	d	SE (%)	SP (%)	d
0.5	99.34	4.05	95.95	99.30	4.51	95.50	99.24	5.09	94.92	98.86	5.21	94.79	98.80	5.12	94.89
1	98.11	12.96	87.06	98.19	14.21	85.81	96.54	16.88	83.19	96.18	17.30	82.79	97.31	16.92	83.12
1.5	96.91	24.08	75.98	96.57	26.38	73.70	94.33	30.38	69.85	93.52	30.96	69.34	95.13	30.32	69.85
2	94.99	34.81	65.39	95.14	37.41	62.78	91.33	42.46	58.19	90.08	43.17	57.69	91.99	42.31	58.24
2.5	93.55	43.20	57.16	93.34	46.11	54.30	88.76	51.31	49.97	87.25	52.27	49.40	89.41	51.39	49.75
3	91.97	50.97	49.68	91.18	54.23	46.61	86.81	59.21	42.87	85.25	60.15	42.49	86.77	59.52	42.59
3.5	90.41	56.50	44.54	88.86	60.14	41.39	84.88	64.49	38.60	83.15	65.56	38.34	84.79	65.04	38.12
4	88.98	61.05	40.48	86.99	64.82	37.51	83.34	68.67	35.49	81.03	69.80	35.66	82.95	69.26	35.15
4.5	87.85	64.83	37.21	85.34	68.57	34.68	81.85	71.93	33.43	79.68	73.18	33.65	81.04	72.70	33.23
5	86.63	67.60	35.05	84.01	71.50	32.68	80.90	74.25	32.06	78.24	75.60	32.69	79.99	75.17	31.89
5.5	85.78	69.95	33.24	82.76	73.86	31.31	80.00	76.27	31.04	77.17	77.49	32.06	78.83	77.20	31.12
6	85.08	71.93	31.79	81.49	75.82	30.46	78.86	77.97	30.53	76.00	79.14	31.80	77.90	78.90	30.56
6.5	84.37	73.63	30.65	80.58	77.46	29.75	77.91	79.30	30.27	75.16	80.34	31.68	77.08	80.24	30.26
7	83.63	75.05	29.84	79.88	78.81	29.22	77.29	80.45	29.96	74.44	81.50	31.55	76.04	81.48	30.29
7.5	83.12	76.23	29.15	78.91	79.99	29.07	76.80	81.33	29.78	73.90	82.41	31.47	75.12	82.37	30.49
8	82.48	77.44	28.56	78.09	81.15	28.90	76.17	82.11	29.79	73.26	83.20	31.58	73.91	83.22	31.03
8.5	81.92	78.42	28.15	77.10	82.15	29.03	75.41	82.99	29.90	72.66	84.01	31.67	73.48	84.04	30.95
9	81.29	79.41	27.82	76.33	83.06	29.11	74.92	83.75	29.88	71.98	84.81	31.87	72.90	84.85	31.05
9.5	80.61	80.19	27.71	75.65	83.94	29.17	74.51	84.41	29.88	71.65	85.42	31.88	72.30	85.51	31.26
10	80.10	80.99	27.52	74.82	84.67	29.48	74.04	85.10	29.93	71.02	86.15	32.12	71.72	86.09	31.52
10.5	79.41	81.64	27.58	74.10	85.30	29.78	73.63	85.63	30.04	70.65	86.63	32.25	71.06	86.60	31.89
11	78.98	82.42	27.40	73.33	86.05	30.10	73.09	86.24	30.23	70.12	87.14	32.53	70.45	87.18	32.21
11.5	78.52	83.06	27.35	72.77	86.65	30.33	72.65	86.74	30.40	69.69	87.64	32.73	70.05	87.74	32.36
12	78.10	83.58	27.37	72.21	87.17	30.61	72.05	87.11	30.78	69.42	88.01	32.84	69.58	88.10	32.66
12.5	77.61	84.10	27.46	71.39	87.64	31.16	71.85	87.51	30.80	68.97	88.43	33.11	69.16	88.54	32.90
13	77.04	84.77	27.55	70.74	88.12	31.58	71.50	87.98	30.93	68.41	88.86	33.50	68.58	88.93	33.31
13.5	76.53	85.25	27.72	70.07	88.56	32.04	70.87	88.38	31.36	68.17	89.24	33.60	68.31	89.35	33.43
14	76.05	85.74	27.88	69.65	88.98	32.29	70.33	88.73	31.74	67.76	89.60	33.88	67.94	89.67	33.69

Table 3 Sensitivity and specificity for choice of best threshold in PAT variations. (d is the distance to the upper left corner of the ROC curve).

Threshold (s)	Foot			Top			20%			50%			80%		
	SE (%)	SP (%)	d	SE (%)	SP (%)	d	SE (%)	SP (%)	d	SE (%)	SP (%)	d	SE (%)	SP (%)	d
0.005	84.97	28.91	72.66	84.04	30.93	70.89	82.23	37.32	65.15	81.80	37.78	64.82	82.17	37.19	65.30
0.01	80.28	51.17	52.67	77.91	54.30	50.76	74.51	64.82	43.45	72.67	65.98	43.64	74.22	64.35	43.99
0.015	75.00	66.29	41.97	72.39	69.02	41.50	67.71	78.78	38.64	64.86	79.96	40.45	66.43	78.55	39.84
0.02	71.80	72.33	39.51	68.56	74.91	40.22	63.65	82.87	40.18	60.55	84.00	42.57	62.56	82.94	41.15
0.025	68.85	76.52	39.01	64.66	79.20	41.01	60.25	85.19	42.42	56.61	86.29	45.51	58.45	85.42	44.04
0.03	67.08	78.75	39.19	62.34	81.53	41.94	58.29	86.32	43.90	53.96	87.33	47.75	56.21	86.55	45.81
0.035	65.83	80.33	39.43	59.98	83.36	43.34	56.91	87.07	44.99	52.09	88.06	49.37	53.91	87.40	47.78
0.04	64.48	81.32	40.14	58.19	84.47	44.60	55.44	87.48	46.29	50.63	88.48	50.70	52.42	87.87	49.10
0.045	63.30	82.35	40.72	56.53	85.50	45.82	54.28	87.91	47.29	49.23	88.81	51.99	50.69	88.28	50.68
0.05	62.36	83.10	41.26	55.26	86.16	46.83	53.29	88.14	48.19	48.27	89.00	52.89	49.59	88.59	51.69
0.055	61.35	83.70	41.95	54.07	86.74	47.80	52.35	88.37	49.05	47.38	89.16	53.72	48.49	88.81	52.71
0.06	60.84	84.20	42.22	53.14	87.19	48.58	51.75	88.54	49.59	46.53	89.29	54.53	47.87	88.97	53.29
0.065	59.27	84.70	43.51	51.99	87.64	49.58	50.68	88.73	50.59	45.92	89.40	55.11	47.00	89.12	54.10
0.07	58.67	85.08	43.94	50.67	87.98	50.77	50.01	88.84	51.22	45.46	89.50	55.54	46.22	89.24	54.85
0.075	57.78	85.50	44.64	49.75	88.28	51.60	49.39	88.99	51.80	44.93	89.63	56.04	45.56	89.37	55.47
0.08	57.04	85.81	45.24	48.91	88.50	52.37	48.79	89.11	52.36	44.52	89.69	56.43	44.73	89.45	56.27
0.085	56.56	86.12	45.61	48.02	88.74	53.18	48.25	89.22	52.86	44.33	89.77	56.60	44.45	89.53	56.53
0.09	55.89	86.39	46.17	47.36	88.92	53.80	47.48	89.28	53.61	43.92	89.86	56.99	44.02	89.63	56.93
0.095	55.36	86.61	46.60	46.35	89.13	54.74	46.85	89.41	54.19	43.17	89.97	57.71	43.58	89.71	57.35
0.005	84.97	28.91	72.66	84.04	30.93	70.89	82.23	37.32	65.15	81.80	37.78	64.82	82.17	37.19	65.30
0.01	80.28	51.17	52.67	77.91	54.30	50.76	74.51	64.82	43.45	72.67	65.98	43.64	74.22	64.35	43.99
0.015	75.00	66.29	41.97	72.39	69.02	41.50	67.71	78.78	38.64	64.86	79.96	40.45	66.43	78.55	39.84
0.02	71.80	72.33	39.51	68.56	74.91	40.22	63.65	82.87	40.18	60.55	84.00	42.57	62.56	82.94	41.15
0.025	68.85	76.52	39.01	64.66	79.20	41.01	60.25	85.19	42.42	56.61	86.29	45.51	58.45	85.42	44.04
0.03	67.08	78.75	39.19	62.34	81.53	41.94	58.29	86.32	43.90	53.96	87.33	47.75	56.21	86.55	45.81
0.035	65.83	80.33	39.43	59.98	83.36	43.34	56.91	87.07	44.99	52.09	88.06	49.37	53.91	87.40	47.78
0.04	64.48	81.32	40.14	58.19	84.47	44.60	55.44	87.48	46.29	50.63	88.48	50.70	52.42	87.87	49.10
0.045	63.30	82.35	40.72	56.53	85.50	45.82	54.28	87.91	47.29	49.23	88.81	51.99	50.69	88.28	50.68
0.005	84.97	28.91	72.66	84.04	30.93	70.89	82.23	37.32	65.15	81.80	37.78	64.82	82.17	37.19	65.30
0.01	80.28	51.17	52.67	77.91	54.30	50.76	74.51	64.82	43.45	72.67	65.98	43.64	74.22	64.35	43.99
0.015	75.00	66.29	41.97	72.39	69.02	41.50	67.71	78.78	38.64	64.86	79.96	40.45	66.43	78.55	39.84
0.02	71.80	72.33	39.51	68.56	74.91	40.22	63.65	82.87	40.18	60.55	84.00	42.57	62.56	82.94	41.15
0.025	68.85	76.52	39.01	64.66	79.20	41.01	60.25	85.19	42.42	56.61	86.29	45.51	58.45	85.42	44.04
0.03	67.08	78.75	39.19	62.34	81.53	41.94	58.29	86.32	43.90	53.96	87.33	47.75	56.21	86.55	45.81
0.035	65.83	80.33	39.43	59.98	83.36	43.34	56.91	87.07	44.99	52.09	88.06	49.37	53.91	87.40	47.78
0.04	64.48	81.32	40.14	58.19	84.47	44.60	55.44	87.48	46.29	50.63	88.48	50.70	52.42	87.87	49.10
0.045	63.30	82.35	40.72	56.53	85.50	45.82	54.28	87.91	47.29	49.23	88.81	51.99	50.69	88.28	50.68
0.05	62.36	83.10	41.26	55.26	86.16	46.83	53.29	88.14	48.19	48.27	89.00	52.89	49.59	88.59	51.69
0.055	61.35	83.70	41.95	54.07	86.74	47.80	52.35	88.37	49.05	47.38	89.16	53.72	48.49	88.81	52.71
0.06	60.84	84.20	42.22	53.14	87.19	48.58	51.75	88.54	49.59	46.53	89.29	54.53	47.87	88.97	53.29
0.065	59.27	84.70	43.51	51.99	87.64	49.58	50.68	88.73	50.59	45.92	89.40	55.11	47.00	89.12	54.10
0.07	58.67	85.08	43.94	50.67	87.98	50.77	50.01	88.84	51.22	45.46	89.50	55.54	46.22	89.24	54.85
0.075	57.78	85.50	44.64	49.75	88.28	51.60	49.39	88.99	51.80	44.93	89.63	56.04	45.56	89.37	55.47
0.08	57.04	85.81	45.24	48.91	88.50	52.37	48.79	89.11	52.36	44.52	89.69	56.43	44.73	89.45	56.27
0.085	56.56	86.12	45.61	48.02	88.74	53.18	48.25	89.22	52.86	44.33	89.77	56.60	44.45	89.53	56.53
0.09	55.89	86.39	46.17	47.36	88.92	53.80	47.48	89.28	53.61	43.92	89.86	56.99	44.02	89.63	56.93
0.095	55.36	86.61	46.60	46.35	89.13	54.74	46.85	89.41	54.19	43.17	89.97	57.71	43.58	89.71	57.35

Table 4 Sensitivity and specificity for choice of best threshold in HR comparison. (d is the distance to the upper left corner of the ROC curve).

Threshold (bpm)	Foot			Top			20%			50%			80%		
	SE (%)	SP (%)	d	SE (%)	SP (%)	d	SE (%)	SP (%)	d	SE (%)	SP (%)	d	SE (%)	SP (%)	d
0.5	93.57	35.66	64.66	93.24	37.82	62.54	90.40	45.72	55.12	90.22	46.45	54.44	91.05	45.47	55.26
0.6	92.48	40.69	59.78	91.58	43.05	57.57	88.66	51.23	50.07	88.16	52.01	49.43	89.38	50.83	50.30
0.7	91.52	45.69	54.97	90.26	48.17	52.74	86.86	56.58	45.37	86.43	57.14	44.96	87.83	55.95	45.70
0.8	90.59	49.71	51.17	89.50	52.44	48.70	85.81	60.51	41.96	85.27	61.03	41.66	86.41	59.90	42.34
0.9	89.87	52.88	48.20	88.49	55.53	45.93	84.81	63.31	39.71	83.77	63.93	39.56	85.24	62.81	40.01
1	89.00	55.62	45.72	87.48	58.44	43.40	84.07	65.80	37.73	82.58	66.37	37.87	84.21	65.31	38.11
1.1	88.41	58.13	43.45	86.90	61.14	41.00	83.24	67.89	36.23	81.28	68.56	36.59	83.09	67.52	36.62
1.2	87.93	60.29	41.51	85.92	63.34	39.27	82.46	69.67	35.03	80.48	70.30	35.54	82.24	69.39	35.38
1.3	87.46	61.97	40.04	85.26	65.03	37.95	81.86	70.95	34.25	79.57	71.58	35.00	81.21	70.85	34.68
1.4	86.88	63.40	38.88	84.51	66.51	36.90	81.20	72.00	33.73	78.77	72.67	34.61	80.68	71.99	34.03
1.5	86.41	64.70	37.82	83.78	67.90	35.96	80.51	72.92	33.36	78.08	73.63	34.29	79.98	72.99	33.62
1.6	85.87	65.78	37.02	83.15	69.01	35.27	79.91	73.74	33.06	77.45	74.45	34.07	79.43	73.83	33.29
1.7	85.20	66.83	36.32	82.62	70.15	34.54	79.25	74.46	32.90	76.81	75.17	33.97	78.75	74.65	33.08
1.8	84.69	67.71	35.73	82.13	71.01	34.06	78.66	75.08	32.81	76.36	75.77	33.85	78.24	75.30	32.92
1.9	84.40	68.50	35.15	81.65	71.73	33.70	78.10	75.57	32.81	75.70	76.26	33.97	77.66	75.85	32.90
2	83.94	69.16	34.77	81.28	72.34	33.40	77.67	75.95	32.81	75.11	76.68	34.11	77.18	76.26	32.93
2.1	83.71	69.79	34.32	80.69	72.96	33.22	77.43	76.36	32.68	74.74	77.09	34.10	76.84	76.65	32.89
2.2	83.41	70.34	33.99	80.42	73.48	32.96	77.09	76.71	32.67	74.51	77.41	34.06	76.42	76.98	32.96
2.3	83.01	70.80	33.79	80.11	74.03	32.71	76.78	76.98	32.70	73.94	77.71	34.30	75.98	77.35	33.02
2.4	82.77	71.30	33.47	79.80	74.52	32.51	76.43	77.23	32.77	73.39	77.97	34.55	75.56	77.62	33.14
2.5	82.37	71.70	33.34	79.36	74.90	32.50	76.13	77.44	32.85	72.96	78.23	34.72	75.11	77.87	33.30
2.6	82.04	72.07	33.20	79.05	75.24	32.43	75.86	77.62	32.91	72.61	78.45	34.85	74.70	78.09	33.47
2.7	81.95	72.42	32.96	78.72	75.54	32.42	75.51	77.82	33.04	72.32	78.60	34.99	74.42	78.26	33.57
2.8	81.74	72.74	32.81	78.25	75.85	32.50	75.25	78.02	33.10	72.03	78.76	35.12	74.00	78.44	33.77
2.9	81.53	73.03	32.69	78.03	76.17	32.41	74.92	78.16	33.25	71.76	78.94	35.23	73.74	78.61	33.87
3	81.22	73.36	32.60	77.69	76.43	32.45	74.60	78.30	33.41	71.55	79.07	35.32	73.52	78.76	33.95
3.1	81.07	73.62	32.47	77.38	76.68	32.49	74.34	78.44	33.52	71.35	79.19	35.41	73.13	78.90	34.16
3.2	80.88	73.85	32.39	77.06	76.91	32.55	74.19	78.57	33.54	71.22	79.32	35.44	72.90	79.04	34.26
3.3	80.71	74.10	32.30	76.49	77.07	32.84	74.00	78.68	33.62	71.04	79.42	35.53	72.50	79.15	34.51
3.4	80.49	74.30	32.27	76.34	77.29	32.80	73.81	78.82	33.69	70.75	79.51	35.71	72.36	79.27	34.55
3.5	80.34	74.52	32.18	76.03	77.48	32.88	73.64	78.93	33.75	70.44	79.59	35.92	72.03	79.39	34.74
3.6	80.17	74.71	32.14	75.67	77.63	33.05	73.52	79.00	33.80	70.22	79.66	36.06	71.65	79.45	35.01
3.7	79.88	74.92	32.16	75.42	77.78	33.13	73.31	79.08	33.91	69.99	79.73	36.22	71.39	79.52	35.19
3.8	79.68	75.06	32.17	75.14	77.93	33.24	73.20	79.15	33.95	69.85	79.82	36.28	71.17	79.60	35.32
3.9	79.45	75.24	32.18	74.86	78.07	33.36	73.01	79.21	34.07	69.55	79.87	36.51	70.86	79.67	35.54
4	79.28	75.39	32.16	74.62	78.22	33.44	72.90	79.25	34.13	69.44	79.93	36.56	70.63	79.76	35.67
4.1	78.98	75.55	32.25	74.36	78.34	33.57	72.77	79.30	34.21	69.36	79.97	36.60	70.35	79.80	35.88
4.2	78.77	75.70	32.27	74.12	78.50	33.64	72.62	79.37	34.29	69.24	80.04	36.67	70.14	79.87	36.01
4.3	78.64	75.84	32.25	74.03	78.64	33.62	72.54	79.42	34.31	69.01	80.08	36.84	70.03	79.93	36.07
4.4	78.35	75.97	32.34	73.86	78.73	33.70	72.43	79.49	34.37	68.88	80.12	36.92	69.79	79.99	36.24
4.5	78.20	76.09	32.36	73.67	78.84	33.78	72.24	79.53	34.49	68.79	80.17	36.98	69.68	80.03	36.31
4.6	77.95	76.17	32.46	73.46	78.93	33.89	72.15	79.57	34.54	68.70	80.19	37.04	69.48	80.07	36.45
4.7	77.78	76.29	32.49	73.28	79.02	33.98	71.97	79.61	34.66	68.54	80.23	37.16	69.35	80.12	36.53
4.8	77.71	76.37	32.48	73.01	79.08	34.15	71.84	79.64	34.75	68.45	80.25	37.22	69.20	80.15	36.64
4.9	77.53	76.45	32.55	72.80	79.16	34.26	71.56	79.69	34.95	68.40	80.27	37.25	69.00	80.18	36.80
5	77.33	76.54	32.62	72.58	79.25	34.38	71.40	79.72	35.06	68.33	80.29	37.30	68.88	80.21	36.88
5.5	76.78	77.01	32.68	71.64	79.62	34.92	70.87	79.90	35.39	67.87	80.44	37.61	68.45	80.43	37.13
6	75.99	77.37	33.00	70.84	79.85	35.44	70.25	80.03	35.83	67.34	80.53	38.02	67.96	80.54	37.49
6.5	75.36	77.65	33.27	70.07	80.07	35.96	69.87	80.15	36.08	66.84	80.61	38.42	67.41	80.65	37.90
7	74.71	77.92	33.57	69.39	80.22	36.45	69.41	80.24	36.42	66.48	80.69	38.69	66.96	80.71	38.25
7.5	73.71	78.18	34.17	68.84	80.36	36.83	68.91	80.32	36.80	66.29	80.75	38.82	66.30	80.80	38.79
8	72.96	78.36	34.63	68.10	80.47	37.41	68.54	80.39	37.07	65.80	80.78	39.23	65.73	80.83	39.26
8.5	72.44	78.56	34.92	67.41	80.57	37.94	68.04	80.45	37.47	65.19	80.81	39.75	65.20	80.88	39.71
9	71.95	78.76	35.19	66.74	80.64	38.49	67.45	80.49	37.95	64.93	80.85	39.96	64.68	80.93	40.14
9.5	71.43	78.92	35.51	66.12	80.73	38.98	66.91	80.56	38.38	64.50	80.92	40.30	64.28	80.97	40.47
10	70.90	79.07	35.84	65.54	80.81	39.45	66.53	80.62	38.68	64.23	80.96	40.52	63.96	81.02	40.73

Table 5 Segmented PAT's for the PCA.

Record	PATtop		PAT80		PAT50		PAT20		PATfoot	
	Start (s)	End (s)	Start (s)	End (s)	Start (s)	End (s)	Start (s)	End (s)	Start (s)	End (s)
6	4349.80	4499.80	4349.76	4499.76	4345.65	4495.65	4353.60	4503.60	4356.78	4506.78
7	3055.87	3205.87	3055.83	3205.83	3055.80	3205.80	3055.78	3205.78	3050.63	3200.63
8	2845.01	2995.01	2844.98	2994.98	2844.96	2994.96	2844.93	2994.93	2844.87	2994.87
9	2323.91	2473.91	2313.83	2463.83	2314.31	2464.31	2309.73	2459.73	2311.61	2461.61
12	2676.75	2826.75	2676.68	2826.68	2676.65	2826.65	2676.61	2826.61	2681.46	2831.46
13	2553.06	2703.06	2551.89	2701.89	2551.85	2701.85	2551.82	2701.82	2546.13	2696.13
15	3311.37	3461.37	3308.19	3458.19	3308.16	3458.16	3303.42	3453.42	3299.29	3449.29
18	2470.04	2620.04	2470.00	2620.00	2469.98	2619.98	2469.94	2619.94	2469.88	2619.88
19	3043.32	3193.32	3081.82	3231.82	3043.26	3193.26	3044.84	3194.84	3044.80	3194.80
24	4245.64	4395.64	4245.59	4395.59	4245.56	4395.56	4245.52	4395.52	4235.40	4385.40
26	2236.51	2386.51	2231.78	2381.78	2229.91	2379.91	2226.15	2376.15	2226.07	2376.07
33	2132.63	2282.63	2132.53	2282.53	2132.47	2282.47	2132.43	2282.43	2132.35	2282.35
34	2607.74	2757.74	2606.85	2756.85	2606.82	2756.82	2606.78	2756.78	2615.56	2765.56
36	3787.81	3937.81	3783.21	3933.21	3783.19	3933.19	3783.15	3933.15	3792.91	3942.91
37	3108.32	3258.32	3089.48	3239.48	3098.07	3248.07	3098.04	3248.04	3077.11	3227.11
39	3989.79	4139.79	3989.75	4139.75	3989.71	4139.71	3997.86	4147.86	3998.79	4148.79
40	1551.22	1701.22	1537.65	1687.65	1537.62	1687.62	1537.59	1687.59	1522.65	1672.65
42	4450.91	4600.91	4450.87	4600.87	4450.83	4600.83	4464.37	4614.37	4464.29	4614.29
44	2356.52	2506.52	2356.49	2506.49	2357.88	2507.88	2357.85	2507.85	2355.45	2505.45
46	3209.18	3359.18	3201.36	3351.36	3209.85	3359.85	3209.82	3359.82	3202.88	3352.88
49	2822.43	2972.43	2822.38	2972.38	2822.35	2972.35	2820.54	2970.54	2822.24	2972.24

Table 6 HUT sequences for patients with syncope.

Record	Baseline					Early Tilt					Late Tilt				
	PATf (ms)	PAT20 (ms)	PAT50 (ms)	PAT80 (ms)	PATt (ms)	PATf (ms)	PAT20 (ms)	PAT50 (ms)	PAT80 (ms)	PATt (ms)	PATf (ms)	PAT20 (ms)	PAT50 (ms)	PAT80 (ms)	PATt (ms)
6	337.53	385.63	409.73	433.23	458.61	333.63	377.37	397.03	416.01	437.36	284.28	418.65	451.60	473.61	513.69
7	337.02	405.19	446.67	502.41	584.49	336.40	404.45	440.76	483.63	574.98	391.71	453.52	483.33	515.34	551.72
8	314.38	371.10	403.68	449.14	544.45	306.13	357.87	381.33	407.63	509.59	330.66	377.08	399.07	418.96	444.34
9	317.68	371.69	391.80	413.99	443.30	338.16	384.72	405.27	424.98	446.52	225.21	310.07	431.11	459.28	475.15
12	335.40	397.49	432.90	487.90	593.53	345.19	410.92	448.66	504.41	586.22	370.87	432.40	461.10	489.70	539.05
13	323.41	387.66	414.24	441.89	493.33	318.57	393.05	418.25	449.14	555.34	409.28	480.03	507.19	539.49	581.21
15	325.44	376.33	400.43	426.11	469.33	336.86	389.81	413.36	438.20	473.13	341.66	410.86	433.79	457.58	489.23
18	307.42	363.05	393.49	433.08	538.51	299.09	354.31	382.58	425.32	524.60	326.73	387.79	410.43	432.75	461.52
19	332.19	390.64	415.32	439.48	471.58	329.26	392.26	417.32	441.53	472.60	375.69	432.06	461.15	488.29	525.25
24	365.42	419.55	446.29	474.11	515.40	364.16	419.80	443.68	468.39	499.84	414.30	470.72	495.25	522.60	558.79
26	357.17	421.46	458.37	499.62	578.42	365.07	446.15	472.65	504.32	546.53	461.40	541.13	575.74	614.55	661.53
33	339.29	401.41	431.79	463.49	535.63	343.77	402.77	428.83	454.69	495.64	394.95	474.45	508.03	554.35	615.16
34	326.33	382.18	407.63	436.30	488.33	337.56	398.84	428.88	459.17	506.70	358.10	413.84	440.32	466.99	499.97
36	355.80	414.55	440.51	469.70	516.25	348.27	406.15	433.32	459.52	498.12	406.45	471.35	497.18	523.69	559.44
37	343.73	403.76	433.69	461.56	504.58	356.46	416.54	445.37	476.14	543.26	382.08	438.20	467.04	490.53	524.64
39	318.41	382.89	413.37	453.12	549.53	330.47	396.44	426.70	468.63	578.92	409.74	470.06	500.05	529.88	570.07
40	380.33	436.92	463.41	492.28	558.89	375.06	440.89	460.81	490.15	552.91	432.46	512.08	545.83	571.17	615.74
42	340.85	396.04	423.42	451.81	495.87	356.15	409.78	433.78	459.55	496.63	395.40	452.42	477.72	503.58	532.32
44	319.11	363.19	384.54	404.41	429.43	319.51	363.35	382.25	399.36	420.46	295.33	378.65	385.20	402.09	433.90
46	364.49	431.55	459.78	487.42	536.07	380.33	453.26	484.21	513.98	557.66	487.74	523.80	569.65	586.74	636.19
49	338.18	417.17	455.01	503.34	584.67	353.18	418.45	448.94	489.41	565.79	360.48	410.67	432.17	453.46	480.39
Average	337.12	396.16	425.05	458.30	518.58	341.58	401.77	428.29	458.77	516.32	374.02	440.94	473.00	499.74	536.63
STD	18.45	21.20	23.62	28.79	46.94	20.48	25.85	27.69	31.85	47.11	58.74	52.86	50.44	53.83	61.08

Table 7 HUT sequences for patients without syncope.

Records	Baseline					Early Tilt					Late Tilt				
	PATf (ms)	PAT20 (ms)	PAT50 (ms)	PAT80 (ms)	PATt (ms)	PATf (ms)	PAT20 (ms)	PAT50 (ms)	PAT80 (ms)	PATt (ms)	PATf (ms)	PAT20 (ms)	PAT50 (ms)	PAT80 (ms)	PATt (ms)
5	339.46	411.31	449.71	508.15	592.17	344.21	410.68	446.77	503.34	589.68	333.53	396.70	420.63	443.84	473.78
10	374.17	417.34	435.64	454.48	475.36	310.81	390.91	411.73	433.15	458.79	432.74	479.60	499.38	524.20	551.90
11	332.02	402.70	431.80	471.28	575.53	354.29	421.60	448.13	482.38	563.33	352.52	415.95	440.15	465.73	513.28
14	326.77	391.23	433.65	500.60	588.18	317.41	371.70	398.72	431.40	531.33	307.10	355.71	376.80	397.75	424.80
16	409.47	502.70	555.77	635.45	695.11	386.48	484.89	533.83	576.71	655.06	359.85	452.38	489.34	547.71	605.32
17	376.06	442.30	507.13	562.20	587.85	343.30	415.94	456.83	511.18	580.63	329.90	388.58	413.05	437.08	466.77
20	340.79	432.77	479.55	533.35	619.38	343.71	428.14	471.22	523.92	610.46	415.30	477.35	504.33	534.34	569.17
21	310.96	374.60	410.74	459.90	561.77	323.25	392.68	425.13	474.13	575.07	328.90	383.52	405.64	427.57	454.17
25	254.01	420.48	452.56	365.97	564.64	228.05	330.35	439.16	382.03	513.45	279.83	335.62	359.53	383.56	413.12
27	333.49	403.92	437.58	476.35	545.93	322.67	376.19	404.40	438.43	515.88	307.56	358.17	380.56	405.46	442.33
28	325.63	383.59	413.40	447.33	506.25	312.04	370.09	396.63	423.34	461.08	348.15	393.65	415.16	435.15	460.91
29	340.34	389.16	412.30	438.39	476.94	348.56	397.93	419.09	442.54	470.29	362.48	407.38	424.07	448.98	475.60
30	323.74	381.01	406.93	436.31	501.51	330.21	382.53	405.07	430.72	460.76	349.09	398.83	420.49	441.29	465.19
31	352.93	409.35	435.72	462.42	509.63	367.20	431.45	459.18	492.55	545.95	363.51	422.02	443.74	464.02	486.72
32	402.44	467.16	506.17	557.79	637.95	354.66	419.14	438.68	490.36	556.01	359.28	419.11	447.39	477.69	519.29
35	318.23	369.96	394.86	420.49	461.02	323.18	379.40	409.24	439.68	490.99	328.48	378.73	401.67	424.58	455.32
38	359.08	448.29	501.81	563.43	637.86	365.64	437.70	477.86	532.21	605.73	343.56	397.98	420.55	445.61	477.40
41	349.34	419.66	451.00	486.46	543.62	357.50	416.41	446.15	476.86	554.99	385.05	441.07	465.39	489.12	518.26
43	360.62	433.86	474.11	529.51	622.23	389.78	457.87	489.87	527.57	589.91	382.23	464.43	503.89	530.96	587.98
45	355.32	423.83	471.91	530.70	624.33	368.51	434.98	472.87	524.30	614.26	368.51	434.70	465.46	499.10	560.67
48	349.98	416.90	458.47	513.87	585.24	360.16	423.88	465.06	519.27	578.38	342.24	399.17	428.57	460.21	509.23
50	329.35	387.98	416.53	447.95	508.15	342.00	402.88	431.52	461.24	521.39	408.13	480.27	509.13	538.67	578.60
51	328.04	374.87	396.31	418.73	446.55	315.57	361.36	383.26	403.13	427.56	346.21	394.94	417.31	440.27	467.11
Average	**343.14**	**413.26**	**449.29**	**487.87**	**559.44**	**339.53**	**406.03**	**440.45**	**474.80**	**542.22**	**353.66**	**411.99**	**437.05**	**463.60**	**499.00**
STD	**30.97**	**31.42**	**39.92**	**59.08**	**63.98**	**32.52**	**33.41**	**34.87**	**47.46**	**58.61**	**34.63**	**39.12**	**41.78**	**45.91**	**53.01**

Table 8 Student's t-test for HUT sequences of Table 6 and Table 7 ($p < 0.05$).

	Non syncope					**Syncope**				
	PATf	PAT20	PAT50	PAT80	PATt	PATf	PAT20	PAT50	PAT80	PATt
Baseline vs. Early Tilt	0.503076	0.204718	0.069247	0.031852	0.00937	0,039717	0,023858	0,240441	0,896231	0,684473
Early Tilt vs. Late Tilt	0.052081	0.386415	0.503891	0.196452	0.001945	0,007899	0,000116	3,99E-06	9,08E-05	0,122881
Baseline vs. Late Tilt	0.099397	0.660434	0.206282	0.042854	0.000299	0,002713	4,50E-05	6,77E-06	0,000276	0,182081

Table 9 Student's t-test HUT sequences comparison of syncope vs. non syncope patients ($p<0.05$).

Baseline					**Early-Tilt**					**Late tilt**				
PATf	PAT20	PAT50	PAT80	PATt	PATf	PAT20	PAT50	PAT80	PATt	PATf	PAT20	PAT50	PAT80	PATt
0.444793	0.046891	0.020662	0.04446	0.024039	0.80628	0.648602	0.220233	0.209974	0.124222	0.186058	0.048852	0.015513	0.02372	0.038457

Table 10 Statistics for optimal threshold determination with the original PAT signal. The optimal threshold is the one closest to the upper left corner of the ROC space (d).

Threshold	PATfoot				PAT20				PAT50				PAT80				PATtop			
	SE (%)	SP (%)	PPV (%)	d (%)	SE (%)	SP (%)	PPV (%)	d (%)	SE (%)	SP (%)	PPV (%)	d (%)	SE (%)	SP (%)	PPV (%)	d (%)	SE (%)	SP (%)	PPV (%)	d (%)
1.05	100.00	0.00	33.33	100.00	95.24	16.67	40.00	83.47	95.24	15.79	38.46	84.35	95.24	19.44	40.82	80.70	76.19	16.22	34.04	87.10
1.06	100.00	0.00	33.87	100.00	95.24	20.59	42.55	79.55	95.24	21.21	43.48	78.93	90.48	20.59	41.30	79.98	76.19	24.24	39.02	79.41
1.07	100.00	0.00	33.87	100.00	95.24	22.58	45.45	77.57	95.24	22.58	45.45	77.57	90.48	24.24	43.18	76.35	76.19	28.13	41.03	75.72
1.08	95.24	5.41	36.36	94.71	95.24	25.81	46.51	74.35	95.24	28.57	50.00	71.59	90.48	40.00	51.35	60.75	71.43	41.94	45.45	64.71
1.09	95.24	15.15	41.67	84.98	95.24	39.29	54.05	60.90	95.24	44.44	57.14	55.76	90.48	46.67	54.29	54.18	66.67	46.67	46.67	62.89
1.1	95.24	25.81	46.51	74.35	95.24	60.00	66.67	40.28	95.24	60.00	66.67	40.28	90.48	55.17	59.38	45.83	61.90	53.57	50.00	60.06
1.11	95.24	26.67	47.62	73.49	95.24	64.00	68.97	36.31	90.48	64.00	67.86	37.24	90.48	61.54	65.52	39.62	61.90	57.69	54.17	56.93
1.12	90.48	32.14	50.00	68.52	90.48	68.00	70.37	33.39	90.48	72.00	73.08	29.58	85.71	64.00	66.67	38.73	61.90	60.00	56.52	55.24
1.13	90.48	35.71	51.35	64.99	85.71	70.83	72.00	32.48	90.48	83.33	82.61	19.20	85.71	70.83	72.00	32.48	61.90	64.00	59.09	52.41
1.14	85.71	42.31	54.55	59.43	85.71	75.00	75.00	28.79	85.71	83.33	81.82	21.95	80.95	82.61	80.95	25.79	52.38	75.00	64.71	53.78
1.15	85.71	52.00	60.00	50.08	76.19	82.61	80.00	29.48	80.95	86.96	85.00	23.09	76.19	82.61	80.00	29.48	52.38	75.00	64.71	53.78
1.16	80.95	58.33	62.96	45.81	71.43	82.61	78.95	33.45	76.19	86.96	84.21	27.15	66.67	82.61	77.78	37.60	42.86	75.00	60.00	62.37
1.17	71.43	58.33	60.00	50.52	71.43	86.96	83.33	31.41	76.19	86.96	84.21	27.15	66.67	82.61	77.78	37.60	38.10	82.61	66.67	64.30
1.18	71.43	66.67	65.22	43.90	71.43	86.96	83.33	31.41	66.67	86.96	82.35	35.79	61.90	82.61	76.47	41.88	38.10	86.96	72.73	63.26
1.19	61.90	78.26	72.22	43.86	66.67	86.96	82.35	35.79	57.14	86.96	80.00	44.80	57.14	82.61	75.00	46.25	38.10	91.30	80.00	62.51
1.2	57.14	82.61	75.00	46.25	61.90	86.96	81.25	40.27	47.62	86.96	76.92	53.98	47.62	82.61	71.43	55.19	33.33	91.30	77.78	67.23
1.21	47.62	82.61	71.43	55.19	57.14	86.96	80.00	44.80	47.62	86.96	76.92	53.98	38.10	82.61	66.67	64.30	28.57	91.30	75.00	71.96
1.22	47.62	82.61	71.43	55.19	47.62	86.96	76.92	53.98	47.62	86.96	76.92	53.98	38.10	82.61	66.67	64.30	28.57	91.30	75.00	71.96
1.23	42.86	82.61	69.23	59.73	47.62	86.96	76.92	53.98	42.86	86.96	75.00	58.61	33.33	82.61	63.64	68.90	28.57	91.30	75.00	71.96
1.24	42.86	82.61	69.23	59.73	42.86	86.96	75.00	58.61	42.86	86.96	75.00	58.61	33.33	82.61	63.64	68.90	23.81	91.30	71.43	76.69
1.25	42.86	82.61	69.23	59.73	38.10	86.96	72.73	63.26	42.86	86.96	75.00	58.61	28.57	82.61	60.00	73.52	19.05	91.30	66.67	81.42

A.2 PCA

Table 11 Explained Variances of each component from the PCA.

	PATtop		PAT80		PAT50		PAT20		PATfoot	
Components	Percentage (%)	Cumulative Percentage (%)	Percentage (%)	Cumulative Percentage (%)	Percentage (%)	Cumulative Percentage (%)	Percentage (%)	Cumulative Percentage (%)	Percentage (%)	Cumulative Percentage (%)
1	86.66	86.66	85.23	85.23	84.82	84.82	85.34	85.34	75.19	75.19
2	5.26	91.92	4.82	90.05	4.78	89.60	3.91	89.25	5.53	80.72
3	2.01	93.93	2.39	92.44	3.05	92.65	2.73	91.99	4.24	84.95
4	1.05	94.98	1.69	94.13	1.49	94.14	1.53	93.52	3.72	88.68
5	0.90	95.87	1.25	95.38	1.08	95.22	1.08	94.59	1.90	90.58
6	0.74	96.62	0.88	96.26	0.73	95.95	0.89	95.49	1.52	92.10
7	0.57	97.19	0.70	96.96	0.67	96.62	0.79	96.27	1.43	93.53
8	0.53	97.72	0.48	97.44	0.49	97.11	0.66	96.94	1.24	94.77
9	0.38	98.10	0.43	97.87	0.43	97.54	0.63	97.57	1.07	95.84
10	0.34	98.44	0.34	98.21	0.38	97.91	0.54	98.11	0.83	96.67
11	0.27	98.71	0.30	98.51	0.34	98.25	0.37	98.48	0.68	97.35
12	0.24	98.95	0.27	98.79	0.28	98.53	0.31	98.79	0.58	97.93
13	0.22	99.17	0.23	99.02	0.26	98.79	0.28	99.07	0.51	98.44
14	0.16	99.33	0.21	99.23	0.25	99.03	0.25	99.32	0.48	98.92
15	0.14	99.46	0.17	99.40	0.21	99.24	0.22	99.54	0.36	99.28
16	0.12	99.59	0.17	99.57	0.19	99.43	0.20	99.74	0.28	99.57
17	0.11	99.69	0.14	99.71	0.15	99.58	0.17	99.91	0.24	99.80
18	0.10	99.79	0.12	99.82	0.13	99.71	0.09	100.00	0.20	100.00
19	0.08	99.87	0.10	99.92	0.12	99.83	-	-	-	-
20	0.07	99.94	0.08	100.00	0.10	99.93	-	-	-	-
21	0.06	100.00	-	-	0.07	100.00	-	-	-	-

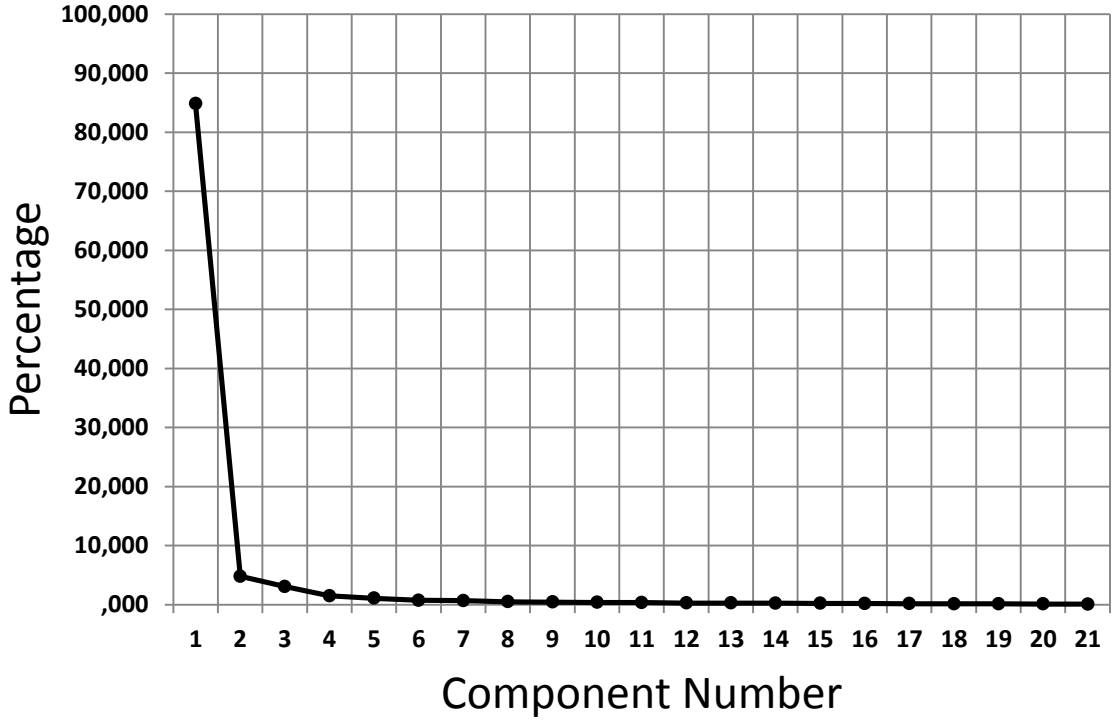

Figure 25 Explained Variance of the PATtop.

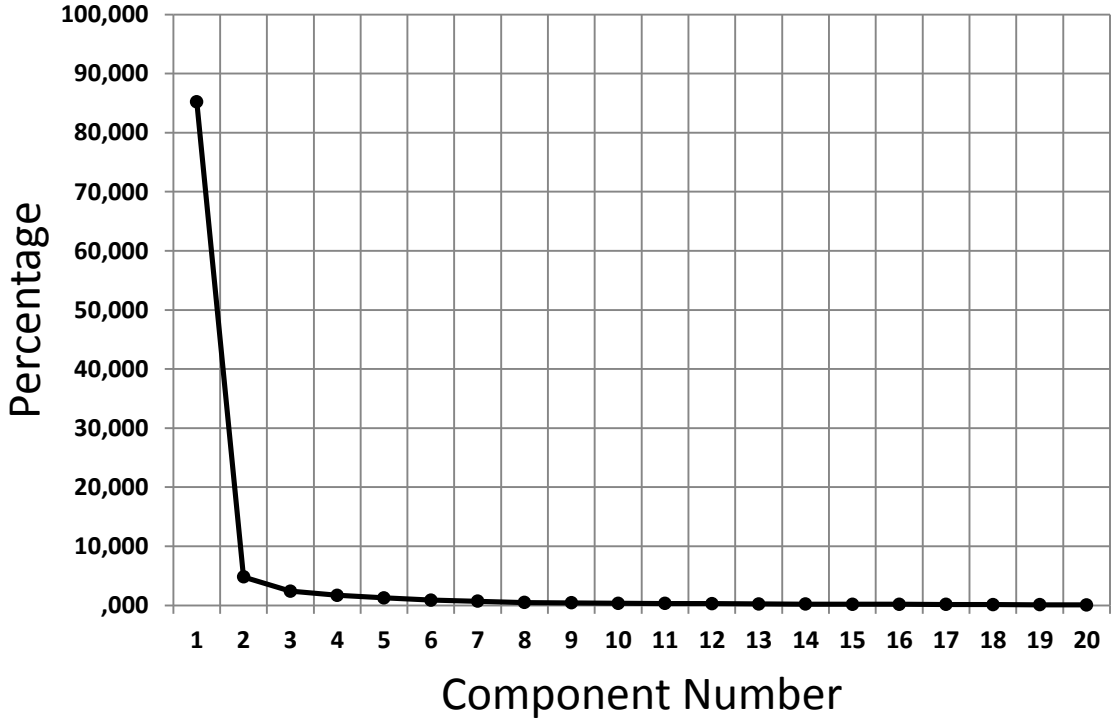

Figure 26 Explained variance of PAT80.

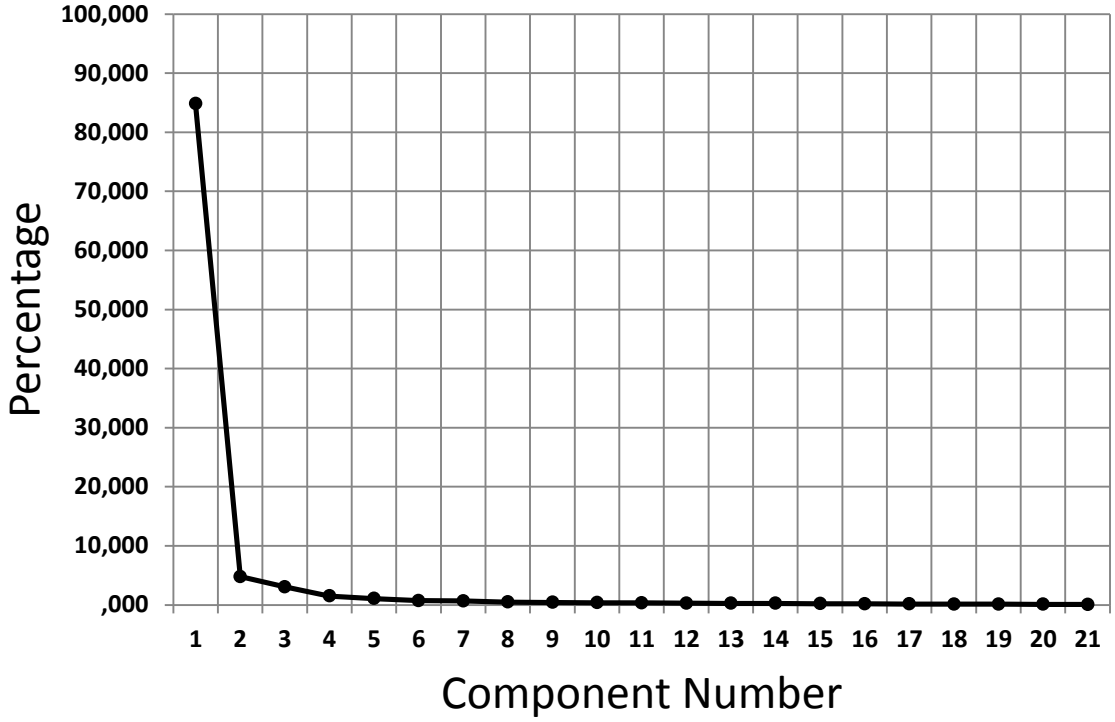

Figure 27 Explained variance of PAT50.

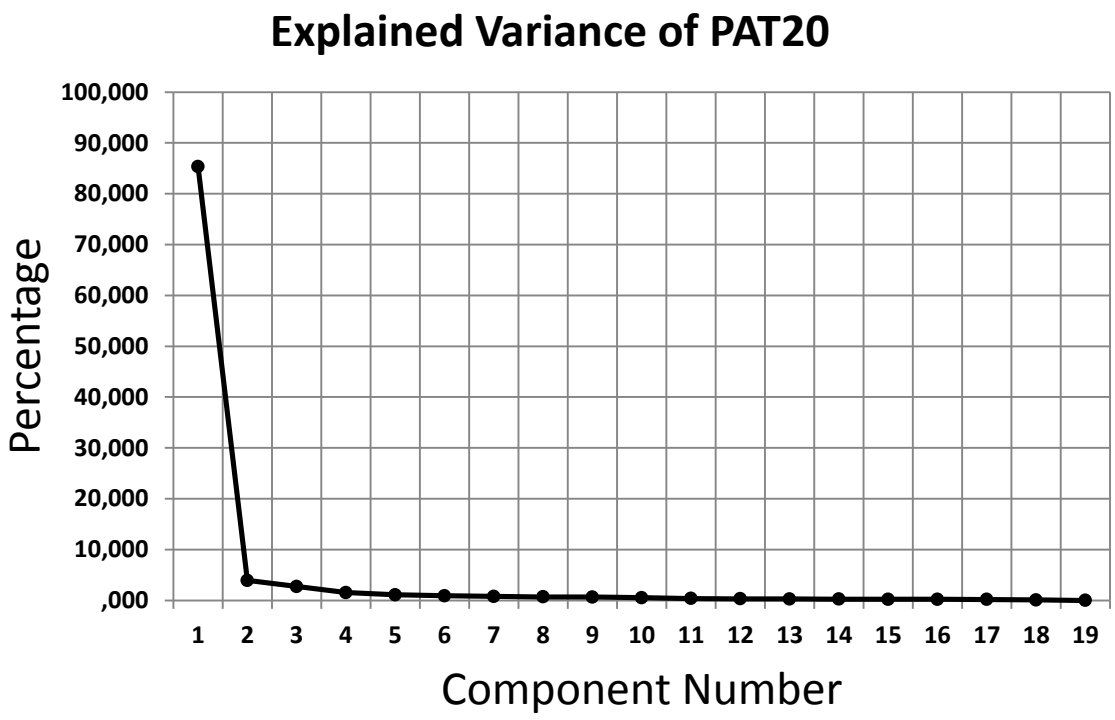

Figure 28 Explained variance of PAT20.

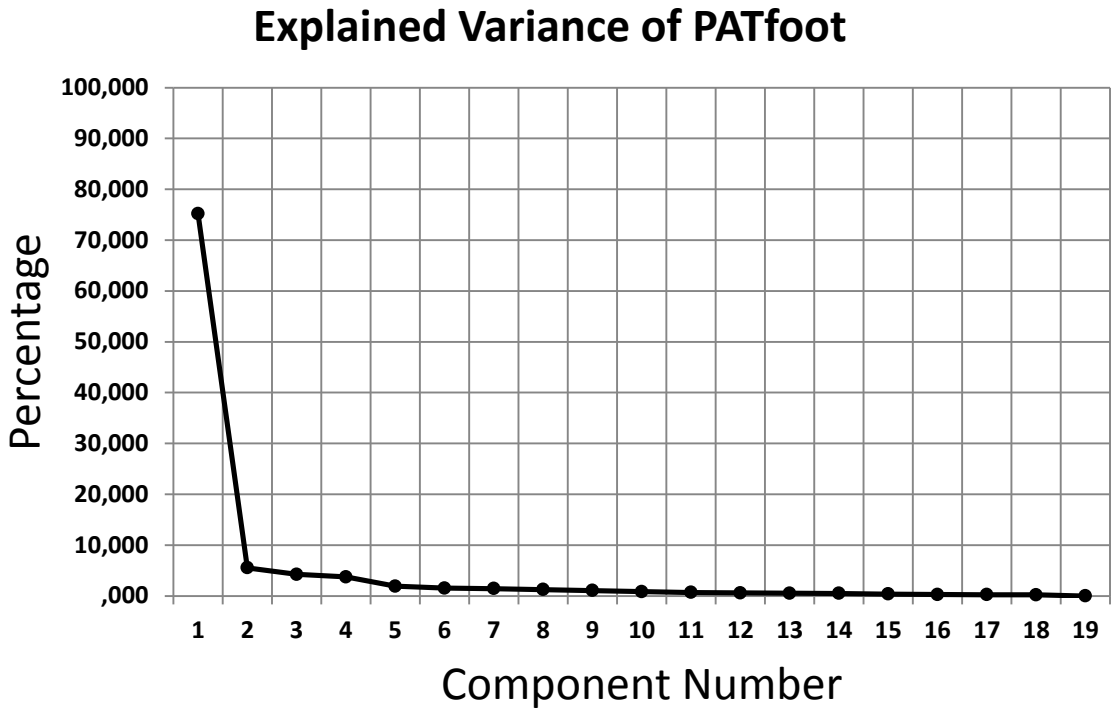

Figure 29 Explained variance of PATfoot.

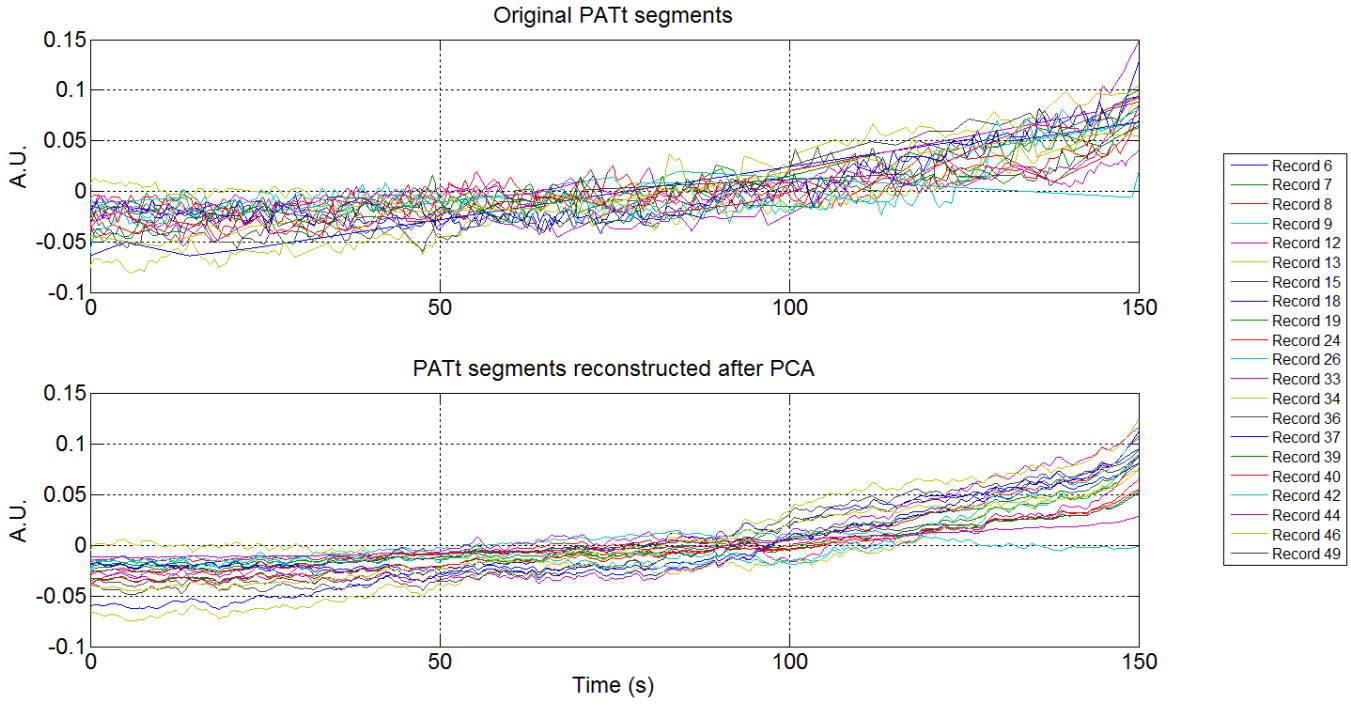

Figure 30 Comparison between original PATtop segments and the reconstructed ones.

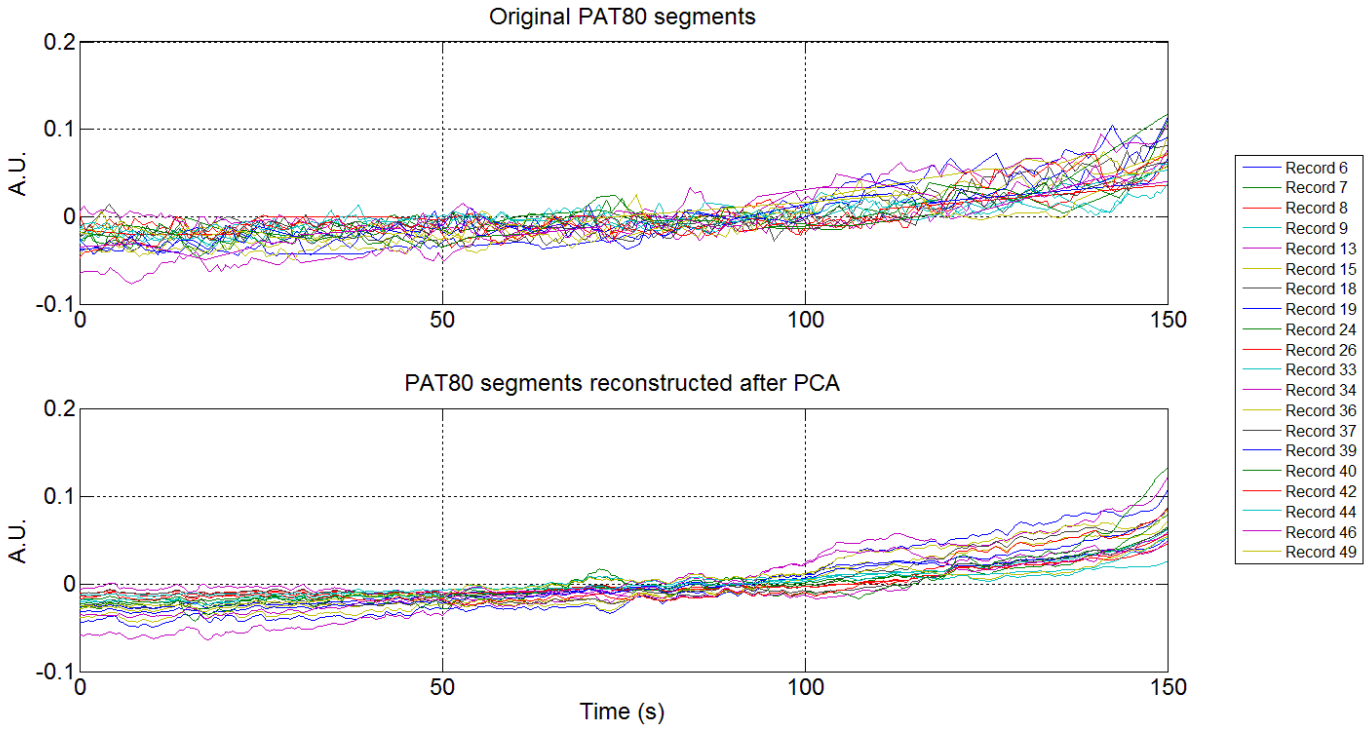

Figure 31 Comparison between original PAT80 segments and the reconstructed ones.

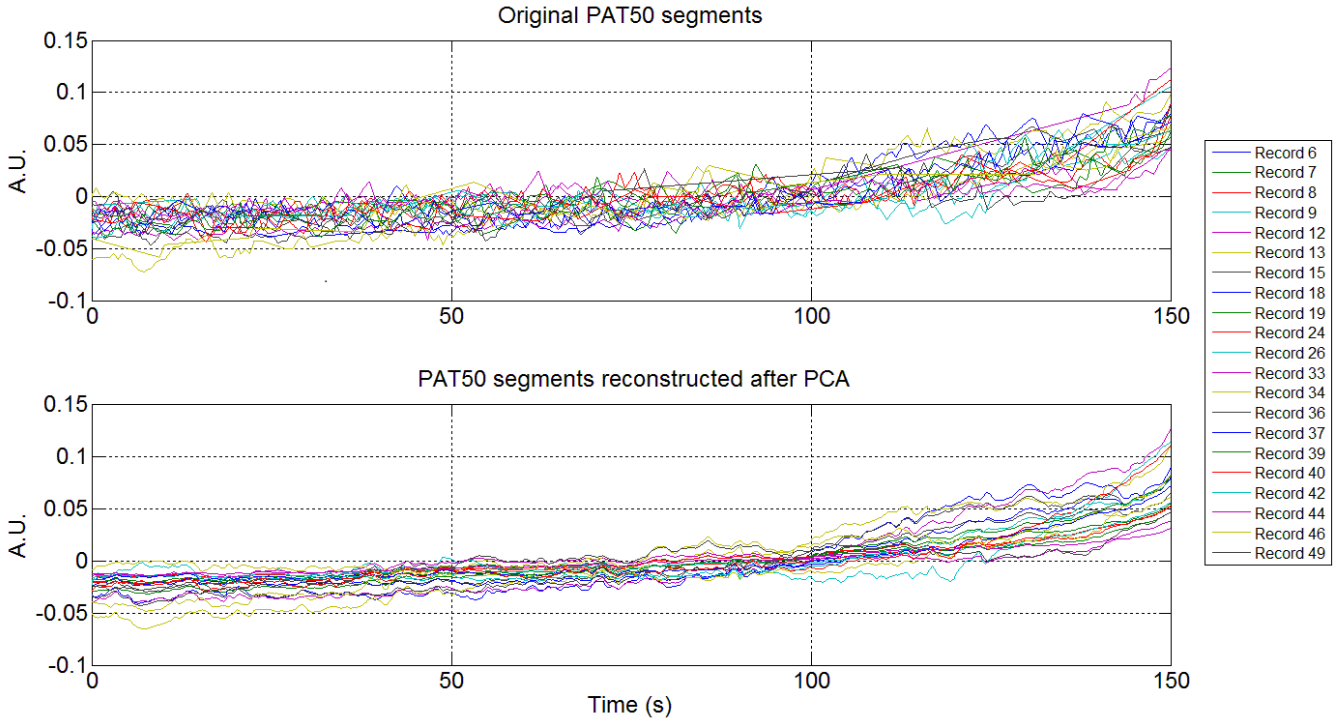

Figure 32 Comparison between original PAT50 segments and the reconstructed ones.

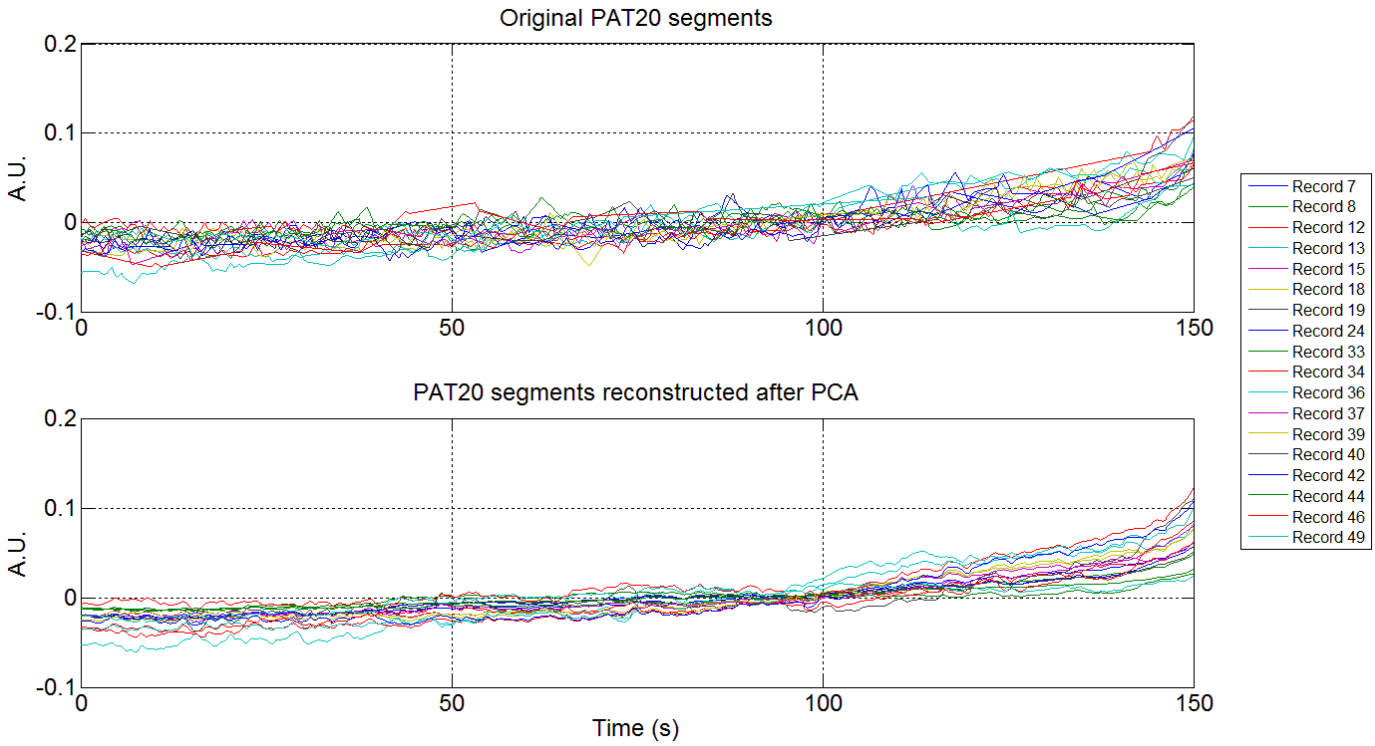

Figure 33 Comparison between original PAT20 segments and the reconstructed ones.

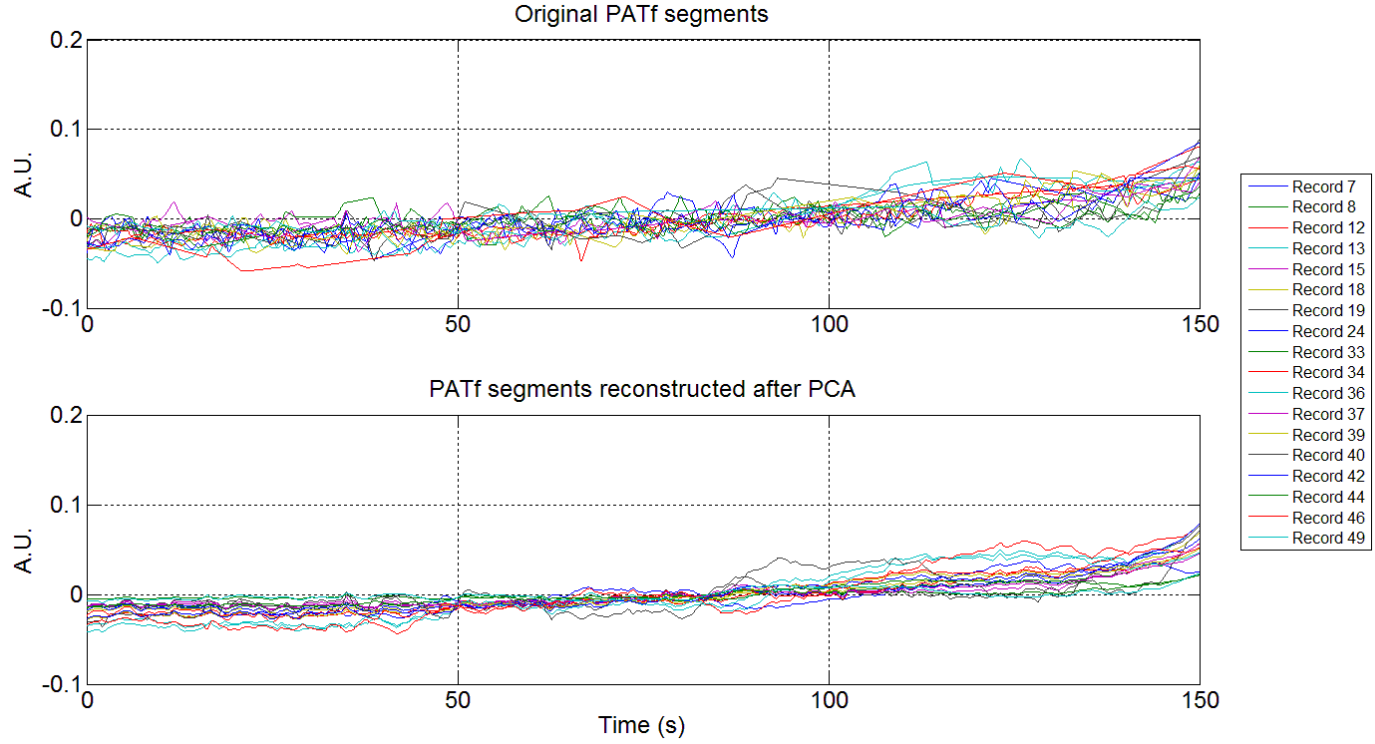

Figure 34 Comparison between original PATfoot segments and the reconstructed ones.

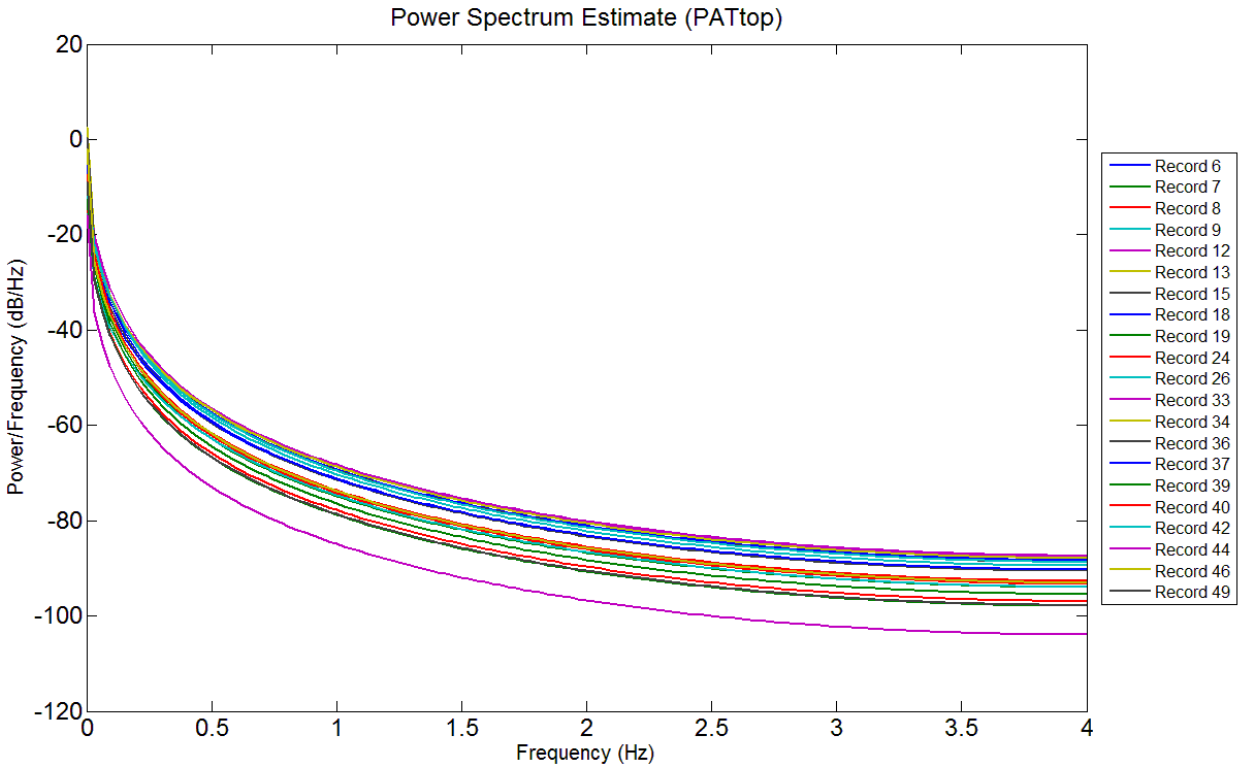

Figure 35 Power spectrum of PATtop segments after PCA reconstruction.

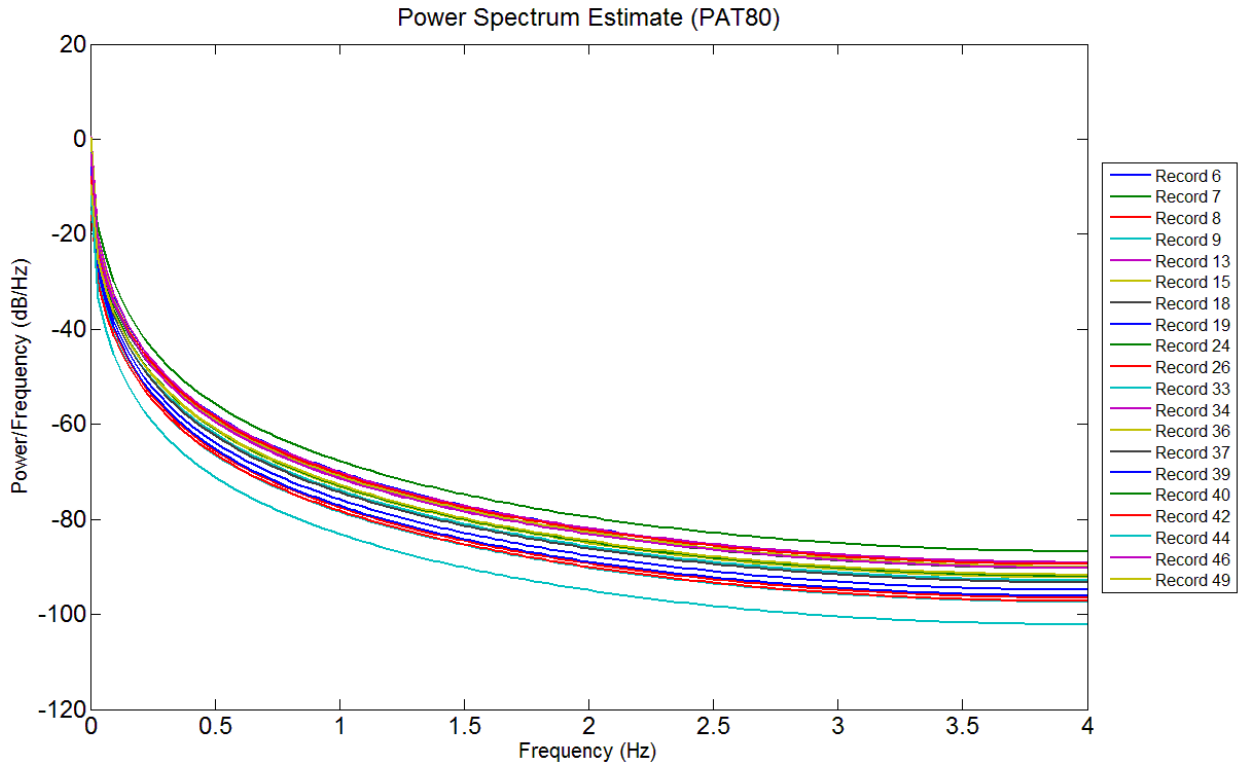

Figure 36 Power spectrum of PAT80 segments after PCA reconstruction.

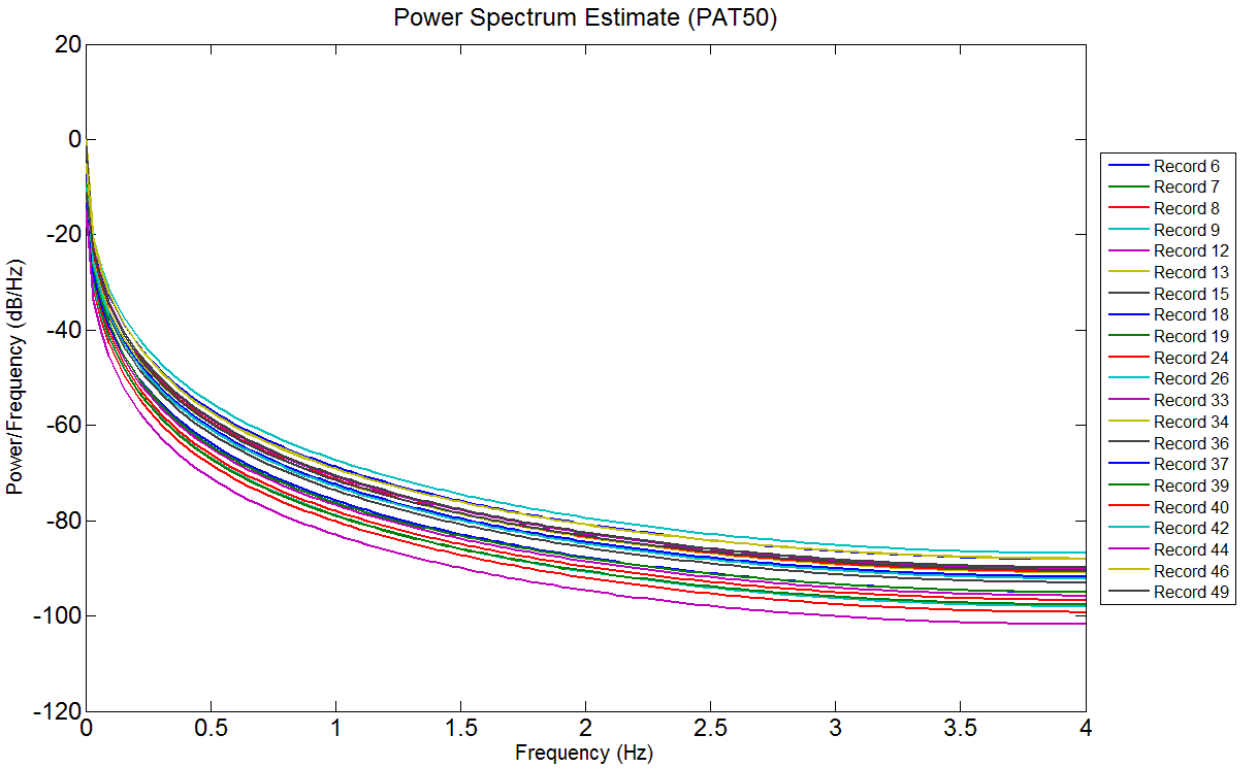

Figure 37 Power spectrum of PAT50 segments after PCA reconstruction.

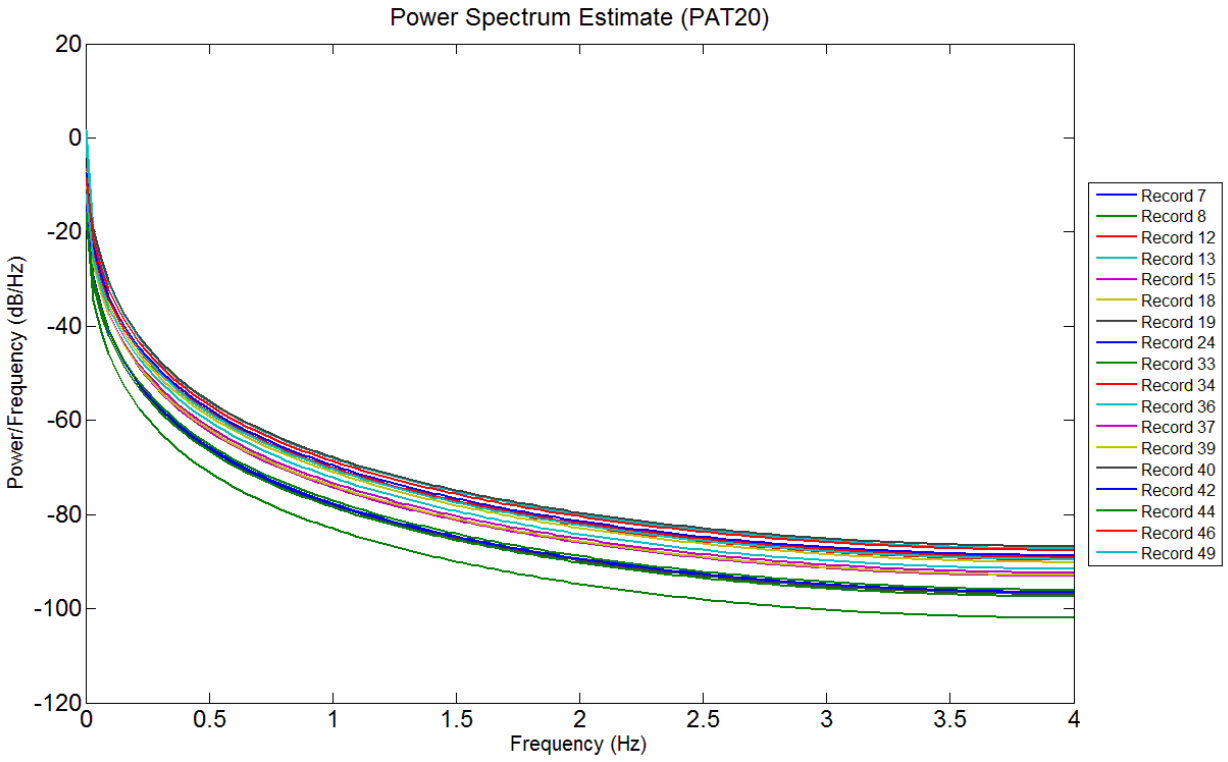

Figure 38 Power spectrum of PAT20 segments after PCA reconstruction.

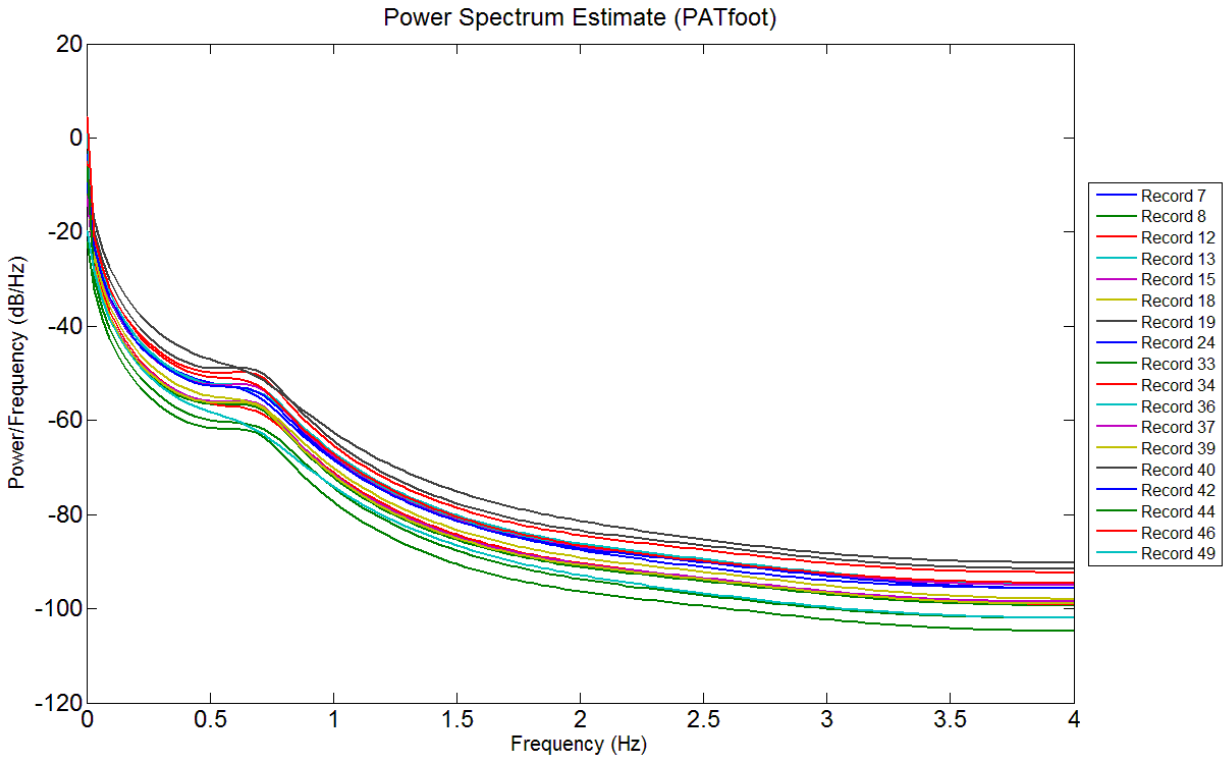

Figure 39 Power spectrum of PATfoot segments after PCA reconstruction.

A.3 ROC curves

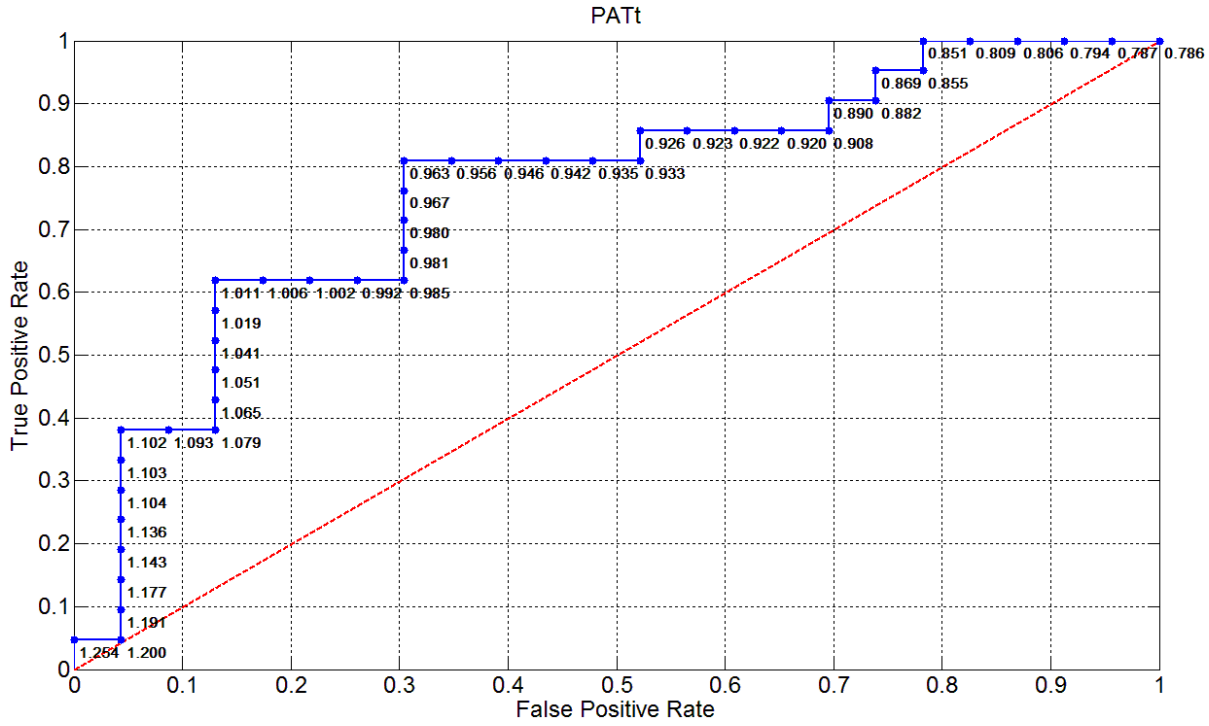

Figure 40 ROC curve for Sensitivity and Specificity of the individual values of the normalized PATt during the late tilt.

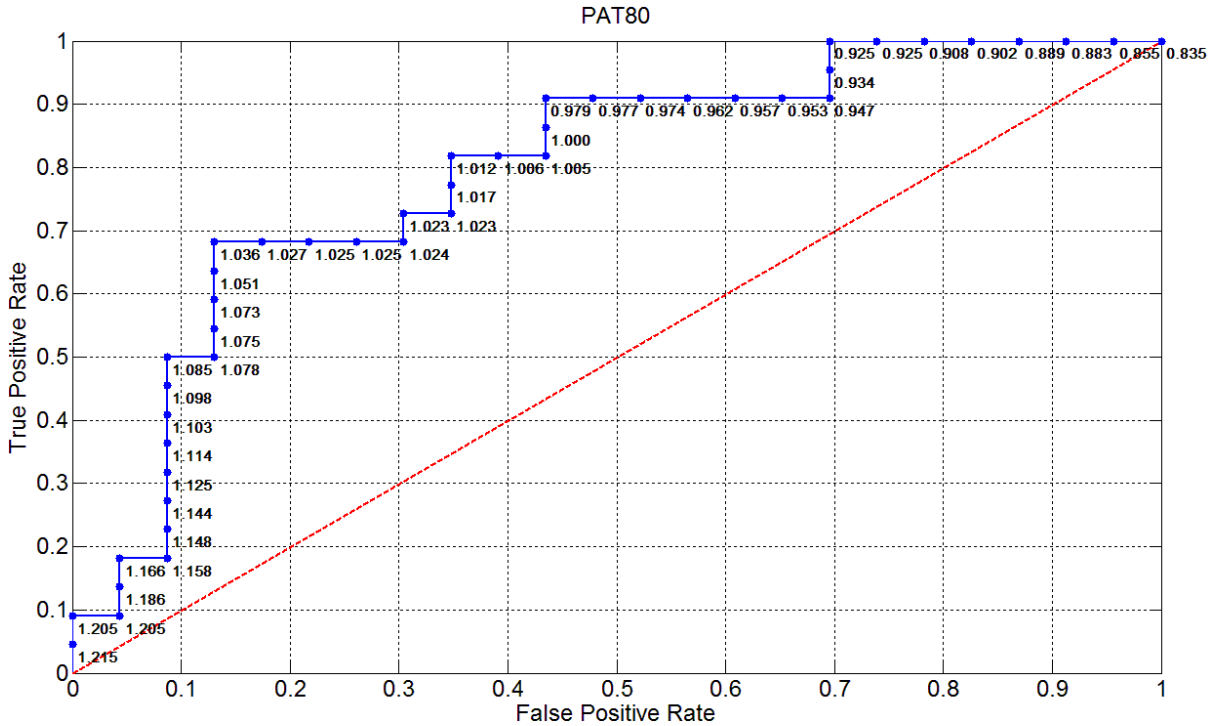

Figure 41 ROC curve for Sensitivity and Specificity of the individual values of the normalized PAT80 during the late tilt.

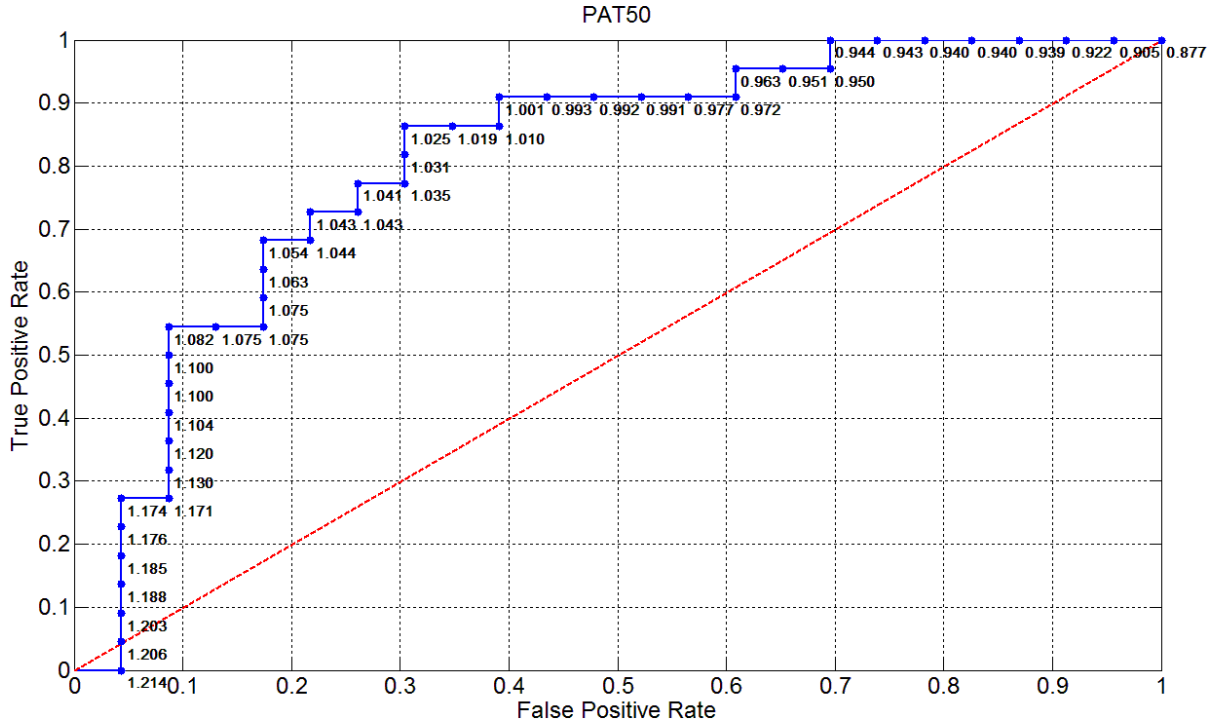

Figure 42 ROC curve for Sensitivity and Specificity of the individual values of the normalized PAT50 during the late tilt.

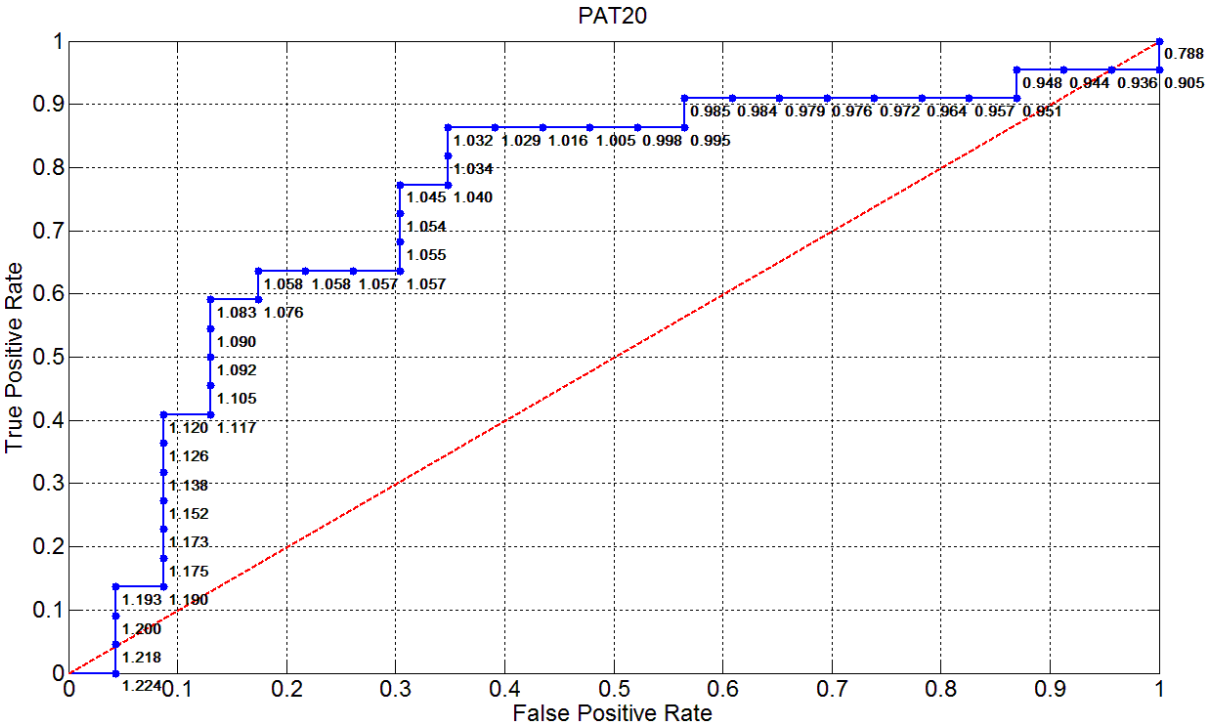

Figure 43 ROC curve for Sensitivity and Specificity of the individual values of the normalized PAT20 during the late tilt.

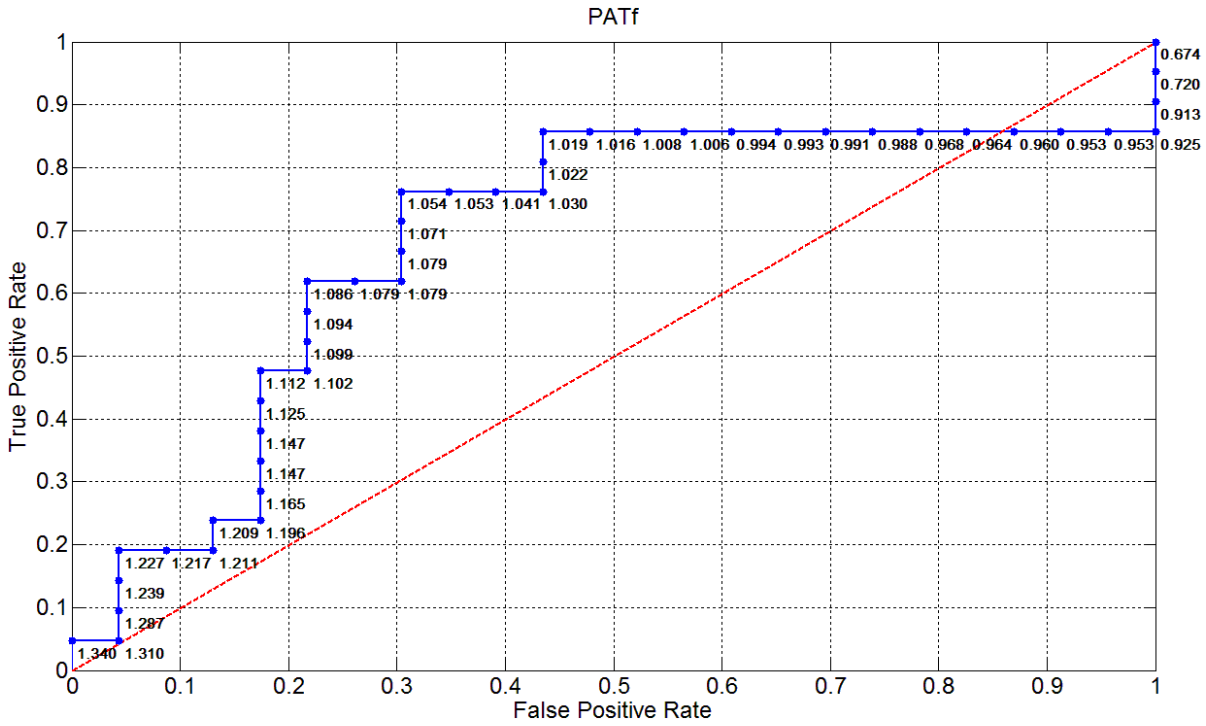

Figure 44 ROC curve for Sensitivity and Specificity of the individual values of the normalized PATf during the late tilt.

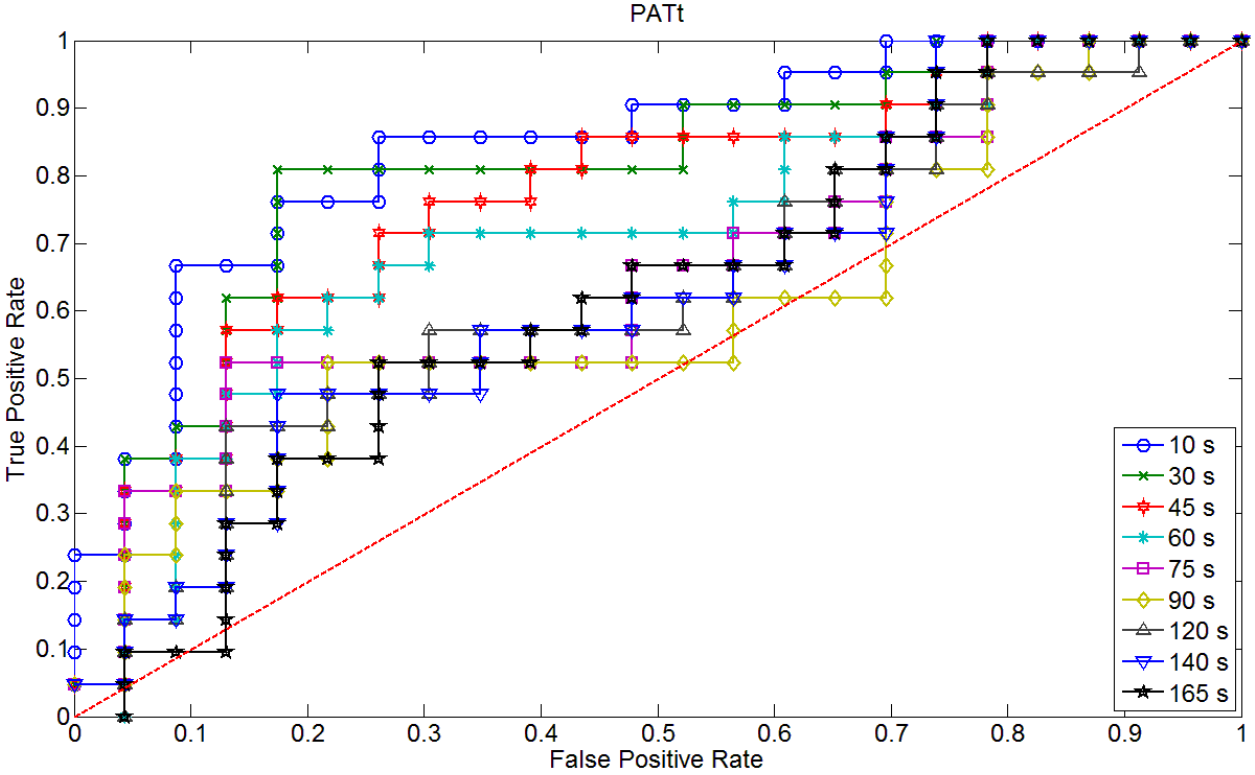

Figure 45 ROC curve for performance of PATt with different prediction times.

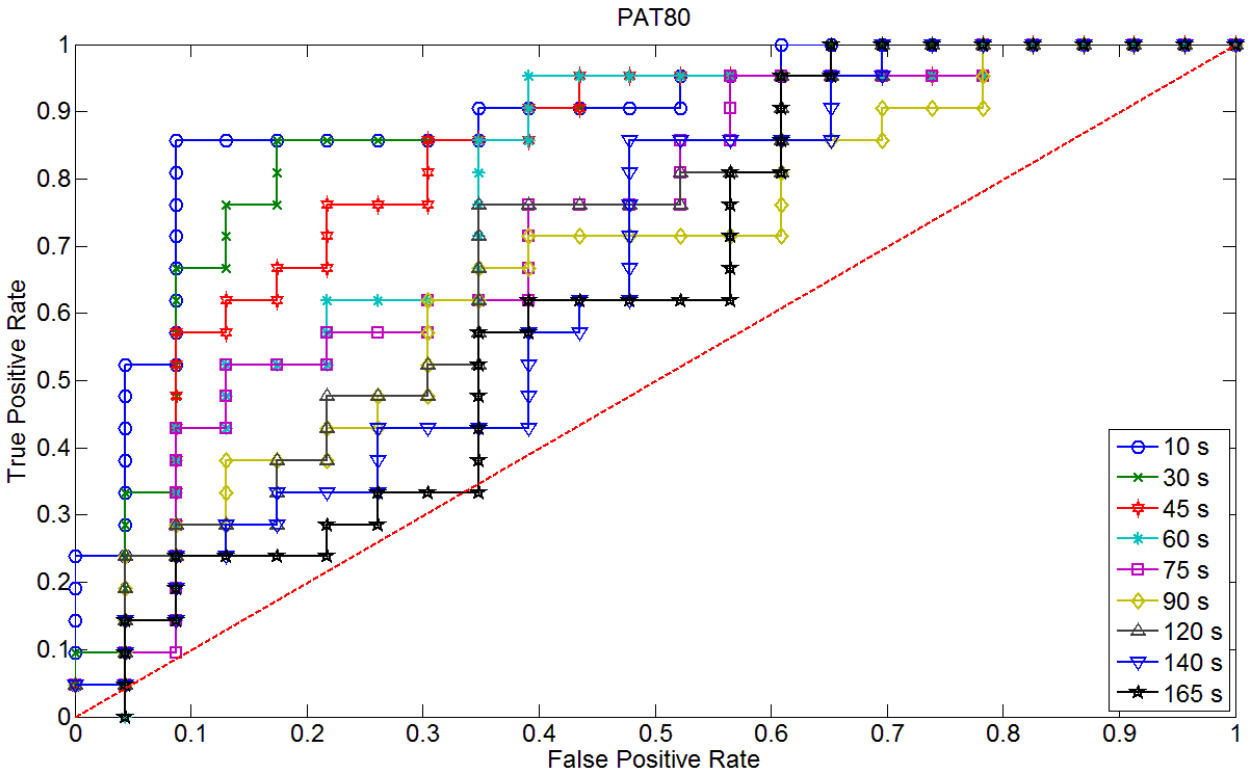

Figure 46 ROC curve for performance of PAT80 with different prediction times.

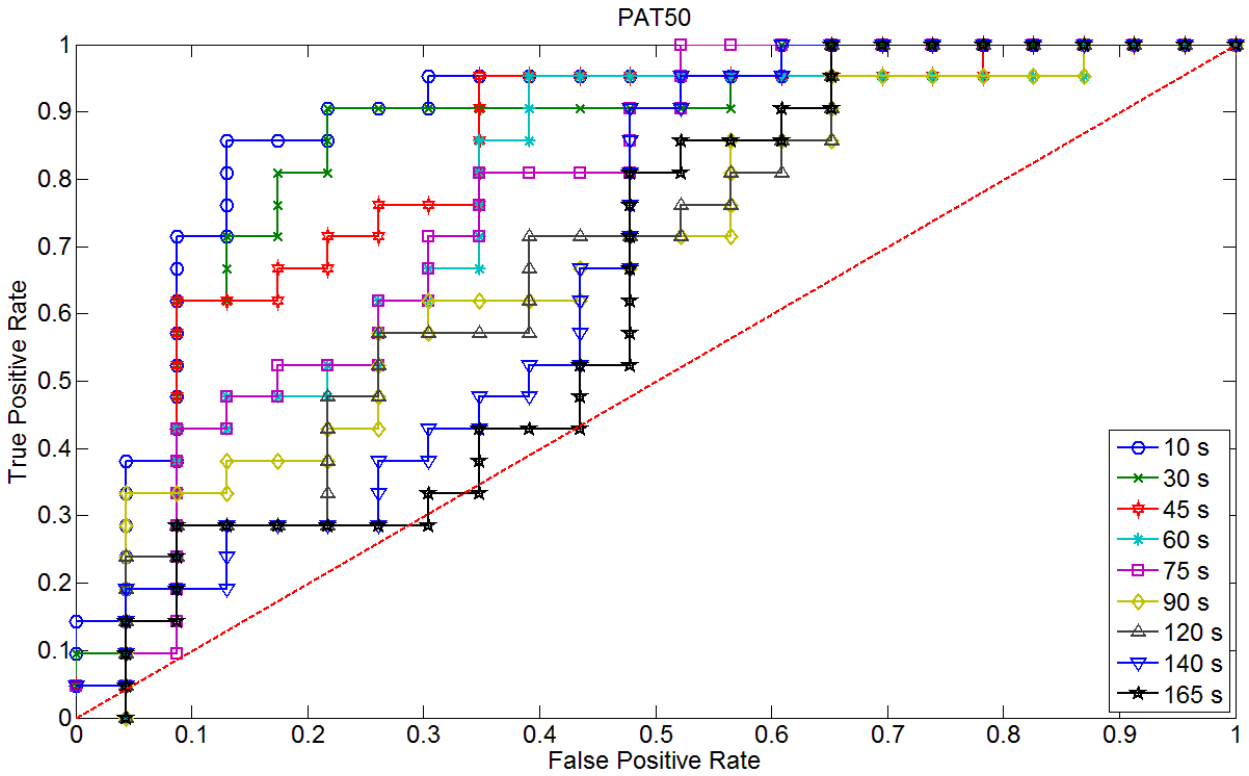

Figure 47 ROC curve for performance of PAT50 with different prediction times.

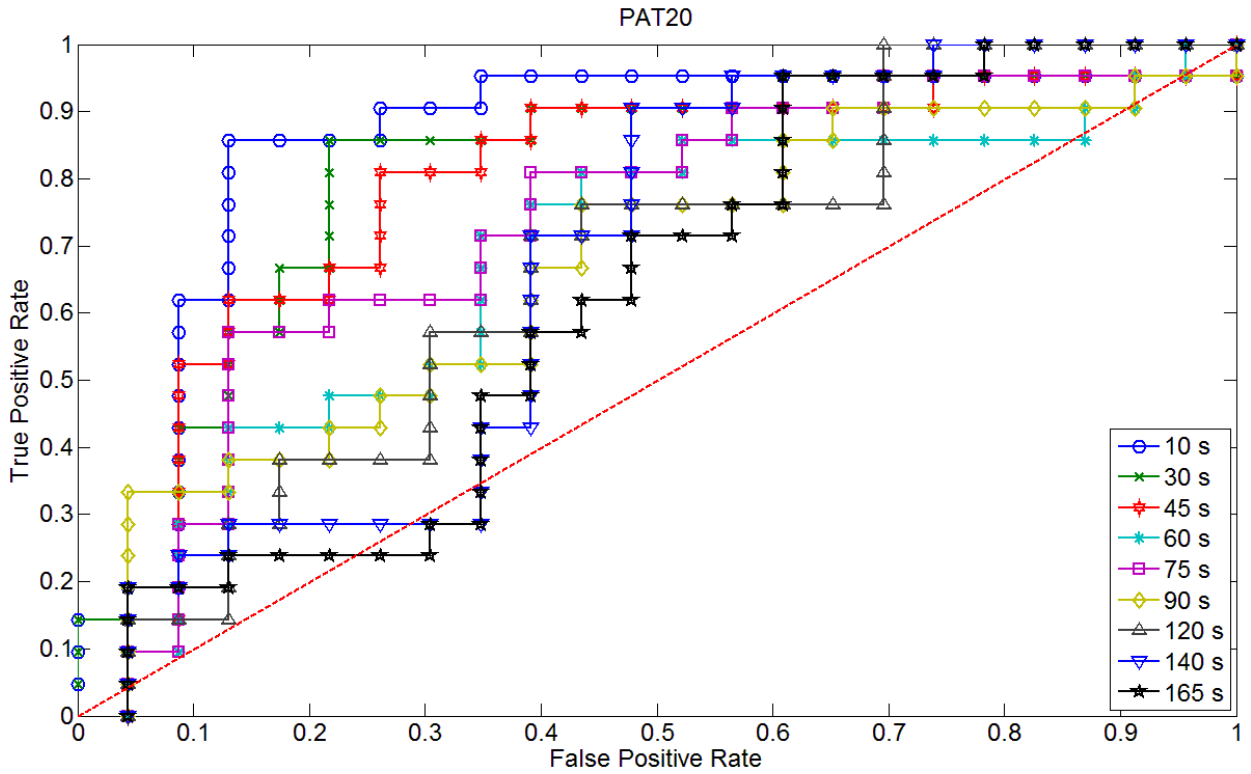

Figure 48 ROC curve for performance of PAT20 with different prediction times.

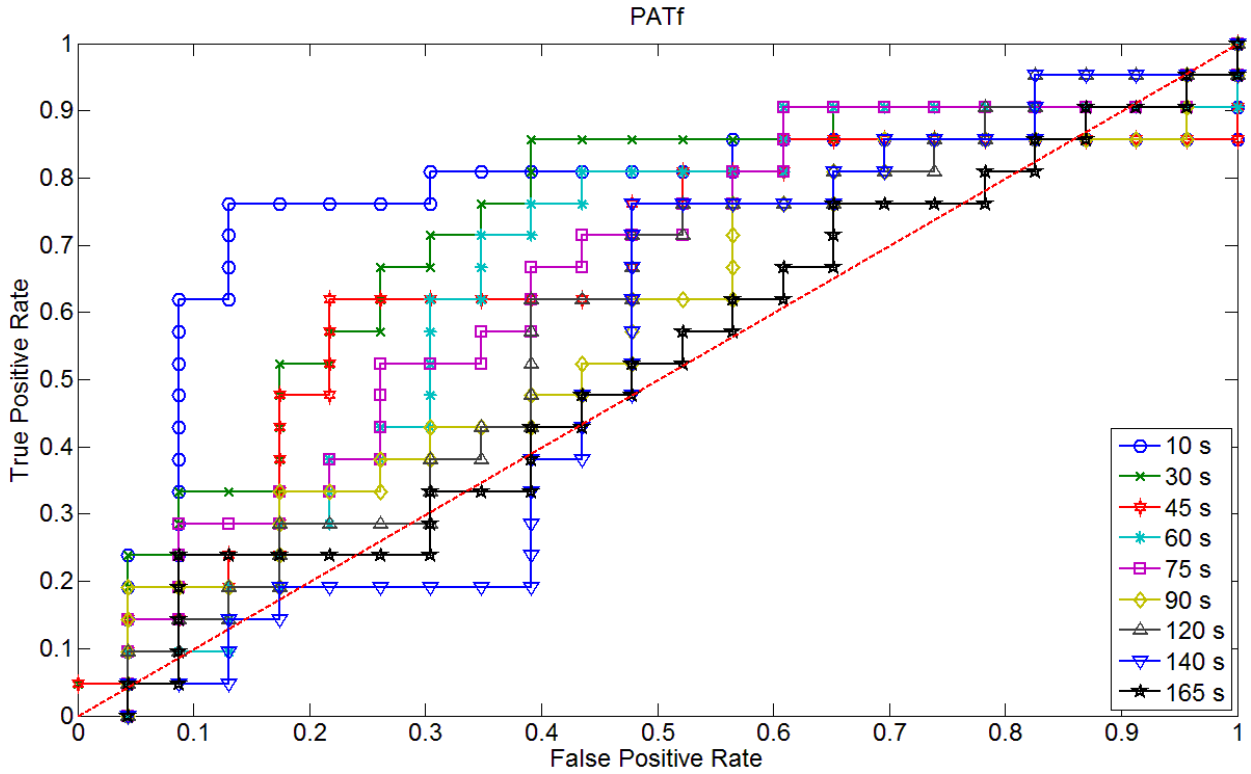

Figure 49 ROC curve for performance of PATf with different prediction times.

A.4 Demonstration of relationship between thresholds of nPAT

Consider a threshold Th1 for a normalized PAT, which is given by:

$$Th1 = \frac{PAT}{PATref} \tag{13}$$

If an offset δ is added to the PAT, we have a new threshold Th2:

$$Th2 = \frac{PAT + \delta}{PATref + \delta} \tag{14}$$

from where,

$$Th2 = \frac{PAT}{PATref + \delta} + \frac{\delta}{PATref + \delta} \tag{15}$$

$$\Leftrightarrow Th2 = \frac{PAT \times PATref}{(PATref + \delta) \times PATref} + \frac{\delta}{PATref + \delta} \tag{16}$$

$$\Leftrightarrow Th2 = Th1 \times \frac{PATref}{PATref + \delta} + \frac{\delta}{PATref + \delta} \tag{17}$$

$$\Leftrightarrow Th2 = \frac{Th1 \times PATref + \delta}{PATref + \delta} \tag{18}$$

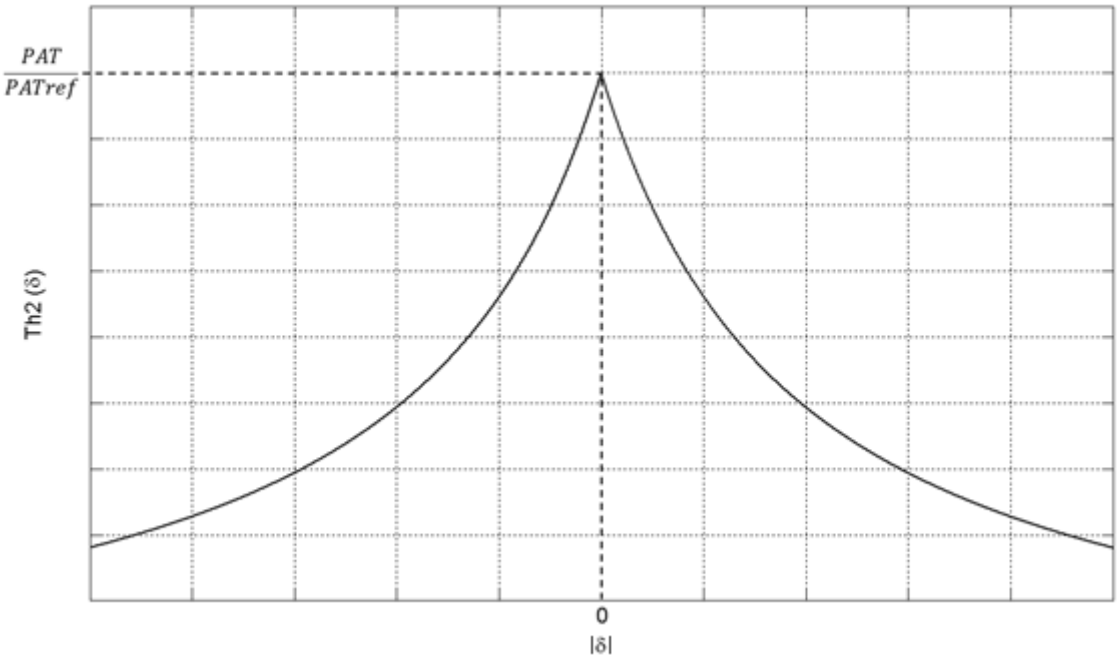

Figure 50 Impact of the offset in the determination of a new threshold.

A.5 Uncertainity of nPAT

The normalized PAT, nPAT, is given by equation (28), so its uncertainty, ΔnPAT, can be obtained through:

$$|\Delta nPAT| = \left|\frac{\delta nPAT}{\delta PAT}\right| \times |\Delta PAT| + \left|\frac{\delta nPAT}{\delta PATref}\right| \times |\Delta PATref| \quad (19)$$

But, ΔPATref is the standard deviation of PATref, σ_{PATref}, and PAT is a constant, so,

$$|\Delta nPAT| = \left|\frac{1}{PATref}\right| \times |\Delta PAT| + \left|-\frac{PAT}{PATref^2}\right| \times \left|\sigma_{PATref}\right| \quad (20)$$

It is also known that the PAT is obtained through the difference of a PPG and an ECG point, so if the precision of the PPG beat and R-peak detection are ignored its uncertainty can be roughly achieved by:

$$|\Delta PAT| = |\Delta PPG| + |\Delta ECG| \quad (21)$$

Where ΔPPG and ΔECG are the precision of the monitors from where the PPG and the ECG are acquired, respectively. Finally,

$$|\Delta nPAT| = \left|\frac{1}{PATref}\right| \times (|\Delta PPG| + |\Delta ECG|) + \left|-\frac{PAT}{PATref^2}\right| \times \left|\sigma_{PATref}\right| \quad (22)$$